



**UNIVERSITY OF SÃO PAULO  
FACULTY OF MEDICINE OF RIBEIRÃO PRETO  
DEPARTAMENT OF ONCOLOGY**

**ISABEL WEINHÄUSER**

**An M2-polarized macrophage microenvironment drives leukemogenesis  
and poor prognosis in acute myeloid leukemia**

**RIBEIRÃO PRETO**

**2021**

**ISABEL WEINHÄUSER**

**An M2-polarized macrophage microenvironment drives leukemogenesis  
and poor prognosis in acute myeloid leukemia**

Tese apresentada à Faculdade de Medicina de  
Ribeirão Preto da Universidade de São Paulo para  
obtenção do título de Doutor em Ciências pelo  
Programa de Pós-Graduação em Oncologia Clínica,  
Células-Tronco e Terapia Celular

Área de concentração: Diferenciação celular Normal  
e Neoplásica

Orientador: Prof Dr Eduardo Magalhães Rego

**RIBEIRÃO PRETO**

**2021**

Autorizo a reprodução total ou parcial deste trabalho, por qualquer meio convencional ou eletrônico, para fins de estudo e pesquisa, desde que citada a fonte.

“Versão corrigida. A versão original encontra-se disponível tanto na Biblioteca da Unidade que aloja o Programa, quanto na Biblioteca Digital de Teses e Dissertações da USP (BDTD)”

## FICHA CATALOGRAFICA

Serviço de Biblioteca e Documentação Médica

Faculdade de Medicina de Ribeirão Preto da Universidade de São Paulo

Weinhäuser, Isabel

An M2-polarized macrophage microenvironment drives leukemogenesis and poor prognosis in acute myeloid leukemia– Ribeirão Preto, 2021.

Um microambiente de macrófagos polarizados em M2 impulsiona a leucemogênese e o mau prognóstico na leucemia mielóide aguda.

108p.: 18il.; 30cm

Tese de doutorado, apresentada à Faculdade de Medicina de Ribeirão Preto – USP

Programa de Pós-Graduação em Oncologia Clínica, Células Tronco e Terapia Celular. Área de concentração: Diferenciação celular e neoplásica.

Orientador: Magalhães Rego, Eduardo

1. Tumor associated macrophages. 2. Therapy resistance. 3. Phagocytosis evasion.

Nome: Isabel Weinhäuser

Título: An M2-polarized macrophage microenvironment drives leukemogenesis and poor prognosis in acute myeloid leukemia

Tese apresentada à Faculdade de Medicina de  
Ribeirão Preto da Universidade de São Paulo para  
obtenção do título de Doutor em Ciências.

Aprovado em:

Banca Examinadora

Prof. Dr.: \_\_\_\_\_ Instituição: \_\_\_\_\_

Julgamento: \_\_\_\_\_ Assinatura: \_\_\_\_\_

Prof. Dr.: \_\_\_\_\_ Instituição: \_\_\_\_\_

Julgamento: \_\_\_\_\_ Assinatura: \_\_\_\_\_

Prof. Dr.: \_\_\_\_\_ Instituição: \_\_\_\_\_

Julgamento: \_\_\_\_\_ Assinatura: \_\_\_\_\_

Prof. Dr.: \_\_\_\_\_ Instituição: \_\_\_\_\_

Julgamento: \_\_\_\_\_ Assinatura: \_\_\_\_\_

Prof. Dr.: \_\_\_\_\_ Instituição: \_\_\_\_\_

Julgamento: \_\_\_\_\_ Assinatura: \_\_\_\_\_

## APOIO E SUPORTE FINANCEIRO

O presente trabalho foi realizado com o apoio financeiro das seguintes entidades e instituições:

- Fundação de Amparo à Pesquisa do Estado de São Paulo (FAPESP) – Projeto 2015/09228-0;
- Fundação Hemocentro de Ribeirão Preto (FUNDHERP);
- Fundação de Apoio ao Ensino, Pesquisa e Assistência do Hospital das Clínicas da Faculdade de Medicina de Ribeirão Preto da Universidade de São Paulo (FAEPA-HC FMRP/USP);
- Instituto Nacional de Ciência, Tecnologia e Inovação (INCT) em Células-Tronco e Terapia Celular – Projeto 14/50947-7;
- Centro de Terapia Celular – Centro de pesquisa, inovação e difusão (CEPID/FAPESP) – Projeto 2013/08135-2.
- Coordenação de Aperfeiçoamento de Pessoal de Nível Superior - Brasil (CAPES) – Código de Financiamento 001

**I dedicate this Thesis to my parents and friends. Science will move medicine Forward and only in a team we can strive and reach our full potential. I hope that this research will one day be part of a bigger picture and help to improve the outcome of acute myeloid leukemia patients.**

## ACKNOWLEDGMENTS

I would like to express my special thanks of gratitude to my first supervisor Prof. Eduardo Rego for accepting me as PhD student and supporting me in my development as a researcher in every possible way. Thanks to him I had the opportunity to get to know a new culture, learn a new language and grow both professionally as well as personally. As supervisor he was kind, always positive, easy to talk to and always willing to discuss and solve scientific problems, qualities I hope to implement myself one day. Second, I would like to express my gratitude to my second supervisor Prof. Jan Jacob Schuringa, who gave me the chance to come to the Netherlands. Prof. Schuringa pushed me in potential, which allowed me to become a better scientist every day. Our weekly scientific discussions will be one of the greatest memories of my PhD as they allowed me to see science from a different perspective and more importantly the bigger picture.

Next, I would like to thank my parents for their lifelong support. Thanks to my father I learned valuable qualities such as independence, to always try to remain calm, be fair and persevere. From my mother I learned honesty and willingness to always help when I can. I am especially grateful that they never pressured me and always wished me to be happy regardless of the path I would choose in life.

Following my parents, I am extremely grateful that I met Diego A P Martins, who was originally my colleague in the laboratory in Brazil and became my partner in life. I feel so lucky to have met someone, with whom I can share my passion for science and at the same time enjoy life. It is for certain that his support, collaboration and humor this thesis significantly contributed to my thesis and most importantly to my happiness.

Furthermore, I wish to thank all my colleagues from the laboratory in Brazil and the Netherlands. I never imagined meeting so many wonderful people and would like to express my special thanks to Luciana, Cleide, Dalva who welcomed me with open arms when I arrived in Brazil. Luise, Thamires, Thiago and Juan with whom I collaborated in Brazil, and I could count on whenever I needed help. Moreover, I am grateful for Ewa and Ayşegül, whom I met in the Netherlands and always supported me with their friendship. Nienke, who was a great help to me to find my way in the laboratory when I first arrived.

Likewise, I would like to thank my friends in Vienna and who supported me from the distance and never gave up on our friendship. My sincere gratitude for this friendship goes to Sonja, Bernard, Layomi, Belinda and Robert.

Finally, I would like to thank all the financial support I received including the Fundação de Amparo à Pesquisa de São Paulo (FAPESP) and the Abel Tasman Talent Program from the Netherlands.

The current work was sponsored by the Coordenação de Aperfeiçoamento de Pessoal de Nível Superior - Brazil (CAPES) – Code number 001

O presente trabalho foi realizado com apoio da Coordenação de Aperfeiçoamento de Pessoal de Nível Superior - Brasil (CAPES) – Código de Financiamento 001

Ao programa de pós-graduação em Oncologia Clínica, Células Tronco e Terapia Celular pelo suporte oferecido durante o doutorado e pela excepcional capacitação oferecida.

O presente trabalho foi realizado com apoio da Fundação de Amparo à Pesquisa do Estado de São Paulo (FAPESP) – Processo 2015/09228-0.



“Logic will take you from A to B. Imagination will take  
you everywhere” Albert Einstein

## RESUMO

**WEINHAUSER, I. Um microambiente de macrófagos polarizados em M2 impulsiona a leucemogênese e o mau prognóstico na leucemia mielóide aguda.** 2021, Ph.D. Tese – Faculdade de Medicina de Ribeirão Preto, Universidade de São Paulo, Ribeirão Preto, 2021.

Embora esteja cada vez mais claro que os cânceres são uma simbiose de diversos tipos celulares e clones tumorais, o microambiente de suporte tumoral (MST) em leucemias mieloides agudas (LMA) ainda permanece pouco compreendido. Nesse trabalho, nos demonstramos que os pacientes com pior prognóstico contem um compartimento de macrófagos polarizados em M2. A co-cultura de blastos leucêmicos com macrófagos M2 promoveu a sobrevivência celular e a resistência a agentes quimioterápicos. A injeção de macrófagos M2 na medula induziu leucemia fatal em animais transplantados com blastos de leucemia promielocítica aguda, usualmente conhecidos por seu baixo potencial de enxertia. Mesmo a exposição *in vitro* por dois dias a macrófagos M2, conseguiu "treinar" os blastos leucêmicos, após os quais as células são protegidas contra a fagocitose, apresentam metabolismo mitocondrial e homing *in vivo* aumentado, resultando em leucemia desenvolvida. Nós desenvolvemos um painel de biomarcadores baseado em macrófagos M2 que supera os preditores de prognóstico para LMA usados atualmente. Nosso estudo fornece uma visão sobre os mecanismos pelos quais o MST contribui para o desenvolvimento de leucemia agressiva e fornece alternativas para estratégias eficazes de tratamento e manejo clínico.

Palavras-chave: Macrófagos associados ao tumor, Desfechos clínicos, Resistência à terapia, Evasão à fagocitose.

## ABSTRACT

**WEINHAUSER, I. An M2-polarized macrophage microenvironment drives leukemogenesis and poor prognosis in acute myeloid leukemia.** 2021, Ph.D. Thesis – Faculdade de Medicina de Ribeirão Preto, Universidade de São Paulo, Ribeirão Preto, 2021.

While it is increasingly becoming clear that cancers are a symbiosis of diverse cell types and tumor clones, the tumor supportive microenvironment (TSM) in acute myeloid leukemias (AML) remains poorly understood. Here, we uncover that patients with the poorest prognosis harbor an M2-polarized macrophage compartment. Coculture of leukemic blasts on M2 macrophages promotes cell survival and drug resistance. Intrabone marrow co-injection of M2-macrophages induces fatal leukemia of acute promyelocytic leukemia blasts, which are otherwise poor grafters. Even a short-term two-day in vitro exposure to M2 macrophages can “train” leukemic blasts after which cells are protected against phagocytosis, display increased mitochondrial metabolism and in vivo homing, resulting in full-blown leukemia. We developed an M2-based biomarker panel that outperforms currently used AML prognosis predictors. Our study provides insight into the mechanisms by which the TSM contributes to aggressive leukemia development and provides alternatives for effective targeting strategies.

**Keywords:** Tumor associated macrophages, Clinical outcomes, Therapy resistance, Phagocytosis evasion.

## LIST OF ABBREVIATIONS AND ACRONYMS

AAM	AML Associated Macrophages
AC220	Quizartinib
AML	Acute Myeloid Leukemia
ACTB	Actin Beta
ANOVA	Analysis of Variance
AGM	Aorta Gonad Mesonephros
ANGPT1	Angiopoietin
APL	Acute Promyelocytic Leukemia
AraC	Cytarabine
ATO	Arsenic Trioxide
ATRA	<i>All-trans</i> Retinoic acid
AUC	Area Under the Curve
BM	Bone Marrow
BiNGO	The Biological Networks Gene Ontology tool
BSA	Bovine Serum Albumin
CB	Cord Blood
CD	Cluster of Differentiation
cDNA	Copy Deoxyribonucleic acid
CLR	Calreticulin
CPHM	Cox Proportional Hazard Model
CR	Complete Remission
CEBPA	CCAAT Enhancer Binding Protein Alpha
CLOUD	Continuum of low-primed undifferentiated hematopoietic stem and progenitor cells
CM	Conditioned Medium
CMP	Common Myeloid Progenitor

CLP	Common Lymphoid Progenitor
CPT1A	Carnitine palmitoyl transferase I
CSFE	Carboxyfluorescein Succinimidyl Ester
CXCL	C-X-C motif chemokine
DAPI	4',6-Diamidine-2'-phenylindole dihydrochloride
DFS	Disease Free Survival
DNA	Deoxyribonucleic acid
DNMT3A	DNA Methyltransferase 3 Alpha
E.7.5	Embryonic Day 7.5
E.9.5	Embryonic Day 9.5
ECAR	Extracellular Acidification Rate
EDTA	Ethylenediaminetetraacetic Acid
ELN	European Leukemia Net
ES	Enrichment Score
Eto	Etomoxir
FAB	French-American-British
FACS	Fluorescence-activated cell sorting
FAO	Fatty Acid Oxidation
FBS	Fetal Bovine Serum
FcR	Fc Receptor
FCS	Fetal Calf Serum
FDR	False Discovery Rate
FLT3	Fms-Like Tyrosine Kinase 3
G-CSF	Granulocyte colony-stimulating factor
GEO	Gene Expression Omnibus
<i>Gfi1</i>	Growth Factor Independent 1 Transcriptional Repressor
GM-CSF	Granulocyte-macrophage colony-stimulating factor

GMP	Granulocyte/Macrophage Progenitor
GO	Gene Ontology
GSEA	Gene Set Enrichment Analysis
GSK1 $\beta$	GSK-like kinase 1B
HCL	Hydrochloric acid
HD	Healthy Donor
Hdc	Histidine Decarboxylase
HMR	HyperPrep Kit with RiboErase
HPCA	Human Primary Cell Atlas
HPRT1	Hypoxanthine Phosphoribosyl transferase 1
HR	Hazard Ratio
HSC	Hematopoietic Stem Cell
IDO1	Indoleamine-pyrrole 2,3-dioxygenase
IFN $\gamma$	Interferon Gamma
IHC	Immunohistochemistry
IL	Interleukin
IT-HSC	Intermediate-Term Hematopoietic Stem Cells
JOVE	Journal of Visualized Experiments
Kit	Stem Cell Factor
KM	Kaplan Meier
LMPP	Lymphoid-Primed-Progenitor
LL	Left Leg
LPS	Lipopolysaccharides
LSC	Leukemic Stem Cells
LT-HSC	Long-Term Hematopoietic Stem Cells
MCSF	Macrophage Colony Stimulating Factor
MCP	Microenvironment Cell Populations-counter

MEM $\alpha$	Modification of Minimum Essential Medium
MEP	Megakaryocyte/Erythrocyte Progenitors
MFI	Mean Fluorescent Intensity
MGG	May Grunwald-Giemsa
MgSO <sub>4</sub>	Magnesium sulfate
MNC	Mononuclear cell
MPP	Multipotent Progenitor
MRC1	Mannose Receptor C-Type 1
MSC	Mesenchymal Stem cells
NaN <sub>3</sub>	Sodium azide
NES	Normalized Enrichment Score
NK	Natural Killer
NPM1	Nucleophosmin
NSG	NOS scid gamma (mice strain)
OCR	Oxidative Consumption Rate
OS	Overall Survival
OXPHOS	Oxidative Phosphorylation
PB	Peripheral Blood
PBS	Phosphate-buffered saline
PBMSC	Peripheral Blood Mononuclear-Stem Cell
PCA	Principal Component Analysis
PCR	Polymerase Chain Reaction
PDX	Patient Derived Xenograft
PH	Proportional Hazards
PKC	Midostaurin
PML	Promyelocytic leukemia protein
PS	Penicillin Streptomycin

RASA3	Ras GTPase-Activating Protein 3
RL	Right Leg
ROC	Receiver Operating Characteristic Curve
RNA	Ribonucleic acid
RPL30	Ribosomal Protein L30
RPMI	Roswell Park Memorial Institute medium (culture medium)
RT-PCR	Real Time Polymerase Chain Reaction
SCF	Stem Cell Factor
SDF1	Stromal Cell-Derived Factor 1
SLAM	Signaling Lymphocyte Molecule
SPSS	Statistical Package for the Social Sciences
STC1	Stanniocalcin 1
ST-HSC	Short-Term Hematopoietic Stem Cells
TAM	Tumor Associated Macrophages
T-bet	T-box transcription factor
TCGA	The Cancer Genome Atlas
TCZ	Tocilizumab
TGF $\beta$	Transforming growth factor beta
TH1	T-Helper Type 1
TH2	T-Helper Type 2
TME	Tumor Microenvironment
TMRE	Tetramethylrhodamine Ethyl Ester
TNF $\alpha$	Tumor Necrosis Factor
Tris	Trisaminomethane
TP53	Tumor protein 53
TPO	Thrombopoietin
TSM	Tumor Supportive Microenvironment



USP	University of São Paulo
UMCG	University Medical Center Groningen
Vcam1	Vascular cell adhesion protein 1
VEGF	Vascular endothelial growth factor
VEN	Venetoclax
VLCAD	Very-long-chain acyl-CoA dehydrogenase deficiency
WT	Wild Type

## LIST OF FIGURES AND ILLUSTRATIONS

<b>Figure 1.</b> Healthy hematopoiesis .....	25
<b>Figure 2.</b> Revised models of the hematopoietic differentiation tree.....	27
<b>Figure 3.</b> AML risk stratification.....	29
<b>Figure 4.</b> Healthy versus malignant hematopoiesis .....	30
<b>Figure 5.</b> AML Clonal evolution .....	31
<b>Figure 6.</b> Different macrophage subpopulations .....	34
<b>Figure 7.</b> The prognostic value of immune cells in cancer.....	34
<b>Figure 8.</b> The poor prognostic value of M2 macrophages in AML.....	62
<b>Figure 9.</b> The macrophage profile across distinct AML patients .....	63
<b>Figure 10.</b> The pro- and anti-leukemic effects of M1 and M2 macrophages <i>in vitro</i> .....	65
<b>Figure 11.</b> The effect of macrophages on AML cells and vice versa.....	66
<b>Figure 12.</b> Human M2 macrophages promote APL leukemogenesis in a PDX model .....	68
<b>Figure 13.</b> Primary APL blast cells pre-cultured on human M2 macrophages generate fatal leukemia .....	71
<b>Figure 14.</b> Primary APL blast cells pre-cultured on human M2 macrophages generate fatal leukemia .....	72
<b>Figure 15.</b> Primary murine APL blast cells pre-cultured on murine M2 macrophages accelerates APL leukemogenesis <i>in vivo</i> .....	73
<b>Figure 16.</b> M2 macrophages reprogram primary AML cells via different biological pathways.....	77
<b>Figure 17.</b> Co-culture of AML blasts with M2 macrophages reprogram AML cells via different biological process .....	78
<b>Figure 18.</b> M2 macrophages reprogram primary AML cells via different biological pathways.....	79

**Figure 19.** Development of a M2 signature for AML patients ..... 81

**LIST OF TABLES**

**Table 1.** Clinical characteristics of AML patients included ..... 90

**Table 2.** Univariable and multivariable analyses ..... 92

## SUMMARY

<b>1 INTRODUCTION .....</b>	<b>223</b>
1.1 Healthy hematopoiesis.....	223
1.2 The hematopoietic stem cell .....	24
1.3 Immunophenotypic characterization of hematopoiesis .....	25
1.4 Transcriptional regulation of hematopoiesis .....	26
1.5 The revised view of healthy hematopoiesis.....	26
1.6 The emergence of acute myeloid leukemia .....	28
1.7 AML clonal evolution .....	30
1.8 The tumor microenvironment in AML.....	32
1.9 Tumor associated macrophages .....	32
1.10 The role of macrophages in the BM during homeostasis and AML .....	343
1.11 The scope of this thesis.....	34
<b>2 OBJECTIVES.....</b>	<b>36</b>
2.1 General objective.....	36
2.2 Specific objectives.....	36
<b>3 MATERIAL AND METHODS .....</b>	<b>38</b>
3.1 Reagents .....	38
3.2 Patient analysis .....	41
3.2.1 Human sample collection and patient information.....	41
3.2.2 Flow cytometry .....	41
3.2.3 Immunohistochemistry .....	42
3.2.4 CIBERSORT analysis .....	42
3.2.5 Clinical endpoint analysis.....	43
3.3 Cell lines .....	43
3.4 Macrophage isolation and generation.....	44
3.4.1 Human and murine macrophages generation .....	44
3.4.2 Human and murine macrophages polarization .....	45
3.4.3 FACS staining of macrophages .....	45
3.5 Cord blood CD34 isolation.....	45
3.6 <i>In vitro</i> co-culture .....	46
3.6.1 <i>In vitro</i> AML cell line proliferation on macrophages.....	46

3.6.2 <i>In vitro</i> primary CB CD34 and AML cell proliferation on macrophages .....	46
3.6.3 Generation of conditioned medium and <i>in vitro</i> primary AML culture .....	47
3.6.4 Cell cycle .....	47
3.6.5 Apoptosis assay .....	47
3.6.6 Apoptosis assay drug screen in the presence of M2-macrophages .....	48
3.7 <i>In vivo</i> intra-BM APL patient derived xenotransplant (PDX) model.....	48
3.7.1 Animal welfare .....	48
3.7.2 <i>In vivo</i> intra-BM APL patient derived xenotransplant (PDX) model.....	48
3.8 <i>In vivo</i> pre-culture models .....	49
3.8.1 <i>In vivo</i> pre-culture APL PDX model .....	49
3.8.2 <i>In vivo</i> Long-Term Culture Initiating Cell assay .....	50
3.8.3 Murine <i>in vivo</i> pre-culture.....	50
3.9 <i>In vitro</i> phagocytosis .....	51
3.9.1 <i>In vitro</i> phagocytosis .....	51
3.9.2 Confocal immunofluorescence microscopy for calreticulin and stanioalcin-1 .....	52
3.10 Oxygen consumption (OCR) and extracellular acidification rate (ECAR) measurements .....	52
3.11 Mitochondrial transfer .....	53
3.12 <i>In vivo</i> homing and <i>in vitro</i> cell migration .....	54
3.12.1 <i>In vivo</i> homing assay .....	54
3.12.2 <i>In vitro</i> migration assay .....	54
3.13 <i>In vitro</i> assays post macrophage and MSC exposure .....	55
3.13.1 Colony forming unit assay.....	55
3.13.2 <i>In vitro</i> AML proliferation in liquid culture.....	55
3.14 RNAseq experiments and GO/GSEA analyzes .....	56
3.15 Development of a M2 signature suitable for AML patients .....	57
<b>4 RESULTS.....</b>	<b>59</b>
4.1 Heterogeneity in the macrophage landscape in AML: the presence of CD163 <sup>+</sup> /CD206 <sup>+</sup> leukemia-associated macrophages, identifies patients with the poor prognosis .....	59
4.2 M1 macrophages possess tumor suppressive activity while M2 macrophages enhance survival and impose drug resistance on AML blasts. ....	63
4.3 M2 macrophages support <i>in vivo</i> engraftment and leukemogenesis .....	66
4.4 M2 macrophages can reprogram primary APL to induce full-blown APL in a patient derived xenograft (PDX) model .....	68
4.5 “Trained” AML/APL blasts are protected against phagocytosis, display improved homing capacity, and adapt a more OXPHOS-like state.....	73

4.6 Development of a poor prognosis M2 macrophage signature.....	79
<b>5 DISCUSSION.....</b>	<b>82</b>
<b>6 CONCLUSION.....</b>	<b>87</b>
<b>7 TABLES.....</b>	<b>90</b>
<b>8 REFERENCES.....</b>	<b>94</b>
<b>9 SUPPLEMENTAL MATERIAL.....</b>	<b>108</b>

## ***Introduction***

---

## 1 INTRODUCTION

### 1.1 Healthy hematopoiesis

Hematopoiesis is the process by which hematopoietic stem cells (HSC) differentiate into different progenitor cells to continuously sustain the supply of blood cells (GRENIER-PLEAU et al., 2020). The notion of a common precursor cell giving rise to all blood lineages was first postulated by Franz Ernst Christian Neumann and Alexander A. Maximow in the beginning of the 19th century, while first experimental evidence was obtained by studies conducted in the 1950s. Lorenz et.al and others, demonstrated that spleen and bone marrow (BM) cell transplants were able to reconstitute hematopoiesis in recipients, which suffered from BM failure due to radiation (GASPARETTO et al., 2017; LORENZ; CONGDON; UPHOFF, 1952; TILL; MCCULLOCH, 1961). Since then, countless studies mostly conducted in mice, have shaped our knowledge about the structure of the hematopoietic system, which led to the classical portraiture of a hierarchically organized hematopoietic differentiation tree.

Studies in mice demonstrated that hematopoiesis first develops in the yolk sac (primitive or embryonic hematopoiesis) at embryonic day 7.5 (E7.5), followed by the para-aortic splanchnopleure region (E7.5-E9.5) and the aorta-gonad-mesonephros (AGM) region (E10.5-E11.5; definitive or adult hematopoiesis) (ANA CUMANO; FRANCOISE DIETERIAN-LIEVRE; ISABELLE GODIN, 1996; LINNEKIN, 1999; MATSUOKA et al., 2001; MEDVINSKY; DZIERZAK, 1996). Subsequently, the process of hematopoiesis ensues in the fetal liver and finally settles in the BM (EMA; NAKAUCHI, 2000). The transition of primitive/embryonic to definitive/adult hematopoiesis is accompanied by vasculogenesis. Endothelial cells, which emerge from the AGM region also possess the ability to differentiate into hematopoietic cells, which led to the hypothesis that hematopoietic precursor originate from the endothelium (NISHIKAWA et al., 1998). The current experimental data provides evidence to support three distinct theories describing the origin of the hematopoietic lineage. The first theory proposes the Haemangioblast, a common mesodermal progenitor cell with bidirectional potential, to generate hematopoietic cells to initiate embryonic hematopoiesis and endothelial cells for the formation of Blood Islands (CHOI et al., 1998; CHUNG et al., 2002; FALOON et al., 2000; HIRAI et al., 2003). Other studies suggest that hematopoietic cells derive from the hemogenic endothelium, a mesodermally-derived primitive endothelium structure, while others presume that hematopoietic and endothelial cells develop independently from a gastrulation-specified progenitor (GARCIA-PORRERO; GODIN; DIETERLEN-LIÈVRE,

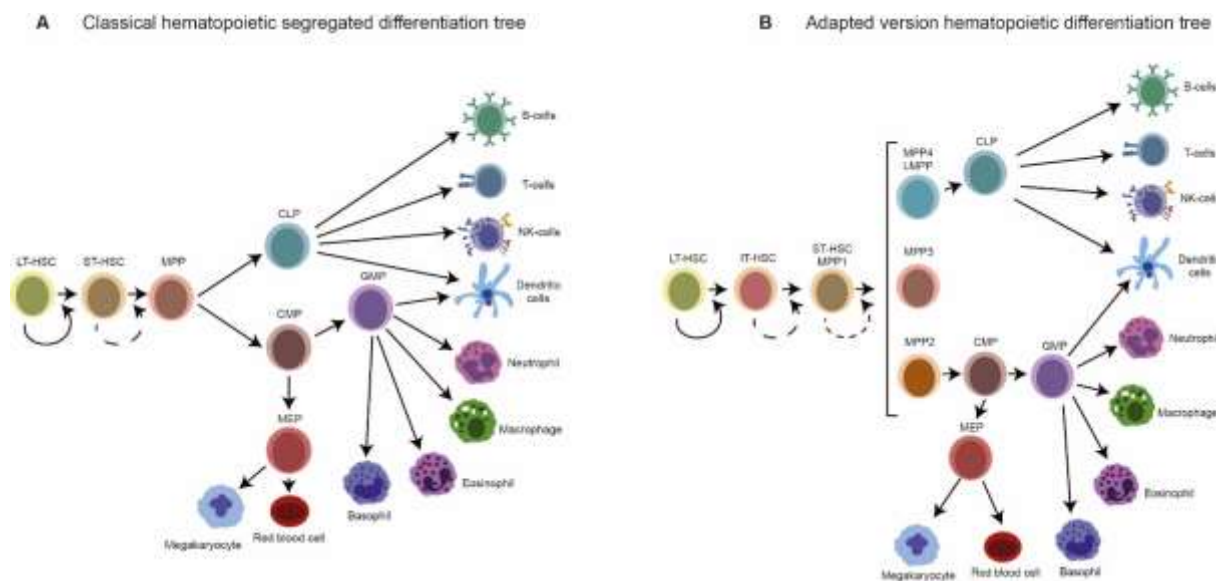


1995; TAM; BEHRINGER, 1997). Although the precise origin and development of the hematopoietic system remains elusive, it is well established that the different blood lineages emanate from HSCs during adult/definitive hematopoiesis.

## 1.2 The hematopoietic stem cell

Being at the apex of the hematopoietic system, the HSC gives rise to different types of blood cells responsible for immune defense, oxygen transport or blood clotting (AKASHI K et al., 2000; CABEZAS-WALLSCHEID et al., 2014). An HSC is a multipotent (ability to generate multiple progenies) cell defined by its ability to self-renew and initiate the lineage differentiation process, which is characterized by the loss of self-renewal ability to generate oligo- (ability to generate few progenies) and subsequently unipotent (ability to generate one specific cell type) progenitor cells.

HSC can be divided into long-term (LT), short term (ST) and more recently intermediate-term (IT) HSC (Figure 1A-B) (HIRAI et al., 2003; IKUTA; WEISSMAN, 1992; MORRISON; WEISSMAN, 1994; SPANGRUDE, 1991). LT, ST and IT distinguish themselves by their self-renewal ability, whereby LT-HSC possess long-lasting abilities to repopulate the BM in the event of lethal irradiation (CHRISTENSEN; WEISSMAN, 2001; SMITH; WEISSMAN; HEIMFELD, 1991), while ST-HSC promotes only short-term reconstitution of the blood lineage (MORRISON; SCADDEN, 2014; MORRISON; WEISSMAN, 1994; YANG et al., 2005) and IT-HSC are found to be in between LT-HSC and ST-HSC (BENVENISTE et al., 2010; YAMAMOTO et al., 2013). LT-HSC are quiescent by nature to avoid HSC exhaustion, except in the event of stress (SCHOEDEL et al., 2016), while ST-HSC differentiate into multipotent progenitors (MPPs) (Figure 1A) (MORRISON et al., 1997). MPP can be classified into four distinct groups: MPP1, MPP2, MPP3, and MPP4 (Figure 1B)(PIETRAS et al., 2015; WILSON et al., 2008) based on their BM abundancy as well as functional and cellular characteristics (CABEZAS-WALLSCHEID et al., 2014; OGURO; DING; MORRISON, 2013; WILSON et al., 2007). MPP1 share characteristics with ST-HSC, while MPP2 and MPP3 differentiate into common myeloid progenitor cells (PIETRAS et al., 2015) and MPP4 are associated with lymphoid-primed multipotent progenitors (LMPPs) to initiate lymphoid lineage development (ADOLFSSON et al., 2001, 2005; BOYER et al., 2011; FORSBERG et al., 2006). Finally, CMP can give rise to megakaryocyte/erythrocyte progenitors (MEP) and granulocyte/macrophage progenitors (GMP) (AKASHI K et al., 2000; NAKORN et al., 2002).

**Figure 1. Healthy hematopoiesis**

**A.** Representation of the hematopoietic differentiation tree depicting the LT-HSC at the apex of the hierarchy giving rise to fully differentiated blood cells. LT-HSC; Long-term Hematopoietic Stem Cell. ST-HSC; Short-term Hematopoietic Stem Cell; MPP; Multipotent Progenitor. CLP; Common Lymphoid Progenitor. CMP; Common Myeloid Progenitor. GMP; Granulocyte-Monocyte Progenitor. MEP; Megakaryocyte-Erythroid Progenitor. **B.** The revised hematopoietic differentiation model includes IT-HSC, which possess intermediate self-renewal capacity and different MPP populations primed to differentiate into distinct progenitor cells and subsequently mature blood cells. LT-HSC; Long-term Hematopoietic Stem Cells. IT-HSC; Intermediate-term Hematopoietic Stem Cells. ST-HSC; Short-term Hematopoietic Stem Cells.

### 1.3 Immunophenotypic characterization of hematopoiesis

The process of hematopoietic cell differentiation is orchestrated by cell intrinsic/extrinsic, epigenetic, and metabolic pathways. In addition, it has been demonstrated that while there is an HSC reigning at the top of the hierarchy, the pool of HSCs from which lineage defined cells derive is not homogenous but heterogeneous (BLACKETT; NECAS; FRINDEL, 1986; COPLEY; BEER; EAVES, 2012; MULLER-SIEBURG et al., 2012). Changes in the epigenetic landscape contributes to HSC heterogeneity and HSC cell fate decision (BUENROSTRO et al., 2018; TANG et al., 2017). Based on murine studies, several markers such as the histidine decarboxylase (Hdc) and the signaling lymphocyte activation molecule (SLAM) receptors have been identified to dictate the outcome of HSCs. While  $Hdc^{high}$ ,  $CD150^{high}$  and  $CD229^{-}$  HSCs are inclined to myeloid differentiation,  $CD150^{low}$  and

CD229<sup>+</sup> HSCs generate lymphoid progenitor cells (CHEN et al., 2017; OGURO; DING; MORRISON, 2013).

#### 1.4 Transcriptional regulation of hematopoiesis

Emanating from a primed HSC cell, a network of transcription factors, which up or down-regulate a set of genes at a certain concentration (level of gene expression), will further drive the process of lineage differentiation. Nonetheless, there are certain genes that are considered key regulators to direct CMP, CLP, GMP and MEP formation. For instance, GATA1 when expressed at low level, GATA1 facilitates eosinophil differentiation, while high expression of GATA1 is associated with erythroid and megakaryocytic maturation. Similar effects have been observed for PU.1, whereby high expression of PU.1 triggers macrophage development and low level of PU.1 promotes the emergence of B cells (DEKOTER; SINGH, 2000; KULESSA; PROGRAMME; MOLECULAR, 1995; MCDEVITT et al., 1997; NERLOV; GRAF, 1998). The up-regulation of lineage-restricting key regulators also means the down-regulation of transcription factors associated with other progenitors. For instance, GATA3 and T-box transcription factor (T-bet) are normally expressed in TH2 and TH1 cells, respectively. As a result, GATA3 and T-bet can both modulate the phenotype of T-cells enabling the conversion of TH1 cells to TH2 cells and vice versa (SZABO et al., 2000).

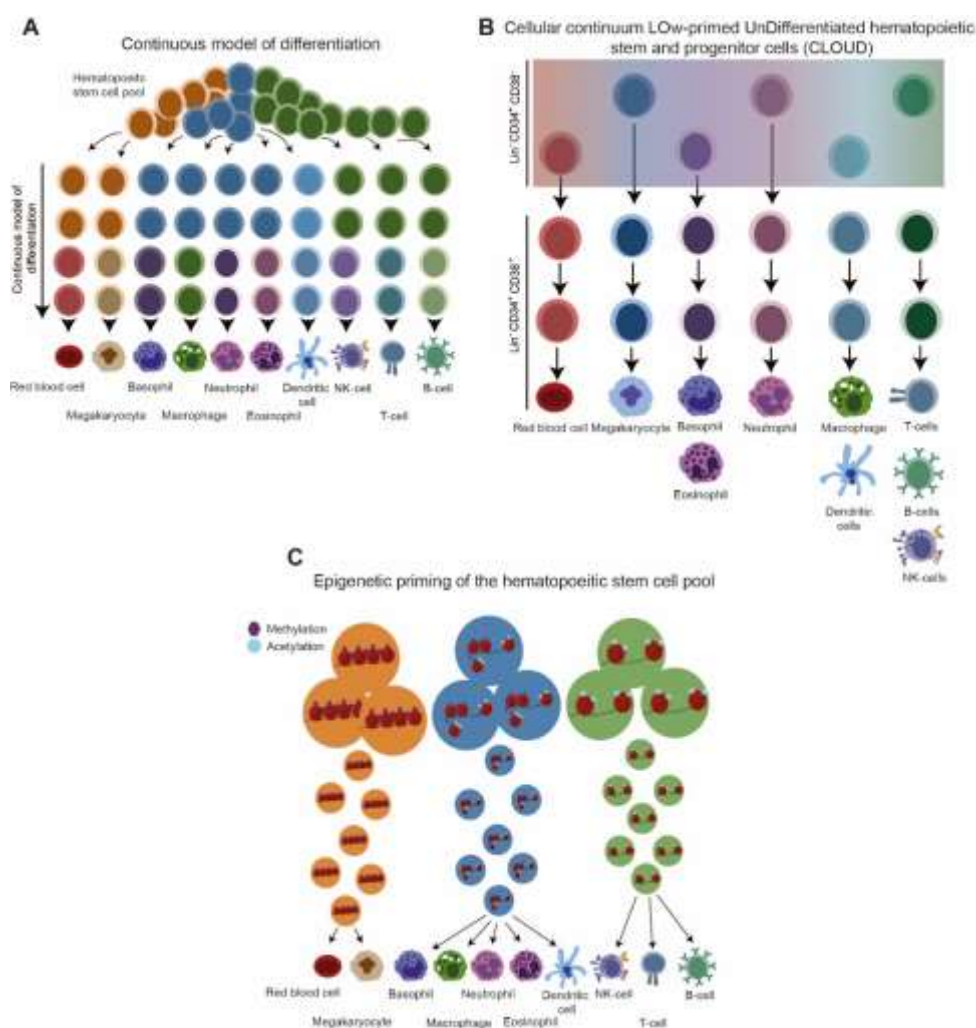
#### 1.5 The revised view of healthy hematopoiesis

In recent years single cell analysis revoke the classical idea of a hematopoietic lineage tree defined by discrete stages of cell differentiation and propose a continuous process without segregation instead (Figure 2A) (LAURENTI; GÖTTGENS, 2018). Initial studies employing single cell analysis, propose the idea of a “cellular continuum of LOw-primed UnDifferentiated hematopoietic stem- and progenitor cells (CLOUD)” (Figure 2B), from which uni-lineage restricted cells emerge. CLOUD-HSPC are Lin<sup>-</sup>CD34<sup>+</sup>CD38<sup>-</sup> cells, while the gain of CD38<sup>+</sup> expression (Lin<sup>-</sup>CD34<sup>+</sup>CD38<sup>+</sup>) marks the beginning of lineage progenitor development (VELTEN et al., 2017).

Yet, more recent studies conducted by Ranzoni et al revealed that even transcriptionally homogenous subpopulations presented diverse chromatin accessibilities along with lineage specific transcription factors. As a result, progenitors isolated based on cell surface marker do not encompass the high heterogeneity of HSC, MPP, CMP, GMP, MEP and CLP progenitor subpopulations. These data support the notion that hematopoiesis does not abide to a segregated differentiation process with the earliest branching point differentiating between myeloid/erythroid and lymphoid, but that HSCs are primed at the chromatin level initiating lineage commitment (Figure 2C) (RANZONI et al., 2021).

Overall, the hematopoietic system must maintain a rigorous balance between HSC self-renewal and differentiation to avoid HSC depletion or the excessive proliferation of undifferentiated cells causing the emergence of hematological malignancies (e.g.: Myeloproliferative diseases or Leukemia) (YAMASHITA et al., 2020).

**Figure 2. Revised models of the hematopoietic differentiation tree**



**A.** Continuous model of hematopoiesis, whereby hematopoietic stem cells differentiate into mature blood cells in a continuum and not in segregated stages. **B.** CLOUD hematopoietic differentiation model depicting an early-stage commitment to develop into distinct mature blood cells. **C.** Hematopoietic differentiation showing a heterogeneous pool of epigenetically distinct HSCs. Different chromatin accessibility induces differentiation into distinct mature blood cells.

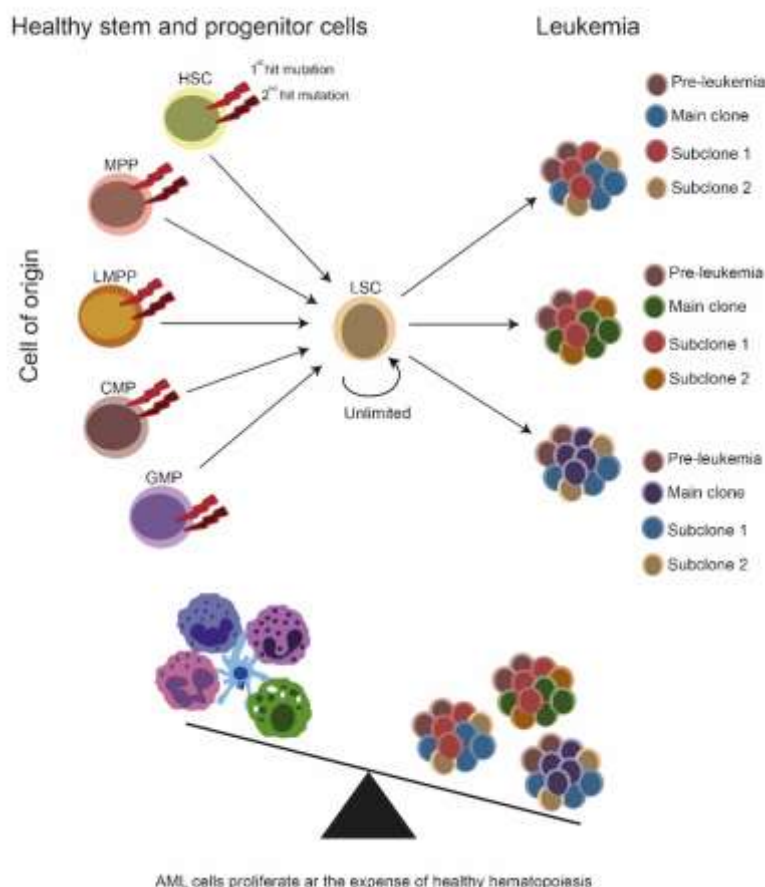
## **1.6 The emergence of acute myeloid leukemia**

In hematological malignancies such as Acute Myeloid Leukemia (AML) the hematopoietic system is disrupted impeding the development of terminally differentiated myeloid cells. AML is characterized by the aberrant proliferation of immature myeloid cells infiltrating the bone marrow and leading to bone marrow failure if left untreated (DE KOUCHKOVSKY; ABDUL-HAY, 2016). The 5-year overall survival rate is approximately 25% and the typical symptoms upon disease progression are anemia, leukocytosis, neutropenia, and thrombocytopenia. One of the major challenges encountered by clinicians and researcher is the cytogenetic, epigenetic, morphological and immunophenotypic heterogeneity of AML blasts between patients, creating the need for a classification system (DE KOUCHKOVSKY; ABDUL-HAY, 2016; KANTARJIAN et al., 2021; LI; MASON; MELNICK, 2016). In an initial attempt to classify patients into different AML subgroups, the French-American-British (FAB) classification system categorized patients based on leukemic cell morphology and cytochemistry into eight subtypes (M0-M7) but neglected many prognostic factors such as age or genetic alterations (BENNETT et al., 1976). Thus, a new system was established by the European LeukemiaNet (ELN) to stratify patients into favorable, intermediate, and adverse risk groups based on their cytogenetic and molecular landscape, age, general health, and comorbidity (DÖHNER et al., 2017).

**Figure 3. AML risk stratification system**

A		B	
FAB subtype	Name	Risk category	Genetic abnormalities
M0	Undifferentiated acute myeloblastic leukemia	Favorable	t(6;21)(q22;q22.1); RUNX1-RUNX1T1 inv(16)(p13.1q22) or t(16;16)(p13.1;q22); CBFB-MYH11 Mutated NPM1 without FLT3-ITD or with FLT3-ITD <sup>low</sup> (<0.5) Biallelic mutated CEBPA
M1	Acute myeloblastic leukemia with minimal maturation	Intermediate	Mutated NPM1 and FLT3-ITD <sup>high</sup> (>0.5) Wild-type NPM1 without FLT3-ITD or with FLT3-ITD <sup>low</sup> (<0.5) without adverse-risk genetic lesion t(8;11)(p21.3;q23.3); MLL73-KMT2A Cytogenetic abnormalities not classified as favorable or adverse
M2	Acute myeloblastic leukemia with maturation	Adverse	t(8;9)(p23;q34.1); DEK-NUP214 t(v;11)(q23.3); KMT2A rearranged t(9;22)(q34.1;q11.2); BCR-ABL1 inv(3)(q21.3;q26.2) or t(3;3)(q21.3;q26.2); GATA2, MECOM(EVI1) -5 or del(5q); -7, -17/abn(17p) Complex karyotype / monosomal karyotype Wild-type NPM1 and FLT3-ITD <sup>low</sup> (<0.5) Mutated RUNX1 Mutated ASXL1 Mutated TP53
M3	Acute promyelocytic leukemia (APL)		
M4	Acute myelomonocytic leukemia		
M4 eos	Acute myelomonocytic leukemia with eosinophilia		
M5	Acute monocytic leukemia		
M6	Acute erythroid leukemia		
M7	Acute megakaryoblastic leukemia		

**A.** AML stratification based on the French American British (FAB) classification system (adapted from Bennett et al., 1976). **B.** The European Leukemia Net (ELN) 2017 AML risk stratification based on molecular genetics and cytogenetic alterations (adapted from Döhner et al., 2017).

**Figure 4. Healthy versus malignant hematopoiesis**

LSCs can either derive from HSC or different progenitor cells that acquire mutations endowing them with unlimited self-renewal potential and a block in differentiation, thereby impairing the maturation of blood cells. Subsequently, LSCs give rise to the leukemic bulk, which expands in the bone marrow niche and comprehends genetically distinct subclones including the presence of pre-leukemic clones

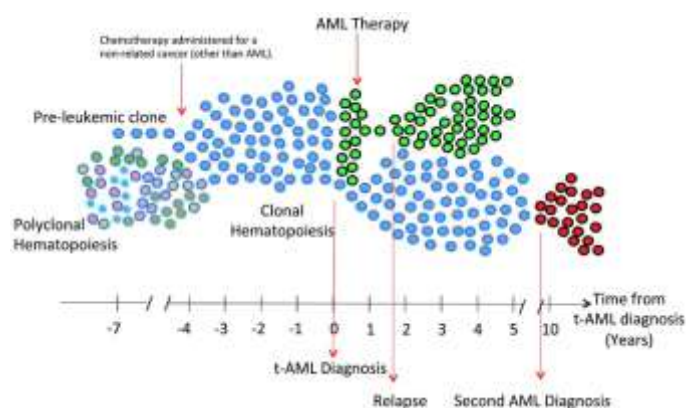
Patients with balanced chromosomal rearrangements such as the promyelocytic leukemia protein (PML) and retinoic acid receptor alpha translocation or inversion of chromosome 16 are commonly associated with favorable prognosis (REGO et al., 2013). The intermediate risk group of patients commonly comprehends AML with normal karyotype, while patients with monosomy 5 or 7, mutations in the *TP53*, and complex karyotype (three or more chromosomal abnormalities) constitute adverse risk patients (DÖHNER; PASCHKA, 2014; HAFERLACH et al., 2008; METZELER et al., 2016; PAPAEMMANUIL et al., 2016). Within this framework the identification of recurrent genetic abnormalities can improve prognostic-risk stratification. For instance, mutation in the fms-like tyrosine kinase 3 (*FLT3*) are frequent

and is considered as a driver mutation which can worsened the patient's clinical outcome (DÖHNER et al., 2017; KANTARJIAN et al., 2021). Hence, proper risk stratification of *de novo* AML patients will help to determine the best possible course of treatment. Nevertheless, the majority of AML patients relapse within the first 5 years after remission, frequently due to the clonal evolution of leukemic cells (KANTARJIAN et al., 2021).

### 1.7 AML clonal evolution

The term AML clonal evolution emerged in the last decade and roots in the idea that a common ancestral cell can give rise to different leukemic cells carrying different mutations known as subclones (MORITA et al., 2021). These data suggest that the AML bulk population is a highly heterogenous population and each cell presents different biological characteristics. Moreover, these differences become also apparent in patient derived xenograft models, whereby commonly only one clone is able to engraft probably due to intrinsic advantages compared to the other subclones injected (KLCO et al., 2014).

**Figure 5. AML Clonal evolution**



Evolutionary trajectory of leukemic clones and its clinical implications, haematologica. Adapted from Tuval et al., 2019. Representative picture depicting the process of AML clonal evolution frequently resulting in relapse.

For patients the presence of distinct subclones means an increased chance that some clones might be resistant to AML therapies and consequently survive and reemerge causing the patient to relapse (SHLUSH et al., 2017). As a result, it a better understanding of AML clonal evolution and patient-tailored therapies become ever so more necessary to prevent AML relapse and improve the clinical outcome of AML patients.





## 1.8 The tumor microenvironment in AML

In addition to the high intrinsic heterogeneity of leukemic cells within the bulk, it has become evident that much like healthy hematopoietic stem cells (HSC), leukemic stem cells (LSC) reside in bone marrow (BM) niches to ensure their survival, facilitate AML progression, and escape cytotoxic therapy (LANE; SCADDEN; GILLILAND, 2009; MORRISON; SCADDEN, 2014). Yet, it remains elusive whether mutations acquired in a permissive BM niche precede the emergence of AML or if a leukemia-supportive BM microenvironment is created upon expansion of a transformed HSC (KIM et al., 2015a, 2015b; VON DER HEIDE et al., 2017). Studies, which reinforce the former hypothesis but do not exclude the latter demonstrated that the deletion of *DICER1* in mesenchymal stem cells (MSC) or the activation of  $\beta$ -catenin in osteoblast can increase the chance of AML development (MORRISON; SCADDEN, 2014; RAAIJMAKERS et al., 2010). Concurrently, the expansion of leukemic cells can usurp the BM niche to form an immunosuppressive environment characterized by high levels of IL10, TGF $\beta$ , Arginase 1/2 and indoleamine 2,3-dioxygenase 1 (IDO1) (MÉNDEZ-FERRER et al., 2020; TURLEY; CREMASCO; ASTARITA, 2015; VON DER HEIDE et al., 2017) and dysfunctional/exhausted natural killer (NK) cells as well as T-cell subpopulations.

Other immune cells, which have been neglected in the context of hematological malignancies are macrophages or also known as tumor associated macrophages (TAM).

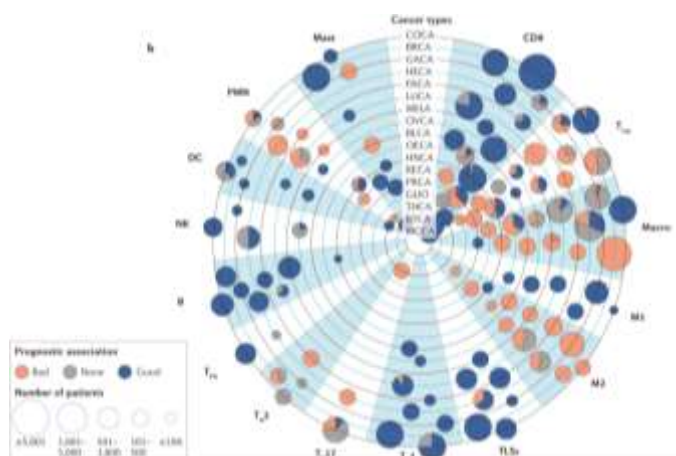
## 1.9 Tumor associated macrophages

Due to their high plasticity, macrophages can polarize to a wide range of distinct subtypes, which reaches well beyond the simplistic classification of M1 (anti-tumorigenic) and M2 (pro-tumorigenic) macrophages (BISWAS; MANTOVANI, 2010). At the extreme end of the scale M1 macrophages are characterized by a pro-inflammatory profile with the aim to kill pathogens and produce pro-inflammatory cytokines such as IL-1 $\beta$ , IL12 and TNF $\alpha$  (MEDREK et al., 2012). Conversely, M2 macrophages are anti-inflammatory engaged in anti-parasitic immune response, wound healing and neoangiogenesis (ITALIANI; BORASCHI, 2014). As a result, M2 macrophages secrete cytokines and growth factors such as IL-10, TGF $\beta$  and VEGF (ITALIANI; BORASCHI, 2014).

**Figure 6. Different macrophage subpopulations**

Scheme depicting different macrophage phenotypes across the spectrum of M1 and M2 macrophages. TNF; Tumor Necrosis Factor. IL-1 $\beta$ ; Interleukin 1 beta. IL12; Interleukin 12. IL10; Interleukin 10. Arg-1; Arginase 1. TGF $\beta$ ; Transforming Growth Factor Beta

Thanks to their inherent plasticity, instructive cues in form of cytokines, chemokines and growth factors elicited by surrounding cells will determine the type of macrophages within a given tissue. TAMs are frequently associated with M2-like features and the term M2-like encapsulates different macrophage subtypes found across and within tumors (MURRAY et al., 2014).

**Figure 7. The prognostic value of immune cells in cancer**

The immune contexture and Immunoscore in cancer prognosis and therapeutic efficacy. Adapted from Bruni et al., 2020. Representative picture depicting the prognostic value of different immune cells in different cancer types.

### 1.10 The role of macrophages in the BM during homeostasis and AML

Within the BM niche, macrophages can regulate the fate of HSC during homeostasis. In vivo macrophage depletion promotes increased mobilization of HSC by reducing *Cxcl12*, *Angpt1*, *Kit* and *Vcam1* expression in BM stromal cells (CHOW et al., 2011). Moreover, Hur

et al., revealed that CD234<sup>+</sup> macrophages can interact with CD82<sup>+</sup> long-term HSC to support quiescence in the endosteal region (HUR et al., 2016), while others identified erythroblastic island macrophages to promote erythropoiesis in the BM (CHOW et al., 2013; JACOBSEN et al., 2014). Thus, it is clear that the BM harbors diverse macrophage populations with many functions which can be exploited by LSCs. In this context, Mussai et al. detected increased ARG2 activity released from AML blast cells to promote M2-macrophage polarization and inhibit T-cell proliferation (MUSSAI et al., 2013). Moreover, Al-Matary et al. observed increased infiltration of monocytes/macrophages with pro-leukemogenic functions using AML murine models and identified the transcriptional repressor *Gfi1* to regulate M2 polarization (AL-MATARY et al., 2016). Finally, a recent single cell RNA (scRNA) sequencing study revealed that the heterogeneity of AML is not only inherent to the leukemic blast cell itself but extends to the stromal and immune cells within the BM (GUO et al., 2021). By sequencing 16 AML patients the authors identified ten distinct macrophage subpopulations where most were immunosuppressive.

### **1.11 The scope of this thesis**

Within this thesis, we uncover clear heterogeneity within the macrophage landscape across different AML patients. We show that this has clinical importance since the presence of M2-polarized macrophages in the bone marrow correlates with the poorest clinical outcomes. We have developed a novel biomarker panel with which patients with dismal prognosis can be identified. Our studies also provide mechanistic insight into the M2-macrophage mediated reprogramming of leukemic blasts into more aggressive leukemia initiating cells in vivo.

*Objectives*

---

## 2 OBJECTIVES

### 2.1 General objective

The overarching aim of the current thesis is to define and study the function of tumor associated macrophages in acute promyelocytic and myeloid leukemia *in vitro* and *in vivo*.

### 2.2 Specific objectives

1. Define different macrophage subtypes in AML bone marrow and healthy subjects by immunophenotypic analysis;
2. Detect the prognostic impact of M1 and M2 macrophages in AML;
3. Study the effect of different macrophage subtypes in AML *in vitro*;
4. Evaluate the phenotypic changes of macrophage after exposure to AML *in vitro*;
5. Determine whether the presence of specific macrophage subtypes can interfere with AML treatment;
6. Investigate the impact of macrophages on APL and AML leukemogenesis *in vivo* (isogenic and xenograft models);
7. Evaluate the changes induced by macrophages on AML on a transcriptional level;
8. Validate the findings of the RNA sequencing analysis.

## *Material and Methods*

---

### 3 MATERIAL AND METHODS

#### 3.1 Reagents

REAGENT or RESOURCE	SOURCE	IDENTIFIER
<b>Antibodies</b>		
Anti-Human CD45 FITC	BioLegend	368508
Anti-Human CD45 PE-Cy7	BioLegend	304016
Anti-Human HLA-DR PE	BioLegend	980416
Anti-Human CD14 PercP Cy5	BioLegend	301848
Anti-Human CD16 APC-Cy7	BioLegend	302018
Anti-Human CD163 PE-Cy7	BioLegend	333614
Anti-Human CD206 BV421	BD Biosciences	564062
Anti-Human CD80 APC	BioLegend	305220
Anti-Human CD47 PE	BD Biosciences	556046
Anti-Human CD33 PE	BD Biosciences	561816
Anti-Human CD117 APC	BD Biosciences	550412
Anti-Human CD34 eFluor 450	eBiosciences	48-0341-82
Anti-Human CD11b FITC	Immunotools	21279113X2
Anti-human CD11 Alexa Fluor 594	BioLegend	101254
Annexin FITC	Immunotools	31490013X2
Annexin APC	Immunotools	31490016X2
Anti-Human CD49d PE	BioLegend	304304
Anti-Human CD49e PE	BioLegend	328010
Anti-Human CD49f PE	BioLegend	313612
Anti-Human CD47 PE	BD Biosciences	556046
Anti-Human CD24 PE	BioLegend	311106
Anti-Mouse Gr1 APC	BioLegend	108412
Anti-Mouse CD117 APC-Cy7	BioLegend	105826
Anti-Mouse CD16/32 FITC	BioLegend	101306
Anti-Mouse CD34 PE-Cy7	BioLegend	128618
Anti-Mouse CD45.1 PE	BioLegend	110708
Anti-Mouse CD45.2 FITC	BioLegend	109806
Anti-Human CD68 (IHC)	DAKO	PG-M1
Anti-Human CD163 (IHC)	Ventana	MRQ-26
<b>Bacterial and virus strains</b>		
<b>Biological samples</b>		
Human AML blast cells	UMCG/USP	Ethical committee NL43844.042.13
Human APL blast cells	UMCG/USP	Ethical committee #13496/2005
Murine hCG-PML-RARa blast cells	USP	Ethical committee #176/2015
HSC from C57/BL6 mice	USP	Ethical committee #176/2015
<b>Chemicals, peptides, and recombinant proteins</b>		
Propidium Iodide	ThermoFisher	P1304MP



4',6-diamidino-2-phenylindole	Sigma-Aldrich	28718-90-3
Paraformaldehyde	Sigma-Aldrich	30525-89-4
RNAse		
Dnase I	Roche	11284932001
MgSO4	Sigma-Aldrich	M7506
Heparin		
Arsenic Trioxide	Sigma-Aldrich	1327-53-3
All Trans Retinoic Acid	Sigma-Aldrich	302-79-4
Midostaurin	Sigma-Aldrich	M1323
Quizartinib	Selleckchem	S1526
Venetoclax	Selleckchem	S8048
Etomoxir	MedChemExpress	HY-50200
Tocilizumab (Actemra/RoActemra)	Roche	
Human Granulocyte-macrophage colony-stimulating factor	Peprotech	300-03
Human Macrophage Colony-Stimulating Factor	Immunotools	11343117
Human Interleukin 6	Peprotech	200-06
Human Interferon Gamma	Peprotech	300-02
Human Interleukin 3	Peprotech	200-03
Human Granulocyte colony-stimulating factor	Peprotech	300-23
Human Thrombopoietin	Amgen	
Lipopolysaccharides	Sigma-Aldrich	L4391
Carboxyfluorescein succinimidyl ester	BioLegend	423801
Incucyte® Cytolight Rapid Red Dye	Sartorius	4706
Hydrocortisone	Sigma-Aldrich	50-23-7
β-mercaptoethanol	Merck Sharp & Dohme BV	60-24-2
SsoAdvanced Universal SYBR® Green Supermix	BioRad	1725274
iScript cDNA synthesis Kit	BioRad	1708891BUN
Tetramethylrhodamine, Ethyl Ester, Perchlorate	Thermofisher	T669
MitoTracker DeepRed™	Thermofisher	M22426
MitoTracker Green™	Thermofisher	M7514
<b>Critical commercial assays</b>		
Seahorse XFe96 Flux Analyzer	Agilent	
<b>Experimental models: Cell lines</b>		
MOLM-13	DSMZ	ACC 554
MV4-11	ATCC	CRL-9591™
HL60	ATCC	CCL-240™
OCI-AML3	DSMZ	ACC 582
NB4	Harvard Medical School	Prof. Pier Paolo Pandolfi
NB4-R2	Harvard Medical School	Prof. Pier Paolo Pandolfi
MS-5	DSMZ	ACC 441
HS27A	ATCC	CRL-9591™
L929*	ATCC	CCL-1™
HEK293T	ATCC	CRL-3216

<b>Experimental models: Organisms/strains</b>		
NSGS (NOD.Cg-Prkdcscid Il2rgtm1 Wjl Tg (CMV-IL3,CSF2,KITLG)1Eav/MloySzJ)	Jackson Laboratory	013062
NSG (NOD.Cg-Prkdcscid Il2rgtm1 Wjl/SzJ)	Jackson Laboratory	005557
C57BL/6J	Jackson Laboratory	000664
B6.SJL-Ptprca Pepcb/BoyJ	Jackson Laboratory	002014
<b>Oligonucleotides</b>		
Staniocalcin 1 Forward primer	Eurofins	TGCTAAATTTGACA CTCAGGGAAA
Staniocalcin 1 Reverse primer	Eurofins	ACCTCAGCAATCAT CCTTTGG
HPRT1 Forward primer	Eurofins	GAACGTCTTGCTCG AGATGTGA
HPRT1 Reverse primer	Eurofins	TCCAGCAGGTCAGC AAAGAAT
ACTB Forward primer	Eurofins	AGGCCAACCGCAA GAAG
ACTB Reverse primer	Eurofins	ACAGCCTGGATAGC AACGTACA
RPL30 Forward primer	Eurofins	ACTGCCCAGCTTTG AGGAAAT
RPL30 Reverse primer	Eurofins	TGCCACTGTAGTGA TGGACAC
<b>Recombinant DNA</b>		
<b>Software and algorithms</b>		
FlowJo v10.0.6	Treestar	<a href="http://www.flowjo.com/">http://www.flowjo.com/</a>
Prism 9	GraphPad	<a href="http://www.graphpad.com/">http://www.graphpad.com/</a>
SPSS Statistical package 19.1	IBM	<a href="https://www.ibm.com/">https://www.ibm.com/</a>
Wave	Agilent	<a href="https://www.agilent.com/">https://www.agilent.com/</a>
RStudio	CRAN	<a href="http://www.r-project.org">www.r-project.org</a>
GSEA 4.0.1	Broad Institute	<a href="https://software.broadinstitute.org/gsea/">https://software.broadinstitute.org/gsea/</a>
Cytoscape 3.4		<a href="http://apps.cytoscape.org/apps/bingo">http://apps.cytoscape.org/apps/bingo</a>
<b>Other</b>		
FcR Blocking reagent, human	Miltenyi Biotec	130-059-901
CD34 MicroBeads Kit UltraPure, Human	Miltenyi Biotec	130-100-453
CD117 MicroBeads Kit, Human	Miltenyi Biotec	130-091-332
CD3 MicroBeads, Human	Miltenyi Biotec	130-050-101
Streptavidin MicroBeads	Miltenyi Biotec	130-048-102
TrypLE™ Express Enzyme	Thermo Fischer Scientific	12604021
MethoCult™	Stemcell	H4435
KAPA RNA HyperPrep Kit with RiboErase (HMR)	Roche	08098131702

## 3.2 Patient analysis

### 3.2.1 Human sample collection and patient information

Bone marrow samples of APL patients used in for in vivo experiments were studied after informed consent and protocol approval by the Ethical Committee in accordance with the Declaration of Helsinki (registry #12920; process number #13496/2005; CAAE: 155.0.004.000-05 and CAAE: 819878.5.1001.5440; Supplemental document A and B, respectively). Mononuclear cells (MNCs) were isolated via Ficoll (Sigma-Aldrich) separation and cryopreserved. Peripheral blood (PB) and bone marrow (BM) samples of AML patients were studied after informed consent and protocol approval by the Medical Ethical committee of the UMCG in accordance with the Declaration of Helsinki. An overview of patient characteristics can be found in Table 1. Neonatal cord blood (CB) was obtained from healthy full-term pregnancies from the Obstetrics departments of the University Medical Center and Martini Hospital in Groningen, The Netherlands, after informed consent. The protocol was approved by the Medical Ethical Committee of the UMCG. Donors are informed about procedures and studies performed with CB by an information sheet that is read and signed by the donor, in line with regulations of the Medical Ethical Committee of the UMCG (protocol #NL43844.042.13). Peripheral blood mononuclear cell derived CD34<sup>+</sup> stem cells (PBMSCs) and CB derived CD34<sup>+</sup> cells were isolated by density gradient separation, followed by a hematopoietic progenitor magnetic associated cell sorting kit from Miltenyi Biotec (#130-046-702) according to the manufacturer's instructions. All CD34<sup>+</sup> healthy cells were pre-stimulated for 24-48hrs prior to experimental use. CB derived cells were pre-stimulated with Stemline II hematopoietic medium (SigmaAldrich; #S0192), 1% penicillin/streptomycin (PS) supplemented with SCF (255-SC, Novus Biologicals), Flt3 ligand (Amgen) and N-plate (TPO) (Amgen) (all 100 ng/ml). PBMSC CD34<sup>+</sup> cells were pre-stimulated with Stemline II, 1% PS, 20% FCS along with SCF, Flt3 ligand, N-plate (all 100 ng/ml) and IL-3 (Sandoz) and IL-6 (both 20 ng/ml). Primary AMLs were grown on MS5 stromal cells with G-CSF (Amgen), N-Plate and IL-3, all 20 ng/ml.

### 3.2.2 Flow cytometry

Cryopreserved MNC fractions of AML/APL patients were thawed, resuspended in newborn calf serum (NCS) supplemented with DNase I (20 Units/mL), 4  $\mu$ M MgSO<sub>4</sub> and

heparin (5 Units/mL) and incubated at 37°C for 15 minutes (min). To analyze the myeloid fraction of the AML/APL bulk sample,  $5 \times 10^5$  mononuclear cells were blocked with human FcR blocking reagent (Miltenyi Biotec) for 5 min and stained with the following antibodies: CD45-FITC, HLA-DR-PE, CD14-PerCP, CD16-APC-Cy7, CD163-Per-Cy7, CD206-BV421 and CD80-APC for 20 min at 4°C. A more mature myeloid population was detected based on the CD45 staining and inside this gate HLA-DR positive cells were selected to analyze the CD14 versus CD16 cellular distribution. The different CD14/CD16 populations (CD14<sup>+</sup>/CD16<sup>-</sup>; CD14<sup>+</sup>/CD16<sup>+</sup>; CD14<sup>-</sup>/CD16<sup>+</sup>) were then analyzed for their expression of the M1 marker CD80 and the M2 markers CD163 and CD206. Fluorescence was measured on the BD LSRII or FACS CantoII and analyzed using Flow Jo (Tree Star, Inc). For each sample a minimum of 5000 events were acquired inside the SSC-A<sup>high</sup> CD45<sup>high</sup> HLA-DR<sup>+</sup> population.

### 3.2.3 Immunohistochemistry

Tissue sections were cut from formalin fixed embedded BM biopsies of AML patients at diagnosis. CD68 and CD163 were visualized by the Ventana Benchmark Ultra automated slide stainer, after antigen retrieval (Ultra CC1, Ventana Medical Systems), using monoclonal antibodies CD68 (PG-M1, 1:100, Dako) and CD163 (MRQ-26, ready to use, Ventana) and Ultraview (Ventana). Digital images of these slides were scored for percentage of positively staining bone marrow cells.

### 3.2.4 CIBERSORT analysis

Relative immune cell fractions were estimated using the CIBERSORT, quantIseq, xCell, MCP-counter and EPIC algorithms, based on several reference expression signatures that distinguish at maximum 64 immune cell subtypes. Briefly, normalized gene expression data were uploaded to the TIMER2.0 web portal ([http:// timer.cistrome.org/](http://timer.cistrome.org/)), with the data matrices prepared according to the example. After 1000 permutations, only samples with p-values < 0.05 were included in subsequent analyses. Kruskal-Wallis were applied to identify immune subpopulations that were differentially enriched between the different AML patients, controlling for the false discovery rate (FDR) by the Benjamini–Hochberg method (FDR < 0.05).

### 3.2.5 Clinical endpoint analysis

Survival analyzes were performed in AML patients treated with intensive chemotherapy (3+7 scheme) as an induction protocol (BEZERRA et al., 2020). According to survival receiver operating characteristic (ROC) curve analysis, the median value of M1 and M2 macrophage markers in the myeloid mature compartment (defined by  $SSC^{\text{high}}CD45^{\text{high}}HLA-DR^+$ ) expression was used to dichotomize patients into two groups (i.e., low infiltration, percentage of M1- and M2-macrophages; high infiltration, percentage of M1- and M2-macrophages). Overall survival was defined as the time from diagnosis to death from any cause related to the disease; those alive or lost to follow-up were censored at the date last known alive. For patients who achieved complete remission (CR), disease-free survival (DFS) was defined as the time from CR achievement to the first adverse event: relapse, development of secondary malignancy, or death from any cause, whichever occurred first. Univariate and multivariate proportional hazards regression analysis was performed for potential prognostic factors for overall survival (OS). Potential prognostic factors examined and included in multivariable regression analysis were ELN2017 risk stratification, age at diagnosis (analyzed as continuous variable), and our proposed clusterization regarding the macrophage content. Proportional hazards (PH) assumption for each continuous variable of interest was tested. Linearity assumption for all continuous variables was examined in logistic and PH models using restricted cubic spline estimates of the relationship between the continuous variable and log relative hazard/risk. Descriptive analyses were performed for patient baseline features. Fisher's exact test or Chi-square test, as appropriate, was used to compare categorical variables. Kruskal-Wallis test was used to compare continuous variables. Details of the statistical analysis and clinical endpoints were described elsewhere. All P values were two sided with a significance level of 0.05. All statistical analyses were performed using the statistical package for the social sciences (SPSS) 19.0 and R 3.3.2 (The CRAN project, [www.r-project.org](http://www.r-project.org)) software.

### 3.3 Cell lines

All cell cultures were maintained in a humidified atmosphere at 37°C with 5% CO<sub>2</sub>. NB4 (all-trans retinoic acid, ATRA-sensitive) and NB4-R2 (ATRA-resistant) cell lines were kindly provided by Dr. Pier Paolo Pandolfi (Harvard Medical School, USA), and maintained in RPMI 1640 (Gibco, USA) supplemented with 10% fetal bovine serum (FBS) (Gibco, USA), L-glutamine (2 mM), 1% penicillin/streptomycin (PS, Invitrogen, USA). Mycoplasma

contamination was routinely tested. All leukaemia cell lines were authenticated by short tandem repeat analysis. The HEK293T (CRL-3216), HS27A (CRL-2496), HL-60 (CCL-240™) and MV4-11 (CRL-9591™) cell lines were obtained from the American Type Culture Collection and grown in DMEM (for HEK293T and HS27A; Gibco, USA) or RPMI (for U937; Gibco, USA) with 10% FBS. The MOLM13 (ACC 554) and OCI-AML3 (ACC 582) cell lines were obtained from the DSMZ-German Collection of Microorganisms and Cell Cultures. All-trans retinoic acid (ATRA), Midostaurin (PKC), and arsenic trioxide (ATO) were obtained from Sigma-Aldrich (St. Louis, USA) and cytarabine (citarax) was obtained from Blau pharmaceuticals (Sao Paulo, Brazil). Venetoclax (VEN) and quizartinib (AC220) were obtained from Selleckchem (Houston, USA). Etomoxir was obtained from MedChemExpress (Groningen, NL).

### **3.4 Macrophage isolation and generation**

#### **3.4.1 Human and murine macrophages generation**

For human macrophage in vitro generation peripheral blood was obtained from healthy donors or allogeneic donors. Mononuclear cells were isolated by a density gradient using Ficoll (Sigma-Aldrich). Next,  $2.5 \times 10^6$  or  $5 \times 10^6$  mononuclear cells were then seeded into 12 or 6-well plates and incubated for 3h at 37°C in RPMI medium supplemented with 10% FBS, 10% heat inactivated and filtered human serum (AB serum, Thermofisher) and 1% penicillin and streptomycin (PS) to allow adherence of monocytes to the tissue plate. After 2h of incubation, the non-adherent cell fraction was removed, and the new RPMI medium supplemented with 10% FBS, 10% human serum and 1% penicillin and streptomycin was added. Additionally, 50 ng/mL of GM-CSF (Preprotech) or M-CSF (Preprotech/Immunotools) growth factors were added to the medium to generate pre-orientated M1 and M2 macrophages, respectively. Monocytes were differentiated into macrophages over a time span of 6 days and at day 3 half of the medium was renewed (with the proper cytokines for each subtype).

To generate murine macrophages mice were anesthetized with an overdose of ketamine/xylazine solution and sacrificed by cervical dislocation to collect femur and tibia. Next the epiphyses were cut off and a syringe of 25 G filled with PBS (1% FBS) was used to flush the bone marrow onto a 70  $\mu$ M cell strainer placed on a 50 ml tube. Red blood cells were lysed for 10 min at 4°C and washed with PBS. Three million bone marrow mononuclear cells

were seeded in a 100x20 mm petri dish and cultured in RPMI medium supplemented with 10% FBS, 15% of L929 supernatant and 1% PS for 7 days. At day 3 half of the medium was renewed.

### **3.4.2 Human and murine macrophages polarization**

Human macrophages were polarized at day 6 into their respective subtype. Cells were washed with PBS and new RPMI medium supplemented with 10% FBS was added. GM-CSF cultured macrophages were polarized to M1 macrophages with 20 ng/ml IFN- $\gamma$  (Peprotech) and 100 ng/ml LPS (Sigma-Aldrich), while M-CSF cultured macrophages were polarized to M2d macrophages with 10 ng/ml M-CSF and 20 ng/ml IL-6 (Peprotech). To generate M0 macrophages, MCSF cultured macrophages were kept with 50 ng/mL of M-CSF in the medium.

Murine macrophages were polarized at day 6 into their respective subtype. Cells were washed with PBS and new RPMI medium supplemented with 10% FBS and 1% PS was added. M-CSF cultured macrophages were polarized to M2d macrophages with 20 ng/mL IL-6 (Peprotech). M0 macrophages were generated by adding new RPMI medium supplemented with 10% FBS, 15% of L929 supernatant and 1% PS.

### **3.4.3 FACS staining of macrophages**

After polarization, macrophages are detached with TrypLE (ThermoFisher) according to manufacturer's instructions. A total of  $1 \times 10^5$  cells were washed in PBS and resuspended in PBS (2 mM EDTA, 2% BSA, 0.02%  $\text{NaN}_3$ ) and 10  $\mu\text{L}$  FcR blocking reagent. Macrophages were incubated 30 min at 4°C. Fluorescence was measured on the BD LSRII or FACS CantoII and analyzed using Flow Jo (Tree Star, Inc). For each sample a minimum of 10 000 viable cells (DAPI negative events) were acquired.

### **3.5 Cord blood CD34 isolation**

Peripheral blood mononuclear cells were isolated by a density gradient using Ficoll (Sigma-Aldrich) from cord blood. Mononuclear cells were washed once at 450g with PBS-EDTA (5 mM) and resuspended in 300  $\mu\text{L}$  of PBS. Next, 100  $\mu\text{L}$  of FcR blocking reagent and 100  $\mu\text{L}$  of CD34 MicroBeads (Miltenyi Biotech) were added to the suspension and incubated for 30 min at 4°C. After incubation cells were washed for 10 min at 450g and resuspended in 2 mL of PBS-EDTA (5 mM). Cells were passed through a cell strainer (70  $\mu\text{M}$ ) and isolated by

magnetic separation on the autoMACS (Program – Possedels, Miltenyi Biotech). The purity of the isolated cells was routinely evaluated by FACS and in the range of 85% to 95%.

### **3.6 *In vitro* co-culture**

#### **3.6.1 *In vitro* AML cell line proliferation on macrophages**

Human macrophages were generated and polarized as described in the sections “Macrophage generation” and “Macrophage polarization”. A total of  $3 \times 10^4$ /mL AML cells (NB4, NB4-R2, OCI-AML3, HL60, MOLM13, MV4-11) were put in co-culture with M1 and M2d macrophages. The co-cultures were performed in RPMI supplemented with 10% fetal bovine serum and 1% PS, except for OCI-AML3 co-cultures, which were performed in Alpha-MEM ( $\alpha$ -MEM) 20% fetal bovine serum and 1% PS. The proliferation rate was assessed by daily cell counts with a hemocytometer and by FACS (LSRII) for a total period of 7 days.

#### **3.6.2 *In vitro* primary CB CD34 and AML cell proliferation on macrophages**

Human macrophages were generated and polarized as described in the sections “Macrophage generation” and “Macrophage polarization”. Cryopreserved MNC fractions of AML patients were thawed as described in the section “Patient analysis by flow cytometry”. CD34<sup>+</sup> cells were isolated from cord blood or primary AML patients on the autoMACS using a magnetically activated cell-sorting progenitor kit (Miltenyi Biotech). In case of NPM1 mutated AMLs with CD34 expression <1% and APL samples, the CD117<sup>+</sup> blast cells were isolated.

A total of  $2 \times 10^5$ - $1 \times 10^6$  primary CB CD34<sup>+</sup>/AML or APL cells (CD117<sup>+</sup>) were cultured on distinct macrophage subtypes and on MS-5/HS27A as a control, for a period of 10 days. HS27A/MS-5 cells were plated on gelatine coated culture flasks and expanded to form a confluent layer (above 70% of confluence). The co-cultures were performed in Gartner’s medium consisting of  $\alpha$ -MEM (Thermo Scientific) supplemented with 12.5% fetal bovine serum (Gibco), 12.5% horse serum (Gibco), 1% penicillin and streptomycin, 2 mM glutamine (Gibco), 57.2 mM  $\beta$ -mercaptoethanol (Merck Sharp & Dohme BV), and 20 ng/mL G-SCF, TPO and IL-3. Co-cultures were grown at 37°C and 5% CO<sub>2</sub> and demi-populated after counting if necessary. Cell proliferation was assessed with a hemocytometer until 14 days of co-culture.



Cell differentiation was assessed by FACS using the CD11b, CD14, CD15, CD34, and CD117 as markers of myeloid differentiation.

### **3.6.3 Generation of conditioned medium and *in vitro* primary AML culture**

Conditioned medium was collected 24h after macrophage polarization as described in the “Human macrophage polarization” section and stored at -80°C until usage. Conditioned medium was only used once after thawing. MS-5 cells were seeded in a gelatin coated 12-well plate and expanded to form a confluent layer. Next,  $2.5 \times 10^5$  primary AML cells were added to the MS5 cells and cultured in 750  $\mu$ L of Gartner’s medium and 750  $\mu$ L of either M1 or M2d macrophage polarization medium to reach a total volume of 1.5 mL. The cytokines G-CSF, TPO and IL-3 were added at a concentration of 20 ng/mL. Co-cultures were grown at 37°C and 5% CO<sub>2</sub> and semi-populated after counting if necessary. Cell proliferation was assessed with a hemocytometer until 10 days of co-culture.

### **3.6.4 Cell cycle**

Cell cycle phases of AML cell lines cultured for 4 days on distinct macrophage subtypes were determined by the BD Cycletest™ Plus DNA Reagent Kit (Becton-Dickinson) according to the manufacturer’s instructions. DNA content distribution was measured with the BD LSRII (Becton-Dickinson) and analysed using FlowJo (Treestar, Inc., USA).

### **3.6.5 Apoptosis assay**

For the apoptosis analysis a minimum of  $1 \times 10^5$  AML cells were stained after 7 days of culture on M1, M2d macrophages or alone (control). The apoptosis rate was determined using the Annexin V-FITC antibody and DAPI as a viability dye. All specimens were acquired by flow cytometry (BD LSRII) and analysed with the FlowJo software (Treestar, Inc., USA). All experiments were performed in triplicate and for each sample a minimum of 10 000 events were acquired.

### **3.6.6 Apoptosis assay drug screen in the presence of M2-macrophages**

Drug screen assays were performed using the co-culture systems employing AML cell lines (NB4, MOLM-13 and MV4-11) and M1- or M2-macrophages, and MS-5 cells as a

control. A total of  $5 \times 10^4$  AML cells were seeded in 24 well plates containing M1 and M2 macrophages, and MS5 cells and incubated in complete medium for 72 hours in the presence of vehicle, ATO (1  $\mu$ M), ATRA (1  $\mu$ M), venetoclax (dose range: 1000 to 5000 nM), midostaurin (PKC, dose range: 40-100 nM) and quizartinib (AC220, dose range: 40 to 100 nM). To evaluate the role of IL-6, AML cells were incubated with M1 macrophages or MS-5 cells in the presence of 20 ng/mL of IL6. Complementary, AML lines were incubated with M2d macrophages or MS-5 cells and cultured in the presence of the IL-6R $\alpha$  monoclonal antibody, Tocilizumab (TCZ, 2 ng/mL, Roche). The apoptosis rate was determined using the Annexin V-APC and DAPI binding assay (BD Biosciences, San Jose, CA, USA). For ATRA treatment, the differentiation rate was determined by evaluating the number of CD11b cells (percentage and MFI levels). All specimens were acquired by flow cytometry (FACSCantoII; Becton-Dickison) and analyzed with the FlowJo software (Treestar, Inc., USA). All experiments were performed in triplicate and for each sample a minimum of 10 000 events were acquired.

### **3.7 *In vivo* intra-BM APL patient derived xenotransplant (PDX) model**

#### **3.7.1 Animal welfare**

All animals were housed under specific pathogen free conditions in individually ventilated cages during the whole experiment. The animals were maintained according to the Guide for Care and Use of Laboratory Animals of the National Research Council, USA, and to the National Council of Animal Experiment Control recommendations. All experiments were approved by the Animal Ethics Committee of the University of São Paulo (protocols #176/2015 and #095/2018).

#### **3.7.2 *In vivo* intra-BM APL patient derived xenotransplant (PDX) model**

Human macrophages were generated and polarized as described in the sections “Macrophage generation” and “Macrophage polarization”. Macrophages were then detached with TrypLE and washed 2 times with PBS at 450g. Macrophages were stained with DAPI, HLA-DR and CD206 to confirm viability and the subtype of macrophage generated. Macrophages were resuspended in PBS at a working concentration of  $1 \times 10^5/10 \mu$ L. Eight to ten weeks old female NSGS (NOD.Cg-Prkdcscid Il2rgtm1Wjl Tg(CMV-IL3,CSF2,KITLG)1Eav/MloySzJ) mice were anesthetized and 25 mg/Kg of Tramadol was

injected subcutaneously. The intra-tibial injection of macrophages was performed according to the percutaneous approach (PARK et al., 2010). In summary, under anesthesia through a nose cone the mouse was placed in a supine position and the pre-shaved knee was cleaned with 70% ethanol and maintained in a flexed position. A 30 G needle was placed percutaneously through the knee joint and inserted by rotating the syringe. Once the BM space was reached, 10  $\mu$ L were of the BM were aspirated (to free BM space). Next, 10  $\mu$ L of macrophages corresponding to 100 000 cells in total were injected into the BM with a new needle. M0 macrophages were injected into the left tibia, while M2d macrophages were injected into the right tibia. Control mice received 10  $\mu$ L of PBS. On the next day, six different cryopreserved MNC fractions of APL patient samples were thaw as described in the section “Flow cytometry” (clinical characteristics in Supplemental table 1) and depleted for CD3<sup>+</sup> cells. Next, 1x10<sup>6</sup> primary APL cells were injected via the retro-orbital sinus into macrophage recipient and control mice. Human CD45<sup>+</sup> levels were measured regularly in blood obtained by sub-mandibular bleeding. Twelve weeks post-transplant mice were sacrificed, and each leg of the macrophage recipient mice was processed separately. Cells from BM, spleen, and spine were collected and stained for human CD45, CD11b, HLA-DR, CD33 and CD117 to detect human APL blast cells (CD45<sup>+</sup>CD33<sup>+</sup>CD117<sup>+</sup>CD11b<sup>-</sup>HLA-DR<sup>-</sup> cells). All specimens were acquired by flow cytometry (FACS CantoII) and analysed with the FlowJo software (Treestar, Inc., USA). For each sample a minimum of 20 000 viable events were acquired. In addition, cytospin preparations stained with May-Grünwald-Giemsa (MGG) were used to evaluate the morphology of human APL blasts.

### **3.8 *In vivo* pre-culture models**

#### **3.8.1 *In vivo* pre-culture APL PDX model**

Human macrophages were generated and polarized as described in the sections “Macrophage generation” and “Macrophage polarization” in 6-well plates. APL patient samples were thaw as described in the section “Flow cytometry” (clinical characteristics in Supplemental table 1) and depleted for CD3<sup>+</sup> cells. In total 5x10<sup>6</sup> APL cells were put in co-culture per well for 48 hours. The co-cultures were performed in Gartner’s medium. After 48 hours, suspension cells were collected and washed 2x with PBS. Primary APL blast cells were counted and 1x10<sup>5</sup> APL cells exposed to macrophages were set aside to evaluate the purity of these cells to ensure no macrophage contamination. Next, 1.5x10<sup>5</sup> APL cells were injected via

the retro-orbital sinus into 8 to 10 weeks old female NSGS (NOD.Cg-Prkdcscid Il2rgtm1Wjl Tg (CMV-IL3, CSF2, KITLG)1Eav/MloySzJ) mice. For control mice the respective paired APL sample, which was used for co-culture was thaw as described in the section “Flow cytometry” and depleted for CD3<sup>+</sup> cells. A total of  $1 \times 10^6$  cells were transplanted via the retro-orbital sinus directly after thawing and the rest of the cells were put in co-culture with primary human mesenchymal stromal cells for 48 hours. The same culture conditions were applied as for the macrophage co-culture. After 48 hours cells were collected and counted to inject 200-350 000 APL blast cells via the retro-orbital sinus. Monitoring of APL engraftment and evaluation of APL blast infiltration post-sacrifice was executed as described in the section “In vivo intra-BM APL PDX model”.

### 3.8.2 In vivo Long-Term Culture Initiating Cell assay

Engrafted primary APL blast cells, which were pre-cultured on M2d macrophages and induced fatal leukemia were sorted post-sacrifice based on the human markers CD45, CD33 and CD117. Sorted APL blast cells from primary transplant were then transplanted via the retro-orbital sinus in secondary mice at different cell dosage:  $1 \times 10^3$ ,  $1 \times 10^5$  and  $1 \times 10^6$ . Control mice received different cell dosage as well:  $5 \times 10^6$ ,  $1 \times 10^6$  and  $5 \times 10^5$  of APL samples at diagnosis. The frequency of leukemic initiating stem cells was calculated with the ELDA software (WIERENGA et al., 2006).

### 3.8.3 Murine in vivo pre-culture

Murine macrophages were generated and polarized in 20x100 petri dishes as described in the section “Macrophage generation” and “Macrophage polarization. Murine primary APL blasts were collected from hCG-PML-RARA mice (CD45.2 background), which developed APL. Once macrophages were polarized, the macrophages were washed and new RPMI supplemented with 10% FBS was added. Murine APL blast cells were then thaw as described in the section “Flow cytometry” and  $5-10 \times 10^6$  were put in co-culture for 48h. After 48 hours, suspension cells were collected and washed 2x with PBS. Murine APL blast cells were counted and  $1 \times 10^5$  APL cells exposed to macrophages were set aside to evaluate the purity of these cells to ensure no macrophage contamination. Next,  $1.5 \times 10^5$  murine APL cells were injected via retro-orbital sinus into sub-lethally irradiated (350 cGy) C57BL/6J. PepBoy recipients (CD45.1). For control mice the respective paired murine APL sample, which was used for co-

culture was thaw and a total of  $1 \times 10^6$  cells were transplanted via the retro-orbital sinus directly after thawing. Chimerism levels were evaluated by measuring the CD45.2 marker by flow cytometry in blood obtained by sub-mandibular bleeding. Mice were followed for overall survival analysis and sacrificed when tumor reached ethical limits (>90% engraftment) or mice showed severe signs of illness. At the end of the experiment, animals were harvested, and the bone marrow was analyzed for the presence of early and late promyelocytes defined by CD34 and CD16/32 (CD34<sup>+</sup>CD16/32<sup>+</sup>, Early Pro/CD34<sup>-</sup>CD16/32<sup>+</sup>, Late Pro) inside the population of lineage negative cells (lineage markers defined by CD3e, CD19, B220, Ter119, NK1.1, CD4, and CD8) positive for CD117 and Gr1intermediate (GAILLARD et al., 2018; WEINHÄUSER et al., 2020).

### **3.9 *In vitro* phagocytosis**

#### **3.9.1 *In vitro* phagocytosis**

Human macrophages were generated and polarized as described in the sections “Macrophage generation” and “Macrophage polarization”. Macrophages, which were generated in a 6 well plate were detached with TrypLE and  $1 \times 10^4$  macrophages were seeded in a flat-bottom 96 well plate to reach a confluence of approximately 80%. Macrophages were then incubated overnight to allow adherence to the plate. Cryopreserved MNC fractions of AML cells were thaw and CD3<sup>+</sup> depleted. For the phagocytosis at day 0, a total of  $1 \times 10^5$  AML cells were washed 2x in serum free medium at 450g for 5 min, resuspended in 100  $\mu$ L and stained with 1  $\mu$ L of Incucyte® Cytolight Rapid Red Dye (0.33  $\mu$ M) or CSFE (concentration, ThermoFisher). Cells were incubated for 20 min at 37°C and washed 2x with medium supplemented with serum. A total of  $5 \times 10^4$  were co-cultured with macrophages in a 96-well plate and incubated for 3h at 37°C and 5% CO<sub>2</sub>. After 3h of incubation AML cells were gently removed by washing with PBS 3x times. To visualize macrophages, residual cells were stained with CD11b-FITC (1  $\mu$ g/mL) (when AML cells labeled with incucyte red dye) or CD11b-AF594 (1  $\mu$ g/mL) (when AML cells labeled with CSFE) 30 min at room temperature in the dark. After 30 min macrophages were fixed with 2% paraformaldehyde and three pictures of randomly chosen fields of view were taken by the EVOS Cell Imaging System (ThermoFisher). The percentage of phagocytosis was equal to the number of macrophages containing labeled AML cells per 100 macrophages. For phagocytosis at day 2, a total of  $5 \times 10^5$  -  $1 \times 10^6$  AML cells were put in co-culture with either M2d macrophages or MS-5 cells seeded in a 12 well plate for

48h. The co-cultures were performed in Gartner's medium. After 48h of co-culture, AML cells were collected, and a phagocytosis assay was performed as described above. In addition to the phagocytosis assay, primary AML cells were stained for CD47 and CD24 at diagnosis and after two-day co-culture on M2d and MS5. All specimens were acquired by flow cytometry (BD LSR II) and analysed with the FlowJo software (Treestar, Inc., USA). For each sample a minimum of 10 000 events were acquired.

### **3.9.2 Confocal immunofluorescence microscopy for calreticulin and staniocalcin-1**

AML cells (primary AML blasts and AML cell lines) co-cultured with M2d macrophages and MS-5 cells for 48 hours were attached to cover slips coated with poly-L-lysine (1 mg/ml), fixed with 4% paraformaldehyde, permeabilized with 0.5% Triton X-phosphate-buffered saline (PBS) and blocked with 3% bovine serum albumin (BSA) PBS. Cells were incubated overnight at 4°C with anti-CLR (1:200 in 3% BSA PBS; PA3-900; ThermoFisher, USA), anti-STC1 (1:200 in 3% BSA PBS; Ab83065; Abcam, USA), followed by incubation with secondary antibody anti-mouse DyLight® 594 and anti-rabbit DyLight® 647 (1:1,000 in 3% BSA PBS, Life Technologies, CA, USA) for 2 hours at room temperature. All incubations were followed by two PBS washes. The slides were mounted in ProLong Diamond Anti-Fade Mounting Medium with DAPI (Life Technologies, CA, USA). Images were generated using a confocal laser-scanning microscope (LSM 510, Carl Zeiss, Welwyn Garden City, UK).

### **3.10 Oxygen consumption (OCR) and extracellular acidification rate (ECAR) measurements**

Oxygen consumption rate (OCR) and Extra Cellular Acidification Rate (ECAR) were measured using Seahorse XF96 analyzer (Seahorse Bioscience, Agilent, US) at 37 °C. For AML cell lines (CD45<sup>+</sup> cells) and sorted CD34<sup>+</sup> or CD117<sup>+</sup> from primary AML patients, 1x10<sup>5</sup> and 2x10<sup>5</sup> viable cells (DAPI<sup>-</sup>) were seeded per well in poly-L-lysine (Sigma-Aldrich) coated Seahorse XF96 plates in 180 µL XF Assay Medium (Modified DMEM, Seahorse Bioscience), respectively. For OCR measurements, XF Assay Medium was supplemented with 10 mM Glucose and 2.5 µM oligomycin A (Port A), 2.5 µM FCCP (carbonyl cyanide-4-(trifluoromethoxy) phenylhydrazone) (Port B) and 2 µM antimycin A together with 2 µM Rotenone (Port C) were sequentially injected in 20 µL volume to measure basal and maximal OCR levels (all

reagents from Sigma-Aldrich). For ECAR measurements, Glucose-free XF Assay medium was added to the cells and 10 mM Glucose (Port A), 2.5  $\mu$ M oligomycin A (Port B) and 100 mM 2-deoxy-D-glucose (Port C) (all reagents from Sigma-Aldrich). For measuring the metabolic activity after M2d or MS-5 co-culture, we initially seeded  $2.5 \times 10^5 - 5 \times 10^5$  AML cells (cell lines and primary samples, respectively) for 2 days and counted remaining viable cells, loading equal amounts of cells. For etomoxir experiments, MS5 and M2d macrophages were treated with Etomoxir (50  $\mu$ M) alone or in combination with VEN (250 nM) for 24 h. After that, cells were washed twice with 1X PBS and HL60 cells or primary AML blasts were added and a co-culture for 24 h was performed, to measure the OCR/ECAR in the AML cells. To exclude off-target effects from treated MS5 or M2d macrophages on the exposed AML cells after co-culture, AML cells were evaluated with the mitochondrial markers – MitoTracker DeepRed and Tetramethylrhodamine, Ethyl Ester, Perchlorate (TMRE; ThermoFisher) by FACS (LSRII). All XF96 protocols consisted of 4 times mix (2 min) and measurement (2 min) cycles, allowing for determination of OCR at basal and also in between injections. Both basal and maximal OCR levels were calculated by assessing metabolic response of the cells in accordance with the manufacturer's suggestions. The OCR measurements were normalized to the viable number of cells used for the assay.

### 3.11 Mitochondrial transfer

Mitochondrial transfer assays were performed as described by Moschoi et al (MOSCHOI et al., 2016). Co-cultures of primary AML blasts or cell lines with M2d macrophages and MS-5 confluent monolayer were performed in Gartners medium or RPMI 1640, respectively. Etomoxir (50  $\mu$ M; MedChemExpress, NL) and Venetoclax (250 nM) treatment were performed in the MS5 and M2d macrophages 24h prior to the co-culture. Viability of the stromal cells was evaluated by DAPI staining. MS-5 and M2d macrophage MitoTracker loading was performed as follows: confluent stromal cells were stained for 10 minutes with 2  $\mu$ M MitoTracker Green FM and 1  $\mu$ M MitoTracker DeepRed FM (Molecular Probes), washed twice, and left 72 hours to allow elimination of the unbound probe. Stromal cells were then washed twice again before initiating co-cultures with AML cells. As a quality control, conditioned medium of stained MS-5 and M2d macrophages 72 hours post staining, was collected and used to stain AML cells, to evaluate the leakage of MitoTracker dyes.

### 3.12 *In vivo* homing and *in vitro* cell migration

### 3.12.1 *In vivo* homing assay

Human macrophages were generated and polarized as described in the sections “Macrophage generation” and “Macrophage polarization” in 6 well plates. Cryopreserved MNC fractions of APL patient samples were thaw as described in the section “Flow cytometry” section and depleted for CD3<sup>+</sup>. In total 5x10<sup>6</sup> APL cells were put in co-culture on M2d macrophages per well for 48 hours. After 48 hours, suspension APL cells were collected and counted. A total of 1x10<sup>6</sup> co-cultured APL blast cells were washed 2x in serum free medium at 450g for 5 min. APL cells were resuspended in 100 µL serum free medium and stained with 1 µL Incucyte® Cytolight Rapid Red Dye (0.33 µM) for 20 min at 37°C. Cells were then washed 2x in medium with serum at 450g for 5 min. For the control group cryopreserved MNC fractions of APL patient samples were thaw, depleted for CD3<sup>+</sup> and 1x10<sup>6</sup> were labelled with the incucyte dye as described above. Labeled APL blast cells (after thawing and M2d co-cultured) were transplanted via the retro-orbital sinus. Additional, 1x10<sup>6</sup> freshly thaw and co-cultured blast cells were set aside to stain for purity and measure the levels of CD49d, CD49e and CD49f. All specimens were acquired by flow cytometry (FACS CantoII) and analysed with the FlowJo software (Treestar, Inc., USA). Eighteen hours post-transplant mice were sacrificed, and legs were first flushed and then crushed to retrieve the maximum number of cells. BM cells were stained with DAPI and human CD45-APC, CD33-PE and the Incucyte dye. A total of 5x10<sup>6</sup> cells DAPI negative cells were acquired by flow cytometry (FACS CantoII) and analysed with the FlowJo software (Treestar, Inc., USA).

### 3.12.2 *In vitro* migration assay

Primary BM stromal cells (passage 3) were plated at a density of 1 × 10<sup>5</sup> per well in a trans well system in a 6-well plate format, 1 day before the migration assay. Migration assay was performed as previously described (JUSTUS et al., 2014). Briefly, primary AML/APL blasts were co-cultured with M2d macrophages for 48 h, and after the co-culture, diagnosis and co-cultured blasts were seeded (1x10<sup>6</sup> cells) in the upper chamber of the 6-well plate and incubated at 37°C at 5% CO<sub>2</sub> for 18 hours to allow the migration upon the SDF-1 stimulus (produced by the MSCs in the lower chamber). After incubation, membranes were fixed with Methanol 99.9% and stained with Violet Crystal. Colonies containing at least 50 cells were



counted and considered as migrating cells. The values were then normalized to the diagnosis samples.

### **3.13 In vitro assays post macrophage and MSC exposure**

#### **3.13.1 Colony forming unit assay**

Colony formation capacity was evaluated out in semisolid methylcellulose medium. Human macrophages were generated and polarized as described in the sections “Macrophage generation” and “Macrophage polarization” in 12 well plates. Cryopreserved MNC fractions of AML cells were thaw and CD3<sup>+</sup> depleted. Primary AML cells ( $1 \times 10^6$ ) were put in co-culture with either macrophages or MS5 cells for 48h. The co-cultures were performed in Gartner’s medium. After 48h cells were collected, washed, and counted. A total of  $1 \times 10^3$  AML cells post co-culture were plated in semisolid methylcellulose medium supplemented with human cytokines MethoCult<sup>TM</sup> H4435 (StemCell). Colonies were detected after 14 days and scored.

#### **3.13.2 In vitro AML proliferation in liquid culture**

Human macrophages were generated and polarized as described in the sections “Macrophage generation” and “Macrophage polarization” in 12 well plates. Cryopreserved MNC fractions of AML cells were thaw and CD3<sup>+</sup> depleted. Primary AML cells ( $5 \times 10^5$ - $1 \times 10^6$ ) were put in co-culture with either macrophages or MS5 cells for 48h. The co-cultures were performed in Gartner’s medium. After 48h, cells were collected, washed, and counted. A minimum of  $1 \times 10^5$  primary AML cells were put in liquid culture with Gartner’s medium. Cultures were grown at 37°C and 5% CO<sub>2</sub> and demi-populated after counting if necessary. Cell proliferation was assessed with a hemocytometer until day 30.

### 3.14 RNAseq experiments and GO/GSEA analyzes

RNA samples for sequencing were prepared for primary AML/APL blast cells at diagnosis and after 48h of co-culture with MS5 or M2d-macrophages. Cells were collected after co-culture, and the human CD34<sup>+</sup> or CD117<sup>+</sup> (for NPM1 mut AMLs and APL) was isolated for posterior RNA extraction. Total RNA was isolated using the RNeasy Micro Kit from Qiagen (Venlo, The Netherlands) according to the manufacturer's recommendations. Initial quality check and RNA quantification of the samples were performed by automated gel electrophoresis on the 2200 TapeStation System (Agilent Technologies). Sequence libraries were generated using the KAPA RNA HyperPrep kit with riboErase (HMR) (Roche Sequencing and Life Sciences) according to manufacturer's protocol. The obtained cDNA fragment libraries were sequenced on an Illumina NextSeq500 using default parameters (25M reads per sample). Quality trimmed reads were aligned to the hg19 reference genome. For normalization and to find differentially expressed genes the DESeq package (Anders and Huber, 2010) was used. Simultaneously, read counts were collected, which were used as input for the DESeq2 package (LOVE; HUBER; ANDERS, 2014) to find differentially expressed genes. Genes with an adjusted p-value < 0.00001 were found to be differentially expressed and were used in further analysis. Differentially expressed genes were clustered using unsupervised hierarchical clustering with Euclidean distances (complete) (stats package in R).

For quantitative RT-PCR, RNA was reverse transcribed using the iScript cDNA synthesis kit (Bio-Rad) and amplified using SsoAdvanced SYBR Green Supermix (Bio-Rad) on a CFX384 Touch Real-Time PCR Detection System (Bio-Rad). The ACTB, HPRT1 and RPL30 were used as housekeeping genes. Primer sequences are listed in the key resources table.

Gene set enrichment analysis (GSEA) was performed using the Broad Institute software (<http://software.broadinstitute.org/gsea/index.jsp>). Gene ontology (GO) was evaluated using the gene ontology resource (<http://geneontology.org/>) and the BinGO plugin using the Cytoscape software v3.8.2 (NIGMS, USA). All genes from the RNA-seq of the different experimental groups (diagnosis, MS5 co-culture and M2d co-culture) cohort were pre-ranked according to their differential expression (fold change). Enrichment scores (ES) were obtained with the Kolmogorov-Smirnov statistic, tested for significance using 1000 permutations, and normalized (NES) to consider the size of each gene set. As suggested by the GSEA, a false discovery rate (FDR) cut-off of 25% (FDR q-value < 0.25) was used. The limma-voom tool (<http://usegalaxy.org>) was used to examine differentially expressed genes and genes with  $\geq 1$  log

difference and adjusted p-value of  $<0.05$  were considered significant. Data visualization was performed with the ClustVis platform (PEREIRA-MARTINS et al., 2021).

### 3.15 Development of a M2 signature suitable for AML patients

The genetic signatures from M1 and M2 macrophages were retrieved from the FANTON, HPCA, BluePrint and CIBERSORT signatures (FINOTELLO et al., 2017; LI et al., 2016; NEWMAN et al., 2015). Genes with unique differential expression in M2 but not M1 macrophages, were selected for survival analysis using AML cohorts (Figure 6A). The gene expression of the two M2 macrophage markers used in our FACS panel (*CD163* and *MRC1* – *CD206*), plus the expression of the M2 genes *FGR*, *CD52*, *RASA3* and *GSK1B* were able to predict poor overall survival in at least two independent cohorts (Figure 18B). Out of those genes, *CD163*, *RASA3*, *FGR* and *GSK1B* exhibited increased expression in the  $CD34^-$  negative cells, when compared to the  $CD34^+$  cells in AML bone marrows (DE JONGE et al., 2011) (Figure 18C). Next, using the TCGA cohort (LEY et al., 2013), patients were dichotomized as a low or high expression using receiving operating characteristics (ROC) curve and the C index and were interrogated for univariate and multivariate Cox proportional hazards model (CPHM) regression analyses for overall survival (OS). Including age, sex and European LeukemiaNet (ELN2010) as cofounders, we identified the independent prognostic predictors by backward elimination using an exclusion significance level of 5%. The M2-UMCG signature was defined as the weighted sums of hazard ratio from the final Cox model from independent prognostic genes (*CD163*, *MRC1*, *FGR*, *CD52*, *RASA3* and *GSK1B*). Internal validation was performed using a non-parametric bootstrap procedure with 1,000 resamplings to get estimates of HR between risk categories corrected for overfitting.

We used the BeatAML cohort (TYNER et al., 2018) to validate our M2-UMCG signature (Figure 18F). Moreover, we correlated the M2-UMCG signature with the drug sensitivity against the 124 compounds evaluated in the BeatAML study, to identify the possible therapeutic opportunities for AML patients with high M2 signature. Area under the curve values (AUC) were used to perform the pearson correlation with the M2-UMCG signature.

***Results***

---

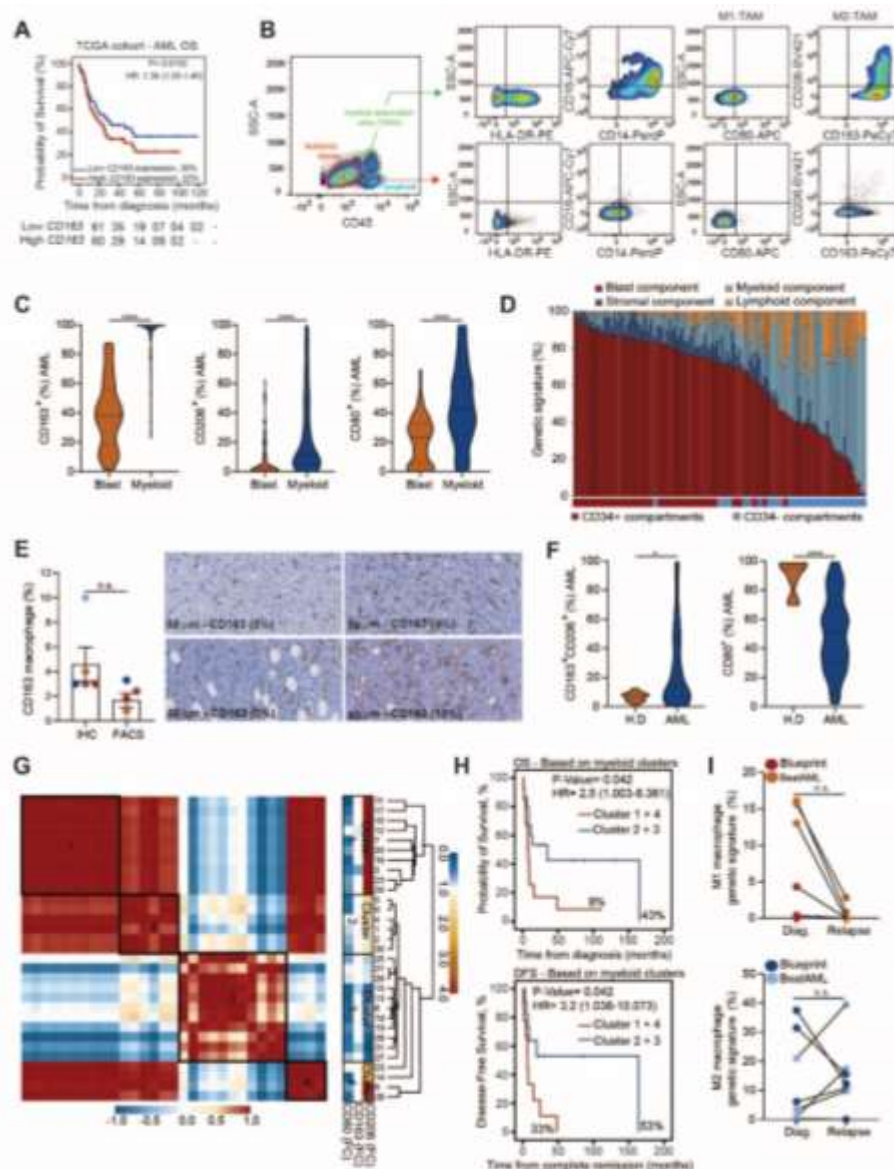
## 4 RESULTS

### 4.1 Heterogeneity in the macrophage landscape in AML: the presence of CD163<sup>+</sup>/CD206<sup>+</sup> leukemia-associated macrophages, identifies patients with the poor prognosis

Using the TCGA cohort (LEY et al., 2013) in which RNA sequencing was performed on the mononuclear cell (MNC) fraction of AML patients, we observed that high expression of CD163 predicted poor overall survival (OS) (Figure 8A). Since CD163 is known to be expressed on more mature myeloid cells, particularly in M2- macrophages, we further investigated the expression of CD163 within the MNC fraction in AML samples. Multiparametric flow cytometry analysis (FACS) revealed that expression of poor prognostic M2 markers CD163/CD206 as well as the M1 marker CD80 primarily emerge from a more mature SSC<sup>high</sup>/CD45<sup>high</sup>/HLA-DR<sup>+</sup>/CD14<sup>+/-</sup>/CD16<sup>+/-</sup> myeloid subpopulation (hereafter called AML-associated macrophages–AAM) (Figure 8B-C and Table 1). CD163 is a scavenger receptor responsible for the clearance of hemoglobin/haptoglobin complexes (GRAVERSEN; MADSEN; MOESTRUP, 2002; MOESTRUP; MOLLER, 2004), while CD206 promotes endocytosis of glycoproteins (AZAD; RAJARAM; SCHLESINGER, 2014) and CD80 induces T-cell activation (SUBAUSTE; DE WAAL MALEFYT; FUH, 1998). CIBERSORT analysis using the published transcriptome analysis of sorted MNC of individual AML patients into paired CD34<sup>+</sup> and CD34<sup>-</sup> compartments (DE JONGE et al., 2011), showed that the more mature myeloid compartment predominantly derives from the CD34<sup>-</sup> fraction (Figure 8D). Next, we questioned whether the quantification of macrophages in the BM by FACS would result in an underrepresentation due to difficulties in efficiently retrieving macrophages using BM aspirates, but comparison of FACS data with immunohistochemistry staining for CD163 indicated no significant differences between the two methods (Figure 8E).

In addition to our M1 and M2 markers, we also included the CD14 and CD16 markers to identify classical (CD14<sup>+</sup>/CD16<sup>-</sup>), intermediate (CD14<sup>+</sup>CD16<sup>+</sup>), and non-classical (CD14<sup>-</sup>/CD16<sup>+</sup>) monocytes/macrophages (PASSLICK; FLIEGER; ZIEGLER-HEITBROCK, 1989). Likewise, to healthy donors, the majority of AML patients primarily comprehended a classical monocyte/macrophage (CD14<sup>+</sup>CD16<sup>-</sup>) subpopulation with some exceptions (Figure 9A-B). We observed considerable heterogeneity between individual patients, with some patients harboring predominantly tumor-suppressive M1 macrophages, some harboring predominantly tumor-supportive M2 macrophages, but also patients harboring both populations were observed (Figure 9C).

On average, AML patients harbored significantly less tumor-suppressive M1 and more tumor-supportive M2 macrophages compared to healthy donors (Figure 8F). Moreover, AMLs defined as M4/M5 by the French-American-British (FAB) classification system harbored the highest proportion of AAMs (Figure 9D). The presence of M2-AAM was more recurrent in *FLT3*-ITD patients (Figure 9E). Next, we performed an unsupervised cluster analysis using the fold change to healthy donors of the expression of CD163, CD206 and CD80 measured on AAMs (excluding patients with a AAM compartment <1%; n=31). Among the 4 generated clusters, patients allocated in clusters 2 and 3, with the lowest CD206 expression, displayed improved OS and disease-free survival (DFS) compared to patients in clusters 1 and 4 (Figure 8G-H and Table 2). In addition, longitudinal CIBERSORT analyses performed on AML patients enrolled in the Blueprint and BeatAML cohorts of which diagnosis and relapse samples were available revealed a consistent reduction of the M1 macrophage signature upon relapse (Figure 8I). Congruent with the nature of AML, heterogeneity exists as well in the macrophage landscape between individual patients, and those patients with an increase in M2-like AAMs display poor prognosis.

**Figure 8. The poor prognostic value of M2 macrophages in AML**

**Figure 8.** (A) Kaplan-Meier (KM) for overall survival (OS) regarding in relation to *CD163* expression in the TCGA cohort. (B) Representative FACS plot of macrophage marker expression in different CD45 subpopulations in an AML sample. (C) Violin plots summarizing the expression of macrophage markers in the AML blasts versus the mature myeloid population. (D) CIBERSORT analysis on the paired CD34<sup>+</sup>/CD34<sup>-</sup> transcriptomes of AML patients. (E) Bar plot displaying the amount of CD163<sup>+</sup> macrophages quantified by IHC and FACS. Representative IHC pictures for CD163 in AML samples. (F) Violin plot comparing the level of M2 (CD163<sup>+</sup>/CD206<sup>+</sup>) and M1 (CD80<sup>+</sup>) markers measured by FACS in healthy donors (HD - BM=5; PB=3; PBSC=5) and AML patients (BM=33; PB=28). (G) Unsupervised hierarchical clustering (Euclidean distance, complete linkage) of the heat map and the correlation matrix generating clusters based on the fold change to HD of the CD206, CD163 and CD80 levels detected in the AML mature myeloid subpopulation (>1%) (BM=14; PB=17) FC=Fold change. (H) KM analysis of OS and Disease-Free survival based on the CD206, CD163 and CD80 clusters. (I) CIBERSORT analysis of the M1 and M2 signatures detected in paired diagnosis and relapse samples from the Blueprint and the BeatAML cohorts.

(A and H) Survival curves were compared using the log-rank test.

(C, E and I) Wilcoxon signed rank test (2-sided). \*\*\*P<0.0001, NS, not significant.

(F) Mann Whitney test for unpaired data (2-sided). \*P<0.05.

Figure 9. The macrophage profile across distinct AML patients

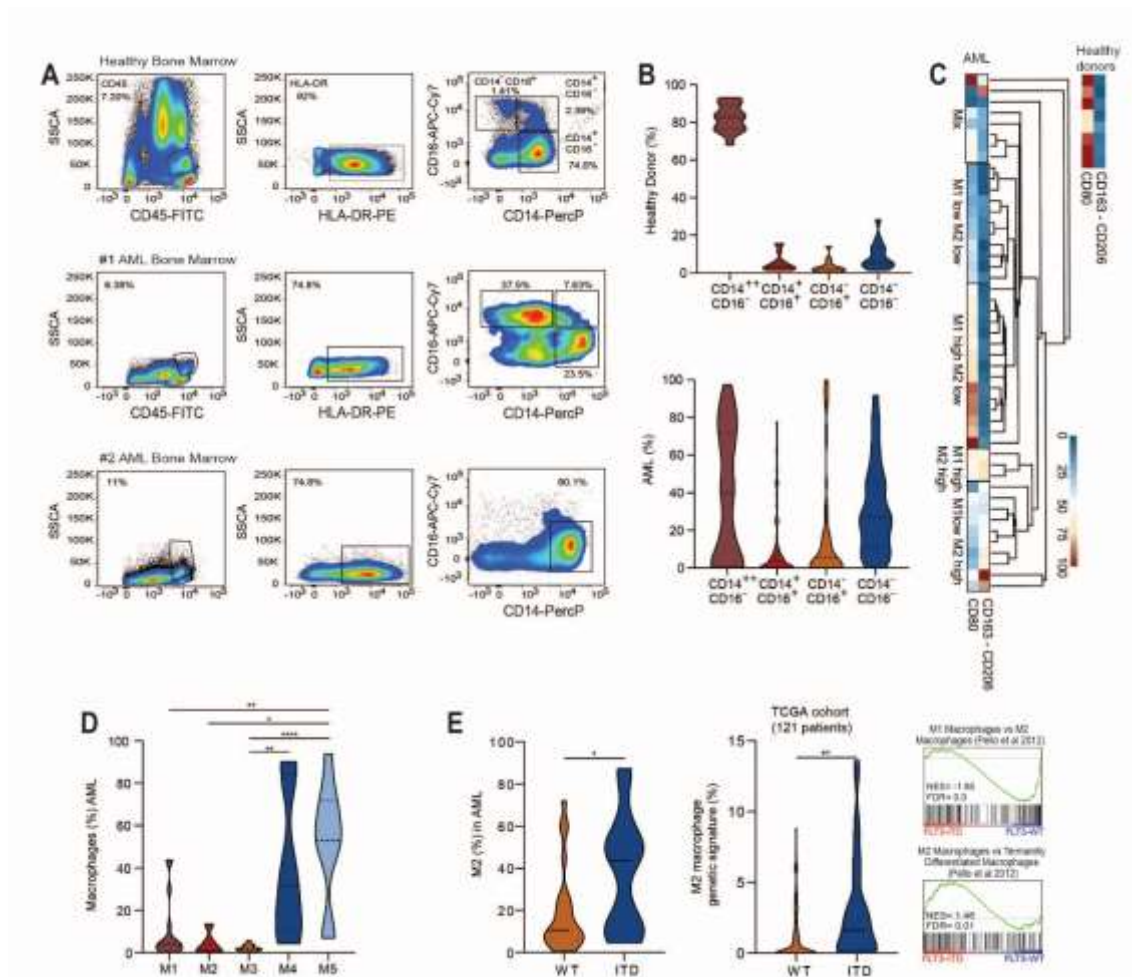


**Figure 9.** (A) Representative FACS plot showing the CD14/CD16 subpopulations inside the  $SSC^{\text{high}}CD45^{\text{high}}HLA-DR^+$  monocyte/macrophage population in healthy donors (H.D) and Acute Myeloid Leukemia (AML) patients. (B) Violin plot of  $CD14^+CD16^-$ ,  $CD14^+CD16^+$  and  $CD14^-CD16^+$  monocyte/macrophage subpopulation in H.D (Bone Marrow, BM= 5; Peripheral Blood, PB= 3; Peripheral Blood mobilized stem cells, PBSC= 5) (Total N=61; BM=33; PB=28). (C) Heat map showing the expression of CD163, CD206 and CD80 detected in monocytes/macrophages of H.D and AML patients. (D) Violin plot depicting the percentage of macrophages detected based on SSC versus CD45 in different AML subtypes defined by the FAB classification system. (E) Violin plot depicting the percentage of M2 macrophages measured within the  $SSC^{\text{high}}CD45^{\text{high}}HLA-DR^+CD14^{+/}CD16^{+/}$  subpopulation and M2 macrophage genetic signature detected in patients with *FLT3* wild-type (WT) and *FLT3*-ITD mutations enrolled in the UMCG (left panel) and TCGA cohort (right panel) respectively. Gene set enrichment analysis displaying decreased M1 macrophage signature (upper panel) and increased M2 macrophage signature (lower panel) in AML patients followed at the UMCG with *FLT3*-ITD mutations in comparison with WT patients. Normalized enrichment score (NES) and False Discovery Rate (FDR) q-values are depicted inside the panels.

Two-way (D) analysis of variance (ANOVA). \* $P < 0.05$ , \*\* $P < 0.01$ , \*\*\* $P < 0.001$ .



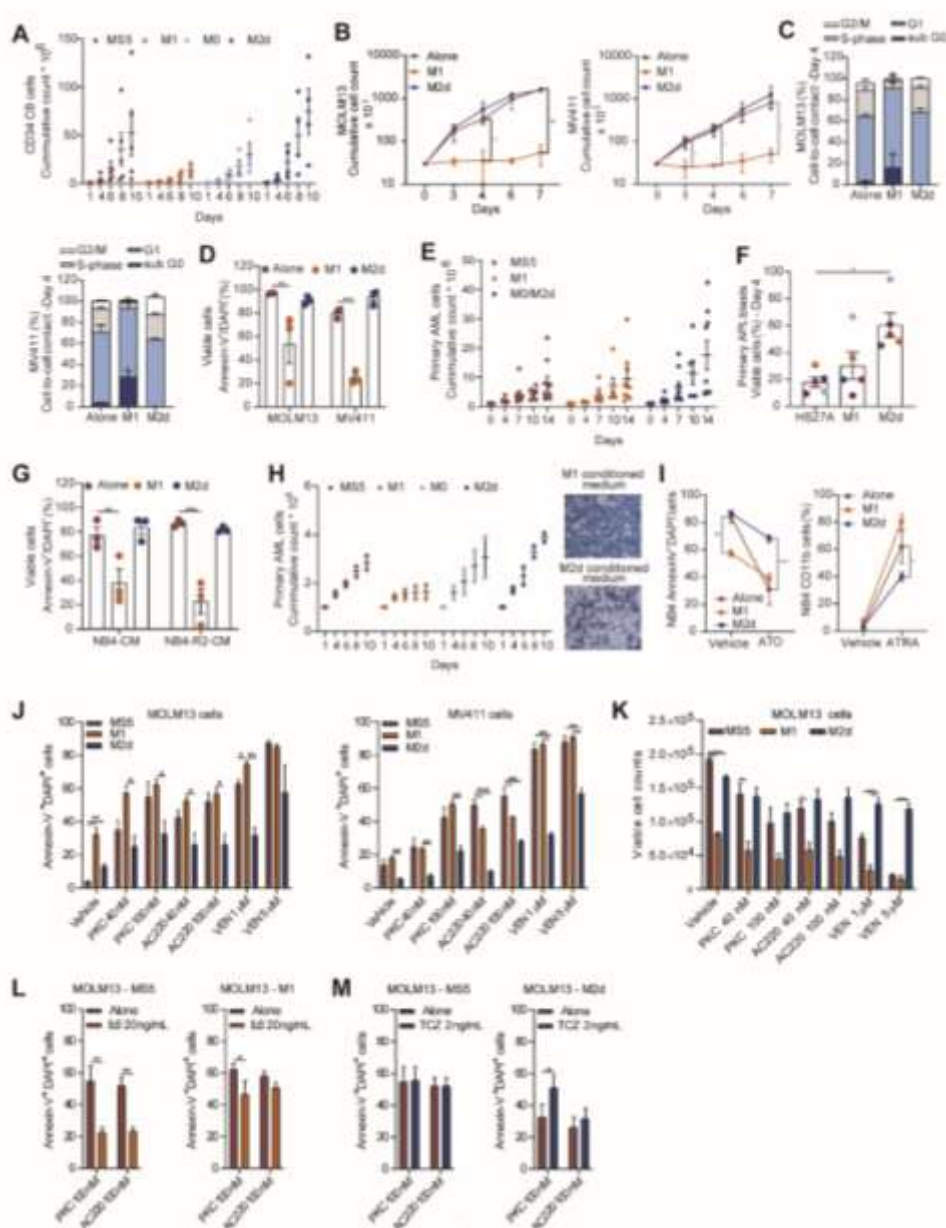
#### **4.2 M1 macrophages possess tumor suppressive activity while M2 macrophages enhance survival and impose drug resistance on AML blasts.**

To understand the dynamics between distinct macrophage subtypes and AML cells, we co-cultured PB-derived M1, M2 and non-polarized (M0) macrophages with cord blood (CB)-derived CD34<sup>+</sup> cells, AML cell lines and primary CD34<sup>+</sup> isolated or MNC AML samples. As controls, cells were grown on murine MS5 bone marrow stromal cells. A prominent anti-leukemic effect of M1 macrophages was observed, associated with an increase in apoptosis and cells accumulating in the sub-G0 phase (Figure 10A-F and 11A-C). In contrast, co-culture on M2d macrophages supported leukemia cell growth and viability (Figure 10E-F). We noted that M1 conditioned medium also induced apoptosis suggesting that tumor suppressive effects might be predominantly mediated by the M1 secretome while the pro-leukemic effects of M0/M2d macrophages appeared to be mediated by a combination of the M2 secretome and direct cell-to-cell contact (Fig 10E-H).

In particular in the case of primary AML cells, we noted that while M1 macrophages initially impaired survival and proliferation, from day seven onwards the M1 macrophages appeared to lose their anti-leukemic effects, possibly due to macrophage repolarization towards a tumor supportive phenotype, which was confirmed by FACS analysis (Figure 11D).

Since high M2 infiltration was associated with low OS and DFS, it is conceivable that the presence of M2-like macrophages could contribute to the resistance of anti-leukemic drugs. Indeed, M2, but not M1 macrophages, significantly reduced arsenic-induced apoptosis and or all-trans retinoic acid-stimulated differentiation in the APL cell line NB4 (Figure 10I). Co-culture on M1 itself did negatively impact viability as noted before (Figure 10I). Likewise, M2 macrophages diminished the cytotoxic effect induced by midostaurin (PKC), quizartinib (AC220-) or venetoclax (VEN-) in MOLM13 and MV4-11 cells (Figure 10J, 10K and 11E). Since M2 macrophages can produce IL6 (GUBERNATOROVA et al., 2018; WANG; LIANG; ZEN, 2014; WANG et al., 2010), we evaluated whether the addition of IL6 could rescue MOLM13 and MV4-11 cells from PKC and AC220 drug-induced apoptosis when cultured on MS5 and M1 macrophages. When cultured on MS5, IL6 was able to significantly counteract PKC or AC220-induced apoptosis, while these effects were less prominent or even abrogated in the presence of M1 macrophages (Figure 10L and 11F). Conversely, we used the monoclonal antibody tocilizumab (TCZ) to block the IL6 receptor, which resulted in increased PKC-induced apoptosis of MOLM13 and MV4-11 cells when cultured on M2 macrophages but not on MS5 cells. Yet, no additional cytotoxic effect was detected when TCZ was combined with AC220 (Figure 10M and 11G). Together, these data indicate that M1 macrophages display tumor suppressive functions while M2 macrophages enhance survival and drug resistance in AML.

**Figure 10.** The pro- and anti-leukemic effects of M1 and M2 macrophages *in vitro*

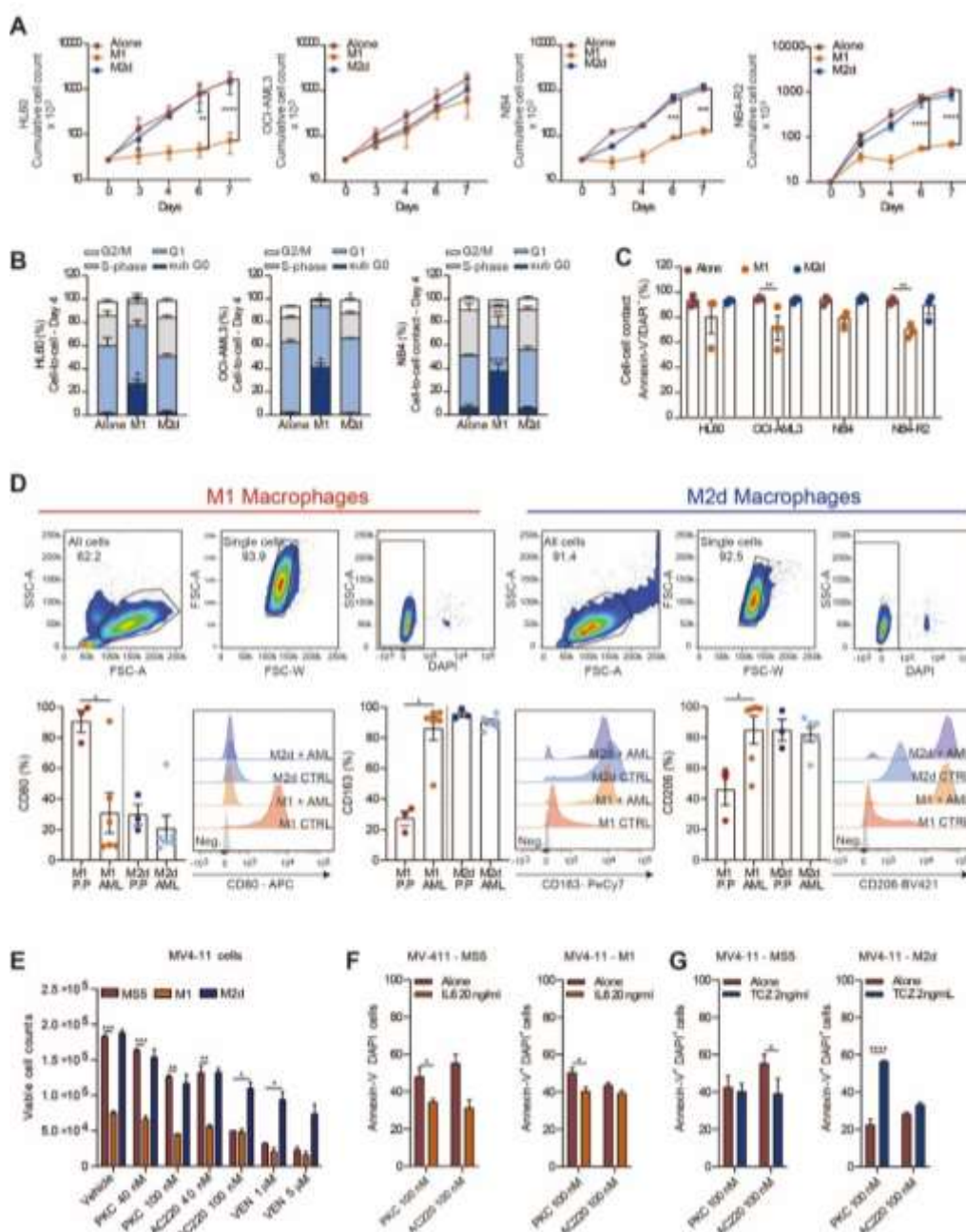


**Figure 10.** (A) Cumulative cell count of CB-derived CD34<sup>+</sup> cells cultured on MS5, M1, M0 and M2 macrophages for 10 days. (B) Cumulative cell count of MOLM13 and MV4-11 AML cell lines cultured on M1 and M2 macrophages or alone (control) for 7 days. (C) Cell cycle distribution analysis of MOLM13 and MV4-11 after 4 days of co-culture on M1 and M2 macrophages or alone. (D) Percentage of viable MOLM13 and MV4-11 cells after 7 days of co-culture on M1 and M2 macrophages or alone. (E) Cumulative cell count of primary AML cells cultured on M1, M0 and M2 macrophages or MS5 (control) for 14 days. (F) Percentage of viable primary APL cells after 4 days of co-culture on M1 and M2 macrophages or HS27A cells (control). (G) Percentage of viable NB4/NB4R2 cells after 7 days of culture in M1 and M2 conditioned medium (CM) or alone. (H) Cumulative cell count of primary AML cells cultured on MS5 cells in M1, M0 and M2 CM or only Gartner's medium (control) for 10 days. Representative pictures of cultures at day 10. (I) Viability and CD11b<sup>+</sup> cells after 72h culture with ATO (1  $\mu$ M) and ATRA (1  $\mu$ M). (J) Percentage of apoptotic MOLM13 and MV4-11 cells when cultured on M1 and M2 macrophages or MS5 (control) for 72h culture with PKC, AC220 and VEN. (K) Percentage of apoptotic MOLM13 cells when cultured on MS5 or M1 macrophages for 72h with PKC/AC220 in the presence or absence of IL6. (L) Percentage of apoptotic MOLM13 cells when cultured on MS5 or M2 macrophages for 72h with PKC/AC220 in the presence or absence of TCZ.

(A and D-H) Each dot represents an independent sample/experiment.

(B-C and I-L) represent at least 3 biological replicates for all experiments.

One-way (F) or two-way (A-E, G, I-L) analysis of variance (ANOVA). \* $P < 0.05$ , \*\* $P < 0.01$ , \*\*\* $P < 0.001$ .

**Figure 11. The effect of macrophages on AML cells and vice versa**

**Figure 11.** (A) Cumulative cell count of HL60, OCI-AML3, NB4, NB4-R2 AML cell lines cultured on M1 and M2 macrophages or alone (control) for 7 days. (B) Cell cycle distribution analysis of HL60, OCI-AML3 and NB4 after 4 days of co-culture on M1 and M2 macrophages or alone. (C) Percentage of viable HL60, OCI-AML3, NB4 and NB4-R2 cells after 7 days of co-culture on M1 and M2 macrophages or alone. (D) Representative FACS plot showing the viability of in vitro generated M1 and M2 macrophages detached at day 7. Bar plot and histogram depicting the percentage of CD80, CD163 and CD206 post-macrophage polarization and after exposure to primary AML cells. Each dot represents an independent experiment with a different AML patient/macrophage donor. (E) Viable cell counts of MV411 cells when cultured on M1 and M2 macrophages or MS5 for 72h culture with PKC (40 and 100 nM), AC220 (40 and 100 nM) and VEN (1 and 5 μM). (F) Percentage of apoptotic MV411 cells when cultured on MS5 or M1 macrophages for 72h with PKC/AC220 in the presence or absence of IL6 (20 ng/mL). (G) Percentage of apoptotic MV411 cells when cultured on MS5 or M2 macrophages for 72h with PKC/AC220 in the presence or absence of Tocilizumab (TCZ, 2 ng/mL). (G)

(A-G) Represent at least 3 biological replicates for all experiments.

One way (C) or two-way (A-B and E) analysis of variance (ANOVA). \*P<0.05, \*\*P<0.01, \*\*\*P<0.001.

(D, F-G) Wilcoxon signed rank test (2-sided) \*P<0.05, \*\*P<0.01, \*\*\*P<0.001.

### 4.3 M2 macrophages support *in vivo* engraftment and leukemogenesis

We evaluated whether M2 macrophages could support leukemogenesis *in vivo*. As a proof of concept, we started with primary APL patient samples as these are notoriously difficult to engraft (REINISCH et al., 2016). Human PB derived macrophages (M0 and M2) were injected into the femur of NSGS mice, while primary human APL blasts were transplanted via the retro-orbital vein (Figure 12A). Control mice only received human APL blasts. As expected, none of the mice receiving APL blasts without macrophages succumbed to leukemia (Figure 12B-C). In stark contrast, at week eight post-transplant mice injected with M0 and M2 macrophages started to present with leukocytosis indicating the manifestation of leukemia (Figure 12B). After 12 weeks post-transplant, the mice were sacrificed to determine the level of human APL blasts (defined as DAPI<sup>-</sup>/hCD45<sup>dim</sup>/hCD117<sup>+</sup>/hCD33<sup>+</sup>) in each leg and spine (as an internal control). FACS analysis confirmed the increased percentage of hCD45 cells in macrophage-injected mice compared to controls (Figure 12C). Similarly, total human APL blast cells were substantially increased for M0 and M2 legs when compared to control (Figure 12C). Cytospins of APL cells retrieved from murine BM displayed human promyelocytes (Figure 12D). When we compared the levels of human CD45<sup>+</sup> chimerism and APL blast cells between M0 and M2 injected tibias, we noticed that the engraftment of primary APL cells was superior in the presence of M2 compared to M0 macrophages (Figure 12C). In line with leukemia onset, macrophage recipient mice displayed APL blast cell infiltration in the spleen and other tissues (Figure 12C and 12E). Collectively, these data indicate that a tolerogenic environment can promote APL leukemogenesis.

**Figure 12. Human M2 macrophages promote APL leukemogenesis in a PDX model**

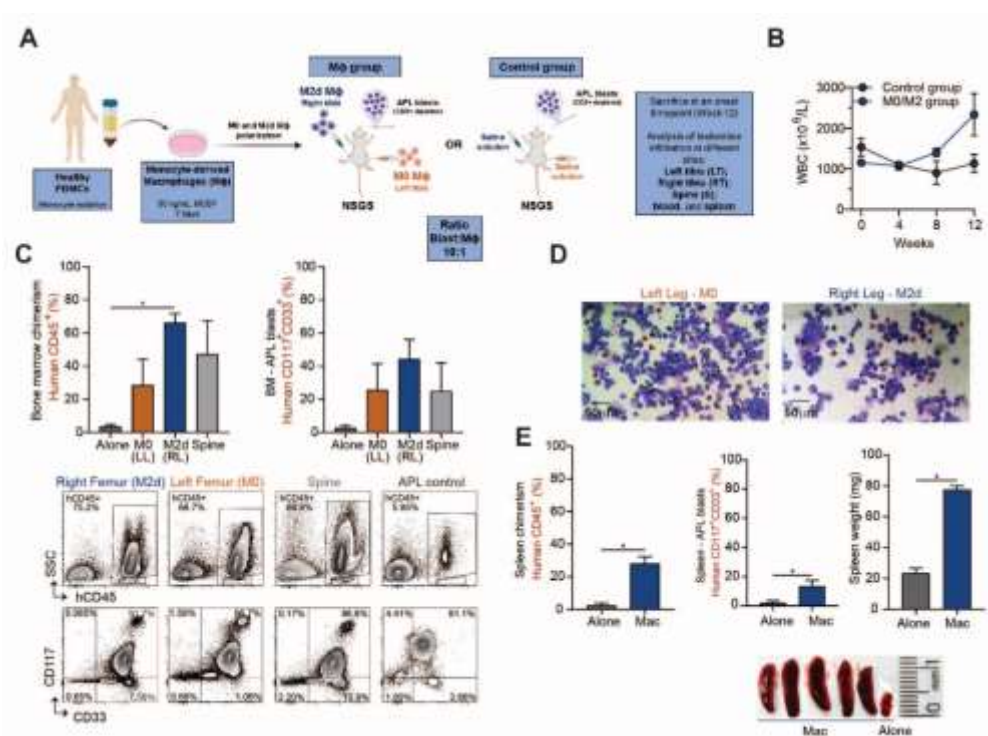


**Figure 12.** (A) Experimental scheme. (B) Dispersion graph showing the leukocyte count. Each dot represents the mean of 6 independent APL patients. (C) Bar graph and representative FACS plot of human CD45<sup>+</sup>/CD117<sup>+</sup>/CD33<sup>+</sup> (APL blast cells, %) detected in the BM (N=6). LL=Left Leg; RL=Right Leg. (D) Representative cytopsin of the M0 and M2 injected murine BM. Arrows indicate human APL blast cells. (E) Bar graph showing of human CD45<sup>+</sup>/CD117<sup>+</sup>/CD33<sup>+</sup> (%) detected in the spleen (N=6) and the spleen weight. Representative spleen pictures of macrophage injected mice and control (APL blast alone). Mac=Macrophage.

Two-way (B) analysis of variance (ANOVA). (C) Kruskal-Wallis test. \*P<0.05. (E) Mann Whitney test for unpaired data (2-sided). \*P<0.05

#### 4.4 M2 macrophages can reprogram primary APL to induce full-blown APL in a patient derived xenograft (PDX) model

Based on the premise that macrophage injected NSGS mice enabled APL engraftment and infiltration of APL cells to distant tissues, we hypothesized that a pre-culture of APL cells on macrophages might be sufficient to induce biological changes that promote fatal leukemia. We co-cultured primary human and murine APL cells on human PB or murine BM derived M0/M2 macrophages for 48hrs. After 48hrs, a substantial fraction of leukemic blasts were phagocytosed leaving 8.3–10.5% of the original input of human and murine blasts, respectively (Figure 14A-B and data not shown). Next, we injected  $1.5 \times 10^5$  “trained” cells retro orbitally into NSGS mice, while control mice received  $1 \times 10^6$  (corresponding to a 6.6-fold increase) non-cultured or MSCs pre-cultured cells (Figure 13A). Indeed, only human APL cells pre-cultured on macrophages were able to induce full-blown leukemia, while no engraftment was detected in control mice (Figure 13B-F and 14C-D). The median OS rate was 18 weeks for M0 pre-cultured cells and 12 weeks for M2 pre-cultured cells (n=6 APL patients) (Figure 13B). The biological changes acquired by APL blast cells upon M2 macrophage co-culture led to a more aggressive course of APL development characterized by leukocytosis, increased human chimerism levels, increased frequency of APL blast cells and spleen weight compared to M0 pre-cultured cells (Figure 13C-F). Similar results were obtained in our murine model, in which transgenic PML-RAR $\alpha$ -expressing blast cells were transplanted into lethally irradiated recipients (WEINHÄUSER et al., 2020). The median OS was 9.5 and 6.2 weeks for M0 and M2 pre-cultured cells respectively compared to 14 weeks for control mice (Figure 15A-C). Cytospins of non-pre-cultured murine APL blasts post-sacrifice displayed a higher frequency of cells with cruller shaped nucleus, characteristic for intermediate myeloid murine cells, while M2-precultured APL cells presented with a more undifferentiated blast-like cell morphology. These observations were confirmed by FACS, with recipients of macrophage precultured APL blasts exhibiting increased levels of early promyelocytes, in comparison with the control (Figure 15D). To determine whether the changes of APL cells pre-cultured on M2 macrophages resulted in increased self-renewal capacity, we sorted hCD45<sup>+</sup>/hCD117<sup>+</sup>/hCD33<sup>+</sup> engrafted APL blast from the primary transplant and performed a secondary transplant with different APL cell dosages ( $1 \times 10^3$ ,  $5 \times 10^5$  and  $1.5 \times 10^6$  APL cells). After passage through primary mice the cells indeed retained self-renewal and secondary transplanted mice developed full-blown APL when transplanted with  $1.5 \times 10^6$  (median OS 10 weeks) or  $5 \times 10^5$  cells (median OS 14 weeks) (Figure 13G-J). Mice transplanted with  $1 \times 10^3$  cells only presented transient engraftment and

never developed fatal APL (Figure 13G-J and 14E). Engrafted mice presented symptoms of leukemia such as leukocytosis, anemia, and thrombocytopenia (Figure 13H). Morphological examination of the BM from leukemic mice confirmed the presence of human promyelocytes characterized by a high nuclear: cytoplasm ratio, visible nucleoli and the presence of primary granules (Figure 13I). FACS analysis further confirmed that engrafted cells were predominantly CD117<sup>+</sup>/CD33<sup>+</sup> (Figure 13I-J). Finally, we calculated the leukemic stem cell frequency, which was  $1/6.4 \times 10^6$  for control mice and  $1/7.2 \times 10^4$  for “trained” APL blasts (Figure 13K). Overall, our data indicate that macrophages can change the biology of APL/AML cells, transforming non-engraftable cells into cells with high leukemic potential, which is preserved over time.

**Figure 13. Primary APL blast cells pre-cultured on human M2 macrophages generate fatal leukemia**

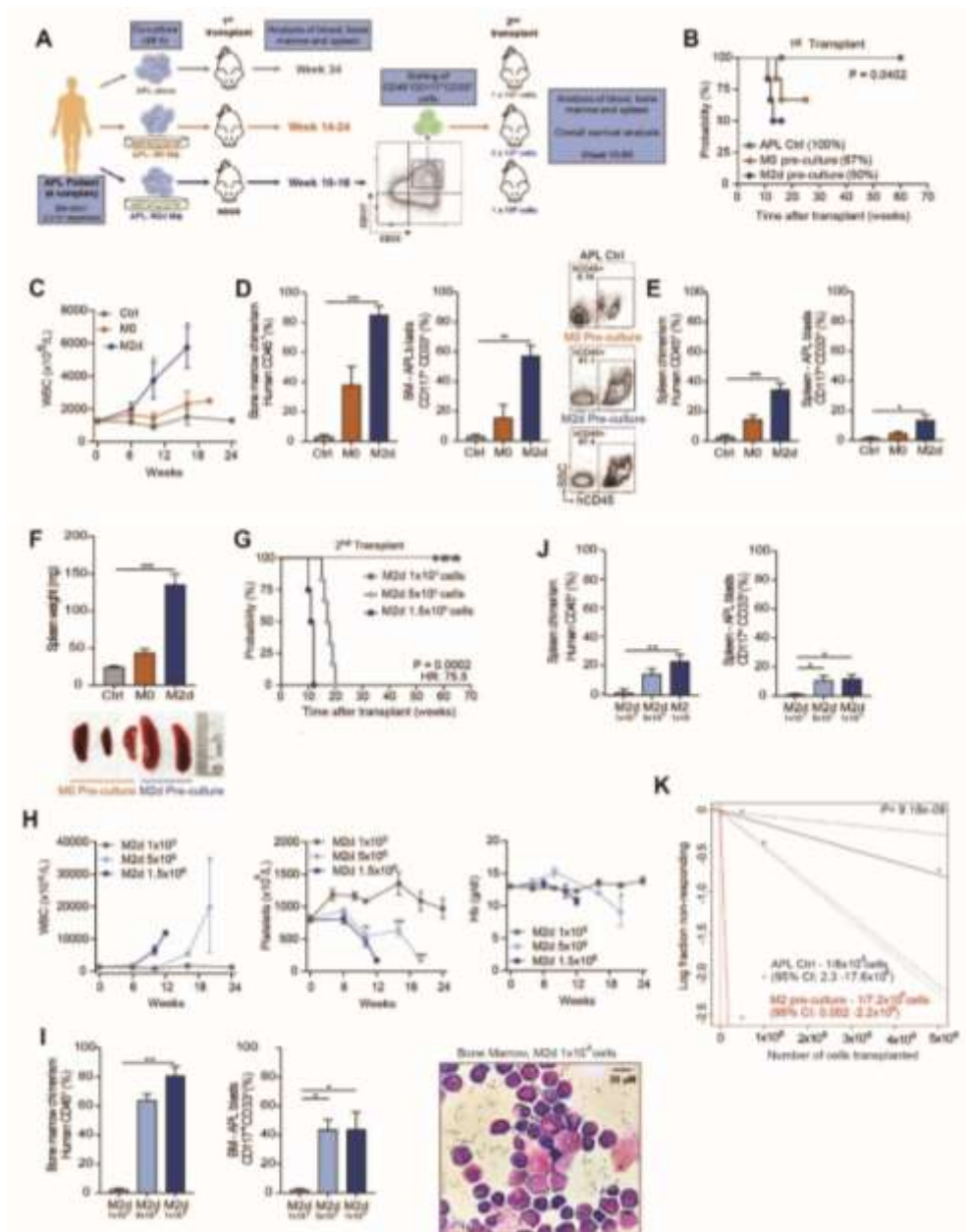


**Figure 13.** (A) Experimental scheme. (B) OS analysis of mice transplanted with primary APL blast transplanted alone or pre-cultured on M0/M2 macrophages for 48h. (C) Dispersion graph showing the leukocyte count. (D) Bar graph and representative FACS plot of human CD45<sup>+</sup>/CD117<sup>+</sup>/CD33<sup>+</sup> (%) measured in the BM of control (alone) and M0/M2 pre-cultured mice. (E) Bar graph of human CD45<sup>+</sup>/CD117<sup>+</sup>/CD33<sup>+</sup> (%) measured in the spleen of control (alone) and M0/M2 pre-cultured mice. (F) Bar graph showing the spleen weight of control (alone) and M0/M2 pre-cultured mice. (G) OS analysis of the secondary transplant of mice transplanted with 1.5x10<sup>6</sup>, 5x10<sup>5</sup> and 1x10<sup>3</sup> (N=3-6 per group) sorted human CD33<sup>+</sup>CD117<sup>+</sup> APL blast cells from the primary transplant. (H) Dispersion graph showing the leukocyte, platelet counts and hemoglobin levels. (I) Bar graph of human CD45<sup>+</sup>/CD117<sup>+</sup>/CD33<sup>+</sup> (%) measured in the BM of mice transplanted with 1x10<sup>3</sup>-1.5x10<sup>6</sup> sorted human CD33<sup>+</sup>CD117<sup>+</sup> APL blasts. Representative cytopsin of human APL blast cells retrieved from the murine BM. (J) Bar graph CD45<sup>+</sup>/CD117<sup>+</sup>/CD33<sup>+</sup> (%) measured in the spleen of mice transplanted with 1x10<sup>3</sup>-1.5x10<sup>6</sup> sorted human CD33<sup>+</sup>CD117<sup>+</sup> APL blast cells. (K) *In vivo* LTC-IC assay.

(B and G) Each dot represents an individual mouse OS curves were estimated using the KM method, and the log-rank test was used for comparison.

(D-F) Represents 6 independent APL patients.

Two-way (C and I) analysis of variance (ANOVA). \*P < 0.05, \*\*P < 0.01, \*\*\*P < 0.001.

(D – G and K-M) Kruskal-Wallis test. \*P < 0.05, \*\*P < 0.01, \*\*\*P < 0.001.



### Figure 14. Primary APL blast cells pre-cultured on human M2 macrophages generate fatal leukemia

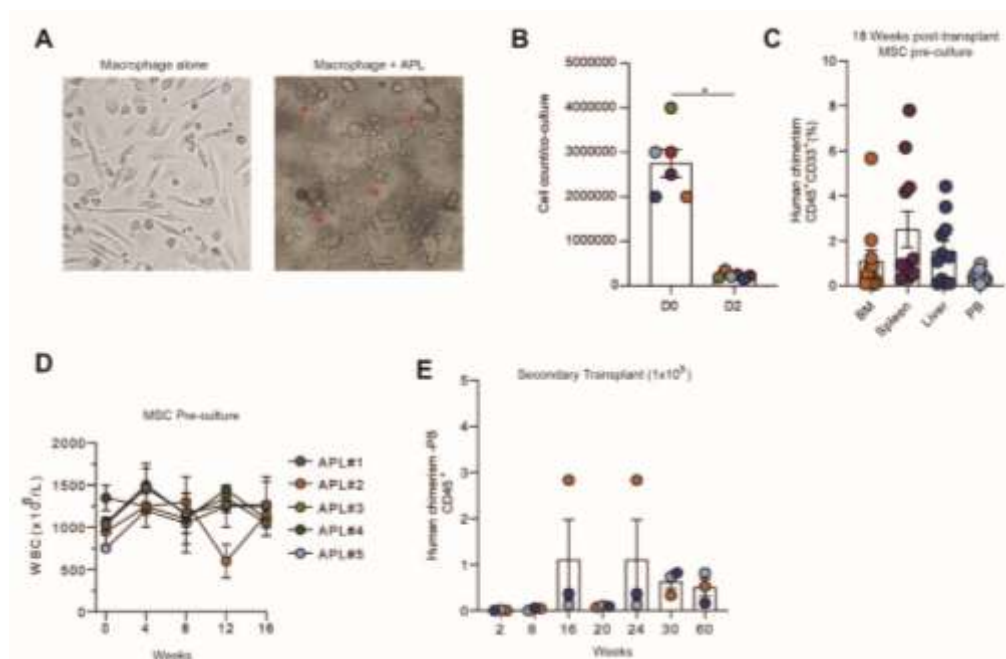


**Figure 14.** (A) Representative picture of M2 macrophages post-polarization (left picture) and after 48h co-culture with primary APL cells (right picture). (B) Bar graph showing the cell counts of primary APL cells when put in co-culture with macrophages at the day 0 (initial input) and after 2 days of co-culture. D0=Day 0, D2=Day2. (C) Human CD45 and CD33 chimerism level detected in different organs at week 18 post-transplant of mice injected with primary APL cells pre-cultured on primary mesenchymal stromal cells (MSCs – Passage 4) isolated from healthy bone marrow for 48h. (D) Dispersion graph showing the leukocyte count over time of mice injected with primary APL cells pre-cultured on primary MSCs for 48h. (E) Bar graph showing the human CD45 chimerism level measured in the blood of mice transplanted with  $1 \times 10^3$  sorted human CD33<sup>+</sup>CD117<sup>+</sup> APL blasts from M2 pre-culture primary transplant.

(B–D) Each dot represents an individual APL patient

(E) Each dot represents an individual mouse

(B) Wilcoxon signed rank test (2-sided) \* $P < 0.05$ .

(C) Kruskal-Wallis test.

Two-way (D) analysis of variance (ANOVA).

**Figure 15. Primary murine APL blast cells pre-cultured on murine M2 macrophages accelerates APL leukemogenesis *in vivo***

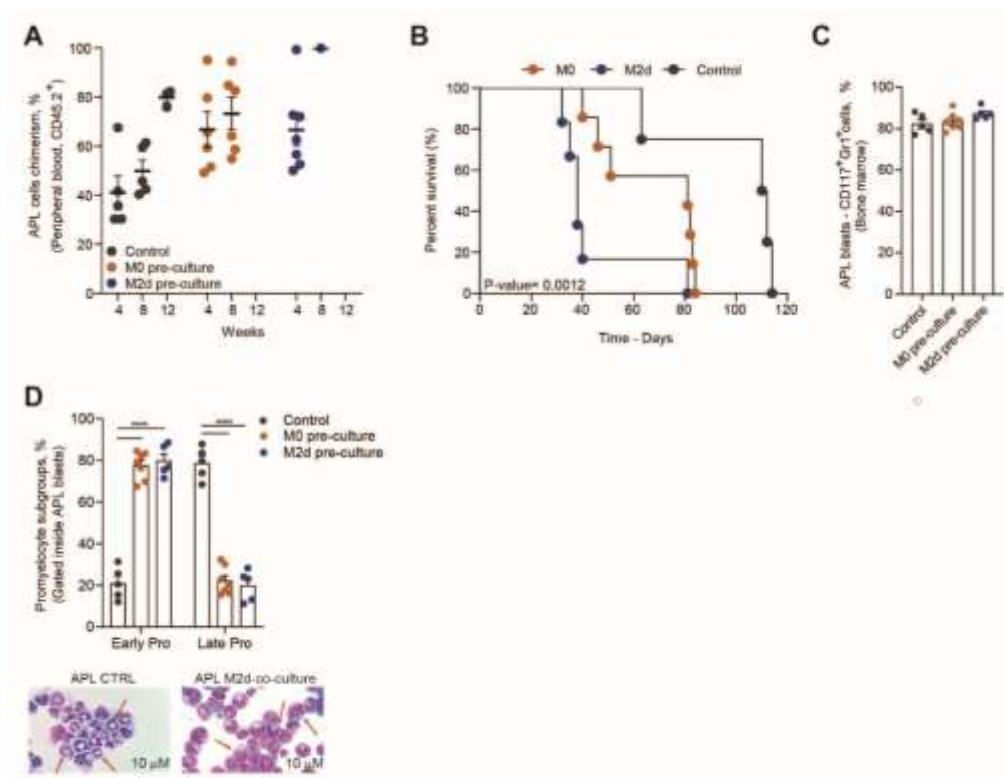


**Figure 15.** (A) Dot plot graph showing the murine CD45.2 chimerism level of mice transplanted with murine primary APL blast cells (from hCG-PML-RARA mice – CD45.2) alone (control) or pre-cultured on either M0 or M2 murine macrophages inside sub-lethally irradiated (350 cGy) C57BL/6J.PepBoy recipients (CD45.1). (B) Overall survival analysis of C57BL/6J transplanted with murine primary APL blast cells alone or pre-cultured on either M0 or M2 murine macrophages. (C) Murine APL blast cells defined by murine CD117<sup>+</sup> and Gr1<sup>+/int</sup> detected in the BM of mice transplanted with murine primary APL blast cells alone or pre-cultured on either M0 or M2 murine macrophages post-sacrifice. (D) Bar graph showing the frequency of early (CD117<sup>+</sup>Gr1<sup>+</sup>CD34<sup>+</sup>CD16/32<sup>-</sup>) and late promyelocytes (CD117<sup>+</sup>Gr1<sup>+</sup>CD34<sup>+</sup>CD16/32<sup>+</sup>) of mice transplanted with murine primary APL blast cells alone or pre-cultured on either M0 or M2 murine macrophages post-sacrifice.

(A-D) Each dot represents an individual mouse

(B) Survival curves were plotted using the Kaplan-Meier method and compared by the log-rank test.

One-way (C) or two-way (D) analysis of variance (ANOVA).

#### 4.5 “Trained” AML/APL blasts are protected against phagocytosis, display improved homing capacity, and adapt a more OXPHOS-like state

Considering that a substantial fraction of leukemic cells was phagocytosed after a two-day co-culture on M2 macrophages, we questioned whether the remaining cells acquired a new mechanism of immune evasion to protect themselves against phagocytosis. Although NSGS mice lack an adaptive immune system, they have functional macrophages with increased phagocytic activity (THOMPSON et al., 2016), which could impede successful engraftment of primary AML cells. Moreover, the latest humanized mice model MISTRG expresses the human protein SIRP $\alpha$  to avoid phagocytosis of human cells (RONGVAUX et al., 2014). To test this hypothesis, leukemic AML blasts were co-cultured on M2 macrophages for two days after which the remaining cells were harvested and used for a new phagocytosis assay on fresh macrophages. Indeed, compared to the level of phagocytosis of uncultured cells (on average 40%) we observed a significant reduction in phagocytosis when leukemic blasts were “trained” on M2 macrophages but not on MSC (Figure 16A and data not shown). Usual suspects that would underlie this phenomenon could be an up-regulation of the “don’t eat me signals” CD47 (CHAO et al., 2010) or CD24 (BARKAL et al., 2019). While there was a negative correlation between AML phagocytosis and CD47 as well as CD24 expression, no increase of these markers was observed after two days on M2 macrophages or MSC (Figure 17A-C and data not shown). In contrast, we noticed that surface calreticulin (CLR), an “eat me signal” predicting better clinical outcome in AML/APL (CHAO et al., 2010) positively correlated with phagocytosis and was downregulated upon M2 co-culture as well as on MSC (Figure 16B, 17B and data not shown). A recent paper described Stanniocalcin 1 (STC1) to trap CLR in the mitochondria as a mechanism to reduce surface CLR expression and evade phagocytosis (LIN et al., 2021). When we evaluated the basal expression of *STC1* in AML patients, we detected very low transcript levels at diagnosis and a significant up-regulation upon M2 macrophages (Figure 16C). Since the expression of CLR was reduced both upon M2 and MSC co-culture, we conclude that CLR is not necessarily the main mechanism, but possibly a contributing factor promoting resistance against phagocytosis.

To obtain a more in depth understanding of underlying mechanisms we performed a whole transcriptome analysis comparing AML samples (AML=4; APL=5) at diagnosis to cells that were “trained” for 48 hrs on M2 macrophages or on MS5. Principal component analyses revealed that the strongest transcriptional changes occurred in leukemic blast cells cultured on M2 macrophages, while MS5 cultured cells clustered in between diagnosis and M2 samples

(Figure 16D). When we compared the differentially expressed genes between all the groups, we found 829 genes that were specifically up regulated in M2-exposed AML samples (Figure 16E). Gene ontology (GO) and gene set enrichment analyses (GSEA) revealed that M2 cultured AML cells were significantly enriched for the terms cell migration, oxidative phosphorylation (OXPHOS) and positive regulation of pro-survival/proliferation pathways. Terms which negatively correlated with M2 cultured AML cells were apoptosis and cell cycle arrest (Figure 16F).

One of the several hurdles AML blast cells must overcome after transplantation is to find their niche. Since cell migration was one of the GO terms associated with M2 cultured AML blast cells, we performed an in vivo homing assay. Indeed, we observed better homing of APL cells to the BM when exposed to M2 macrophages compared to uncultured cells of the same patient (Figure 16G). Using the same APL and additional AML samples, we detected similar results in an in vitro transwell migration assay (Figure 17D). Concurrently, we detected enhanced surface expression of the adhesion receptors CD49d (%) and an increase of the CD49d-f mean fluorescence intensity upon M2 co-cultured versus AML diagnosis (Figure 16H and 17E). Furthermore, APL blast cells harvested from of primary and secondary transplants presented with increased CD49d expression (Figure 17F).

Furthermore, we functionally evaluated the changes in cellular metabolism of leukemic cells after M2 macrophage co-culture. Seahorse measurements confirmed that the functional respiration and extracellular acidification rate were enhanced in HL60 cells and primary AML samples (n=11) when co-cultured on M2 macrophages compared to MS5 (Figure 16I and 18A-B). The increased basal and maximum oxygen consumption rate (OCR) could suggest enhanced mitochondrial metabolism, which prompted us to determine whether macrophages can transfer mitochondria to primary AML cells as reported for MSC cells (MOSCHOI et al., 2016), schematically depicted in Figure 16J. AML cell lines and primary AML cells were co-cultured for 48hrs on mitochondria labeled M2 macrophages or MS5 cells. FACS analysis revealed an efficient mitochondrial transfer from M2 macrophages to leukemic blasts, which was more efficient compared to mitochondrial exchange from MS5 cells (Figure 16J and 18C). Real-time qPCR evaluation of the mitochondrial DNA content further confirmed mitochondrial transfer (Figure 18D). Fatty acid oxidation (FAO) is one of the main mechanisms used by macrophages to fuel the tricarboxylic acid cycle, culminating in M2 polarization (NOMURA et al., 2016). To evaluate whether FAO is the driver of OXPHOS in M2-exposed AML cells we treated M2 macrophages with etomoxir (Eto) for 24h. After 24h macrophages were washed and co-cultured with primary AML cells for 24h to measure their functional respiration. Eto-treated M2

macrophages exhibited decreased OCR (Figure 18E). Moreover, HL60 and primary AML cells co-cultured on Eto-treated macrophages displayed decreased OCR compared to vehicle, although no changes in the mitochondrial potential were observed in the AML cells (Figure 16K and 18F-G). These data indicate that FAO-driven respiration in M2 macrophages can be hijacked by leukemic cells via mitochondrial transfer to drive their own metabolic demands. In contrast, AML cells co-cultured on Eto-treated MS5 cells remained unaffected (Figure 16K). Enhanced FAO metabolism has been linked to AML drug resistance (FARGE et al., 2017). Notably, Steven et al., showed that LSC cells that are more reliant on FAO are also resistant to VEN (STEVENS et al., 2020). Treatment with Eto plus VEN in M2 macrophages, but not in MS5 cells, resulted in decreased OCR of VEN insensitive primary AML cells and HL60 (Figure 16K and 18H). Altogether, our data suggests that the macrophage-supported resistance to VEN in AML, can be circumvented by the FAO inhibition in the TME.

Finally, we assessed the long-term effects of macrophages on leukemic cells by evaluating the colony unit formation and proliferation capacity post macrophage exposure compared to MS5. Two day “training” on M2 macrophages significantly increased colony formation capacity and endowed AML cells with long term proliferation in liquid cultures (Figure 16L). In summary, our data indicate that macrophages can support leukemogenesis via several biological pathways contributing to a more aggressive nature of the disease.

**Figure 16. M2 macrophages reprogram primary AML cells via different biological pathways**

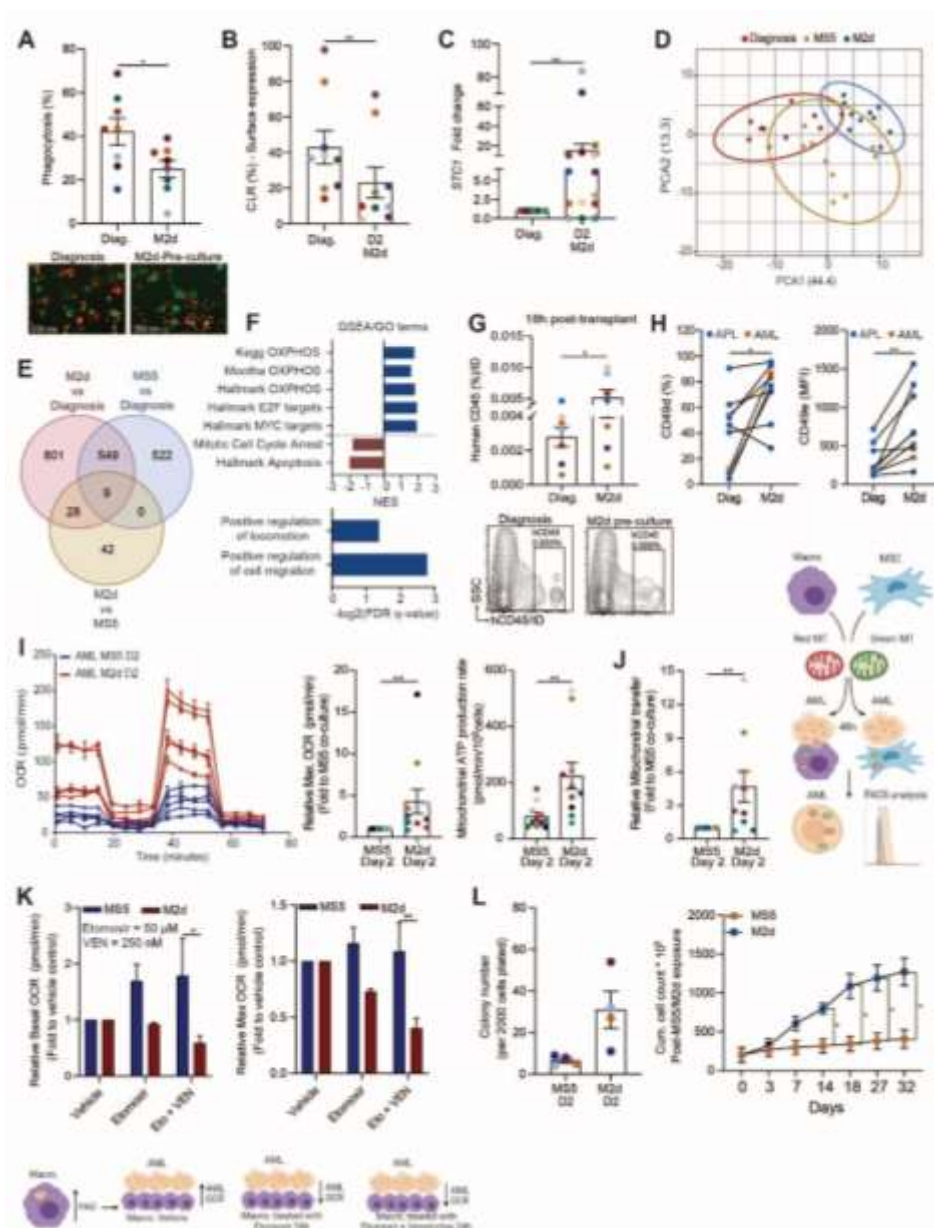


**Figure 16.** (A) Phagocytosis of primary AML at diagnosis and after a 48h co-culture on M2 macrophages. (B) Protein expression of Calreticulin (CLR) measured on primary AML cells at diagnosis and after a 48h co-culture on M2 macrophages. (C) *STC1* gene expression measured in primary AML samples at diagnosis and after a 48h co-culture on M2 macrophages. Data is plotted as a fold change to diagnosis. (D) PCA plot of primary AML transcriptomes at diagnosis and after a 48h co-culture on MS5 or M2d macrophages. (E) Venn diagram depicting up-regulated genes (F) GSEA and GO terms of genes exclusively up-regulated upon M2 co-culture. (G) Human CD45 (%) detected in the BM after 18h post-transplant when mice were injected with diagnosis APL samples or after a 48h co-culture on M2 macrophages. Representative FACS plot. (H) CD49d (%) and CD49e (MFI levels) in primary APL/AML samples at diagnosis and after a 48h co-culture on M2 macrophages. (I) Oxygen consumption rate (OCR) of primary AML blasts exposed to either MS5 or M2 macrophages for 48h. (J) Mitochondrial (mt) transfer measured in primary AML cells after being exposed to mt labelled MS5 and M2 cells for 48h. Experimental scheme. (K) OCR of primary AML blasts exposed to either MS5 or M2 cells pre-treated with vehicle, etomoxir or etomoxir+VEN for 24h. (L) Colony formation of primary AML blasts (methylcellulose) scored after 14 days. Cumulative cell count in liquid culture of primary AML cells exposed to either MS5 or M2 macrophages for 48h.

(A-C; G-I and L) Wilcoxon signed rank test (2-sided). \* $P < 0.05$ , \*\* $P < 0.01$ , \*\*\* $P < 0.001$ . Two-way (K and L) analysis of variance (ANOVA). \* $P < 0.05$ , \*\* $P < 0.01$ .

**Figure 17. Co-culture of AML blasts with M2 macrophages reprogram AML cells via different biological process**

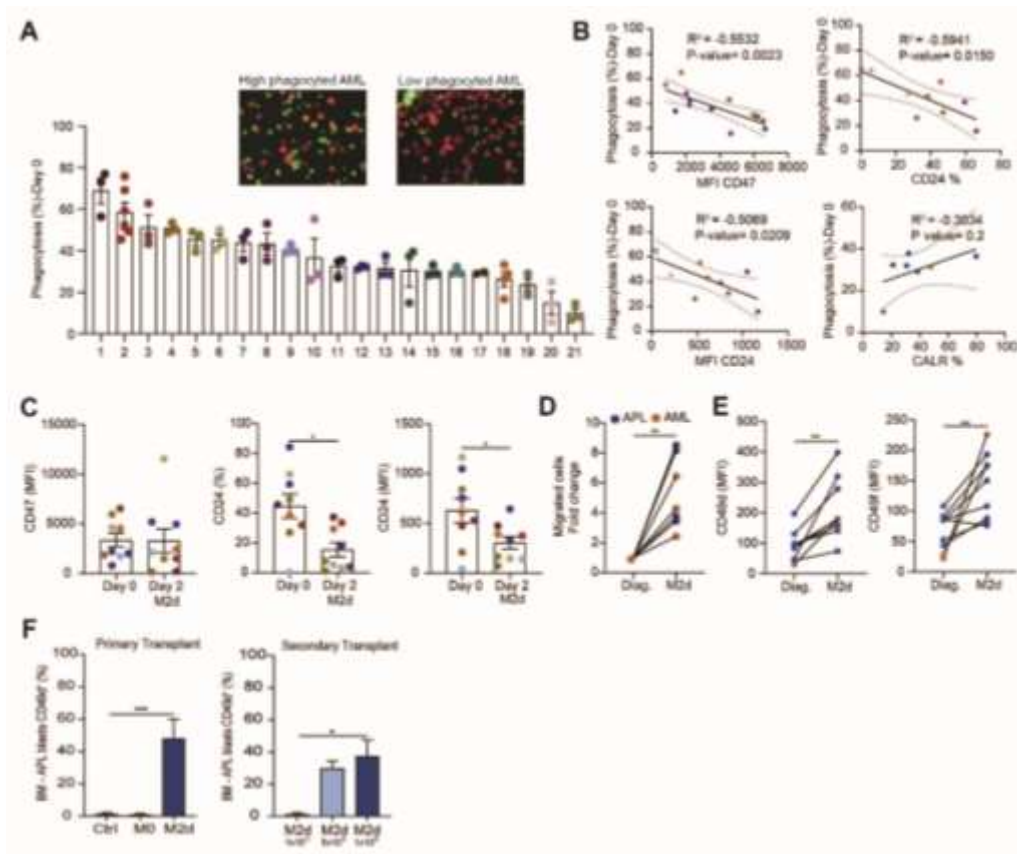


**Figure 17.** (A) Bar graph showing the level of primary AML phagocytosis at diagnosis (day 0) on non-polarized (M0) macrophages. Representative pictures of low and high phagocytosed AML cells. Macrophages are labelled in red (CD11b-AF594) and tumor cells in green (CellTrace™ CFSE Cell proliferation AF488). (B) Pearson correlation graphs between the level of phagocytosis measured at diagnosis and the CD47 and CD24 MFI level as well as the percentage of CD24 and Calreticulin measured on the respective AML blast population ( $SSC^{\text{low}}CD45^{\text{dim}}CD34^+$  or  $CD117^+$  for  $CD34^-$  AMLs). MFI= Mean intense fluorescence, CLR=Calreticulin. (C) Bar graph showing the MFI of CD47/CD24 and CD24 percentage at diagnosis and after two-day co-culture on M2 macrophages. (D) Dot plot graph showing the fold change to diagnosis of APL/AML cells migrated post M2 macrophage exposure for 48h. Migration assay was performed using Trans well system, with healthy MSCs plated in the lower chamber (Passage 4) (E) MFI levels of CD49d and CD49f measured in primary AML and APL blasts ( $CD45^+CD34^+$  for AML samples and  $CD45^+CD117^+$  for APL samples) cells at diagnosis and after a 2 day co-culture on M2 macrophages. (F) Percentage of CD49d measured in human APL blasts ( $CD45^+CD117^+CD33^+$ ) cells post-sacrifice of primary and secondary APL xenograft.

(A) Each dot represents a different counted field  
 (C) Each dot represents an independent AML patient.  
 (C-E) Wilcoxon signed rank test (2-sided) \* $P < 0.05$ .  
 One-way (F) analysis of variance (ANOVA).

**Figure 18. M2 macrophages reprogram primary AML cells via different biological pathways**

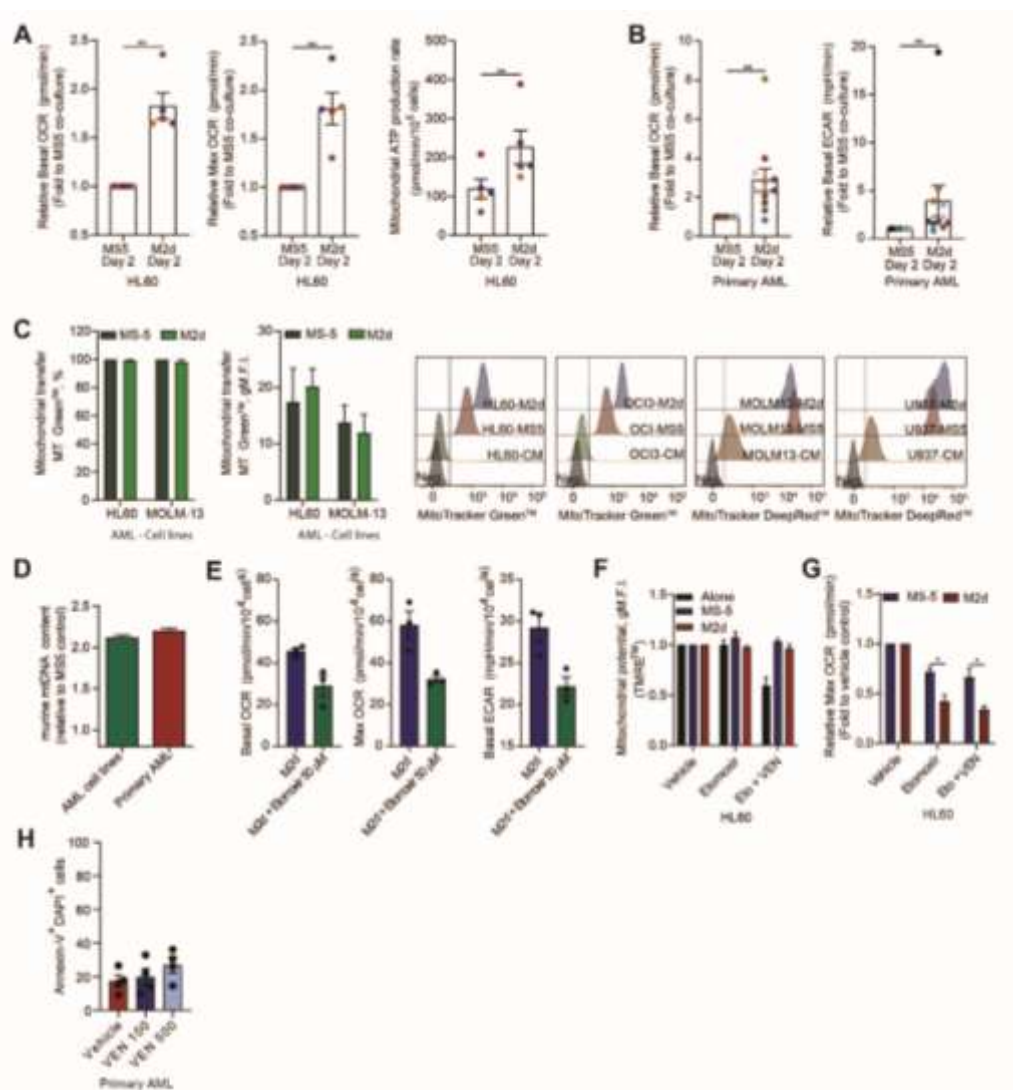


**Figure 18.** (A) Bar graph of basal and maximum oxygen consumption rate (OCR) of HL60 cells after two day co-culture on MS5 cells and M2 macrophages. (B) Bar graph of OCR and extracellular acidification rate (ECAR) of primary AMLs after two day co-culture on MS5 cells and M2 macrophages. (C) Mitochondrial transfer measured in HL60 and MOLM13 cells after co-culture on mitochondrial labelled MS5 cells and M2 macrophages. MS5 and M2 macrophages were labelled with MitoTracker Green™ and DeepRed™ for 15 min and incubated for 48 hours to remove potential dye leakage. Conditioned medium (CM) of stained macrophages were used as negative control of unspecific staining. Mitochondrial transfer was determined by measuring the MitoTracker in the AML cell lines. Representative histogram showing the mitochondrial content and mass (Right panels). (D) Evaluation by real-time quantitative polymerase chain reaction of murine mitochondrial DNA content on AML cell lines (MOLM13, HL60, U937 and OCI-AML3) and primary AML samples after 48h of co-cultures with MS5 and M2 macrophages. Values are normalized to MS5 control cells (E) Basal, maximum OCR and ECAR of M2 macrophages treated with vehicle (DMSO) or etomoxir (50  $\mu$ M). (F) Mitochondrial potential of HL60 cells cultured on either MS5 or M2 cells pre-treated with vehicle, etomoxir (50  $\mu$ M) or etomoxir (50  $\mu$ M) + VEN (250 nM) for 24h. (G) Maximum OCR of HL60 cells cultured on either MS5 or M2 cells pre-treated with vehicle, etomoxir or etomoxir + VEN for 24h. (H) Percentage of viable primary AML cells when cultured in the presence of venetoclax (100 and 500 nM).

(A-B and H) Each dot represents an independent AML patient.

(E) Each dot represents an independent experiment

(D and F-G) Represent at least 3 biological replicates for all experiments.

(A-C and E) Wilcoxon signed rank test (2-sided) \*\* $P < 0.01$ .

One-way (H) or two-way (F-G) analysis of variance (ANOVA).



#### 4.6 Development of a poor prognosis M2 macrophage signature

Given the deteriorating M2-mediated effects observed in AML it would be of interest to incorporate the characterization of macrophages as a predictive marker in the routine diagnostics of AML. To reduce the ciphersort M2 macrophage signature defined by over 500 genes, we generated a new simplified and clinically applicable M2 signature by selecting genes exclusively expressed by M2 macrophages (92 genes) from four different datasets (FANTON, BLUEPRINT, CIBERSORT and HPCA) (Figure 19A). From these 92, 10 genes could predict OS in at least 2 AML cohorts (Figure 19B). Next, we determined whether these 10 genes were differentially expressed between the paired CD34<sup>+</sup> or CD34<sup>-</sup> compartments of AML patients (Figure 19C). Together with *MRC1* and *CD163* (M2-markers–validated in this study) we identified *CD52*, *FGR*, *GASK1B* and *RASA3* to be potential M2 markers in AML (Figure 19C). When we tested the specificity of our signature, we confirmed that our new M2-UMCG signature could predict OS and DFS survival in a “training” cohort (TCGA). Moreover, ROC curve analysis indicated superior OS prediction compared to the M2 ciphersort signature and the ELN2010 risk stratification (Figure 19D-E). We also confirmed that our signature is specific for M2 macrophages (Figure 19F) and validated our results in the BeatAML cohort (Figure 19G-H).

Finally, we took advantage of the ex-vivo drug screen performed in the BeatAML study to determine the drug efficiency in patients with high and low M2-UMCG signature. High M2-UMCG signature was associated with resistance to pan-kinase inhibitors, while low M2 signature was associated with increased sensitivity to MEK inhibitors (Figure 19I). Hence, the quantification and classification of M2 macrophages could improve AML risk stratification in AML clinics.

Figure 19. Development of a M2 signature for AML patients

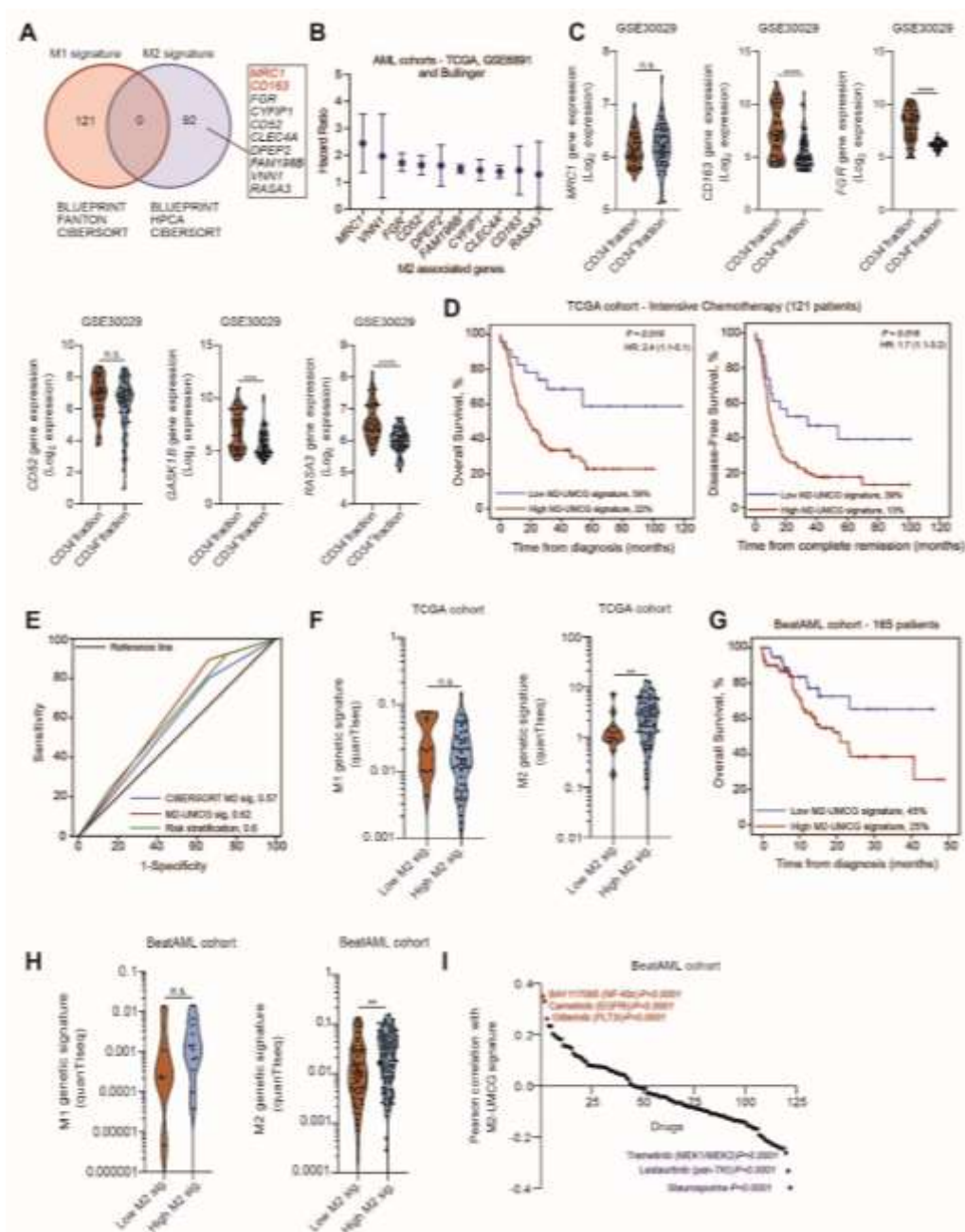


**Figure 19.** (A) Venn diagram of genes exclusively expressed by M1 and M2 macrophages using the BLUEPRINT, FANTOM, HPCA and CIBERSORT datasets. (B) Forest plot depicting the HR of each M2-associated gene (n=10) able to predict OS in at least 2 AML cohorts. (C) Violin plot showing the expression of M2 genes in the CD34<sup>-</sup>/CD34<sup>+</sup> compartments. (D) KM analysis of OS and DSF using the M2-UMCG signature in the TCGA cohort. (E) Area under receiver operating characteristic (AUROC) curve plot of the predictive capacity of the M2-UMCG signature (red curve) versus the CIBERSORT M2 signature (blue curve) and the ELN2010 risk stratification (green curve) for OS. AUROC=1 would denote perfect prediction and AUROC=0.5 would denote no predictive ability (F) Violin plot showing the levels of M1 and M2 macrophages measured by QuanTIseq according to the M2-UMCG signature groups in the TCGA cohort. (G) KM analysis of OS using the M2-UMCG signature in the BeatAML cohort. (H) Violin plot showing the levels of M1 and M2 macrophages measured by QuanTIseq according to the M2-UMCG signature groups in the BeatAML cohort. (I) Pearson correlation between the M2-UMCG signature and the *ex vivo* drug screening of the BeatAML cohort.

(D and G) Patients were dichotomized into low and high M2-UMCG signature. Survival curves were estimated using the KM method, and the log-rank test was used for comparison.

(C, F and H) Mann-Whitney test. \*\*P < 0.01, \*\*\*P < 0.0001, NS, not significant.

*Discussion*

---

## 5 DISCUSSION

We characterized the macrophage landscape in AML and demonstrate the pro-tumorigenic effects of M2 macrophages on leukemia progression. Clear heterogeneity exists in the macrophage landscape across different AML patients, whereby patients with the poorest prognosis have the highest expression of M2 markers. *In vitro*, M2 macrophages support proliferation and mediate drug resistance. *In vivo*, we show that presence of M2 macrophages transform poorly engrafting AML patient samples into fatal leukemia in xenograft models. The M2 pro-leukemogenic effects are most likely multifactorial contributing to immune evasion, AML homing, metabolic reprogramming and enhanced stemness as well as proliferation.

Being an essential part of the TME of solid tumors, TAMs are often associated with poor prognosis due to their pro-tumorigenic functions promoting proliferation, dissemination, and immune evasion of cancer cells (PASSLICK; FLIEGER; ZIEGLER-HEITBROCK, 1989). *In vivo* intra-BM co-injection of M2-macrophages allowed the induction of full-blown leukemia, while APL patient cells were unable to expand in NSGS mice without co-injected macrophages. The leukemic burden was consistently superior in M2 injected bones compared to M0-bones, suggesting that in particular M2-type macrophages provide the leukemia-propagating signals. Perhaps even more intriguingly, even a two-day *in vitro* exposure of APL blasts to M2-macrophages - which we refer to as “training” - allowed efficient engraftment followed by fatal leukemia in NSGS mice. Apparently, the fate of leukemic blasts when encountering M2-macrophages can be two-fold: either they are phagocytosed, or they are altered in such a way that their leukemic potential has increased. Chao et al., showed that the process of programmed cell removal relies on an equilibrium of pro and anti-phagocytic signals (CHAO et al., 2010). We find that remaining cells after the two day “training” are protected against phagocytosis. Indeed, NSG mice do have functional macrophages with increased phagocytic activity (THOMPSON et al., 2016), which could impede successful engraftment of primary AML cells. While we did not observe an increase of “don’t eat me” signals, CLR expression was decreased after the two-day “training”. In line, we find enhanced expression of STC1, which can trap CLR in the mitochondria as a mechanism of immune evasion (LIN et al., 2021). Furthermore, also  $\alpha$ -integrins have been identified to regulate the expression of surface CLR in T-lymphoblasts during immunogenic cell death. The authors demonstrate increased binding of CLR to the  $\alpha$ -integrin GFFKR motif preventing translocation of CLR from the cytosol to the surface upon  $\alpha$ -integrin activation (LIU et al., 2016). We show that M2 macrophages can upregulate the protein expression of CD49d-f on AML cells, which could be

partly responsible for the reduction of surface CLR. Moreover, integrins play an essential role during HSC homing and engraftment (SUBRAMANIAN et al., 2005; YAHATA et al., 2003). Studies, which either deleted or blocked CD49d demonstrated decreased homing and engraftment of HSPCs, even when CD34<sup>+</sup> cells were directly injected into the BM (YAHATA et al., 2003). In line with this notion, we demonstrate that M2-exposed primary APL cells acquire improved homing capacities in vivo, and it is conceivable that the up-regulation of integrins further facilitates APL engraftment and leukemogenesis.

While our data show that conditioned medium of M2 macrophages can improve primary AML cell growth, these effects were not as prominent as when AML cells were placed into direct contact with macrophages. Thus, it is possible that direct cell-to-cell contacts with M2-macrophages are critically important to improve the transformation potential of leukemic blasts. A study published by Hur et al. indicated that LT-HSC quiescence is facilitated by the crosstalk of CD82 expressed by LT-HSC interacting with DARC<sup>+</sup> macrophages (HUR et al., 2016). More recently, Wattrus et al. showed that the depletion of macrophages significantly decreased the number of HSC clones using the brainbow zebrafish model (WATTRUS et al., 2020). The authors identified CLR expressed by HSC to interact with the Lrp1ab present on macrophages. As a result, the HSC was either completely engulfed or a portion of the HSC was removed to promote HSC cell cycle progression (WATTRUS et al., 2020). The notion that malignant tumor cells can fuse with healthy somatic cells to generate a more aggressive hybrid tumor cell is not new but poorly understood (DUELLI; LAZEBNIK, 2003). Here, we show that AML blast cells can in fact uptake mitochondria from macrophages, thereby driving oxidative phosphorylation. Mitochondrial transfer from MSCs has been well described to confer chemotherapy resistance (MOSCHOI et al., 2016), which we now also demonstrate for macrophages. Accordingly, studies also showed that AMLs and especially monocytic subclones characterized by an OXPHOS-driven metabolism fueled by FAO, are more resistant to cytarabine, venetoclax and azacitidine (FARGE et al., 2017; PEI et al., 2020). More recently, Tscheng et al., functionally validated the importance of very long chain acyl-CoA dehydrogenase (VLCAD) to promote AML proliferation, clonogenic growth and engraftment (KLCO et al., 2014; MORITA et al., 2021). To overcome AML venetoclax resistance, Stevens et al., suggested to block the fatty acid transporter CTP1A using etomoxir (STEVENS et al., 2020). In our study we indeed also observe that macrophages that are initially resistant to venetoclax, become sensitive in the presence of Eto and are no longer able to alter the metabolic state of AML cells. Thus, inhibition of FAO could be clinically interesting for AML patients with high M2-profiles. Together, these data indicate that direct interactions with macrophages can have a profound impact on tumor

cell biology, in part mediated via the exchange of organelles such as mitochondria. On the other hand, it is also quite conceivable that exchange of other factors, including plasma membrane proteins, participate in the aggressive leukemic phenotype that cells adopt after exposure to M2 macrophages, which will be investigated in detail in future studies.

Congruent with the notion that AML is a highly heterogeneous disease we could classify patients based on their macrophage marker expression into the following groups: M2<sup>high</sup>M1<sup>low</sup>, M2<sup>high</sup>M1<sup>high</sup> or M2<sup>low</sup>M1<sup>high</sup>. Like previous studies we identified the M2-macrophage markers CD163 and CD206 to predict poor prognosis in AML (MEDREK et al., 2012; XU et al., 2020). Interestingly, CD163 and CD206 were not expressed by the main leukemic blast population but by a subpopulation, representing 0.08-44% of the total bulk (monocytic AMLs excluded). These differences could stem from the cell-of-origin, whereby a GMP-like AML being more mature than an HSC-like leukemia (GOARDON et al., 2011), could be equipped with the ability to form an M2-skewed myeloid support system. A recent study which employed scRNA sequencing analysis to characterize different immune components in AML identified 10 different subsets of macrophages with M2-like characteristics. Among those 10 macrophage subtypes four could be identified by our FACS panel (CD163<sup>high</sup>, CD206<sup>+</sup>, CD14<sup>high</sup> and CD16<sup>+</sup>)(GUO et al., 2021). A detailed functional understanding of these macrophage subtypes would be of interest for future studies to effectively target these AML supportive subpopulations. Here, we chose to first understand how healthy macrophages can affect the biology of AML blast cells assuming that leukemic cells are initially surrounded by healthy macrophages. Due to the inherent plasticity of macrophages, one could imagine that the malignant transformation generates AML supportive macrophages which in response promote the expansion of leukemic cells. Nevertheless, it remains to be determined whether the macrophages detected at diagnosis are wt or an intrinsic part of the leukemic clone. While in general leukemias are characterized by impaired differentiation, it has been described that some cells can escape the differentiation block (KLCO et al., 2014). A study published by Van Galen et al., isolated CD14<sup>-</sup> and CD14<sup>+</sup> from AML patients and demonstrated that solely the CD14<sup>+</sup> was able to inhibit T-cell activation suggesting immune modulatory functions. AML CD14<sup>+</sup> monocytes showed transcriptional similarities with healthy monocytes with the exception of cytotoxic gene signatures being down-regulated (VAN GALEN et al., 2019). Hence, it is conceivable that the leukemic cells can generate a tumor supportive microenvironment and raises the question whether malignant macrophages can provide even better tumor support than wild type M2-like macrophages.

Finally, with immunotherapies being on the rise, the identification of clinical predictive markers becomes indispensable. Currently, the AML risk stratification system relies on genetic alterations detected in the leukemic blast cell itself to infer the course of disease progression (KOEFFLER; LEONG, 2017). Here, we generated an M2-signature based on six M2 markers to evaluate the prognostic value of the TME. Since the TME often contributes to chemoresistance and relapse, we also correlated our M2-signature to the therapeutic efficacy of several drugs. Our results show that incorporation of TME as a clinical variable can improve AML risk stratification, facilitate the design of personalized treatment regimens, and provide the possibility of drug repurposing.

### **Limitation of the study**

Here, we provide insights on the AML macrophage landscape and their impact on leukemogenesis using primary in vitro co-culture systems and patient derived xenograft models by using healthy macrophages. While it is true that the bone marrow is initially surrounded by healthy macrophages, our study did not functionally define primary AML patient derived macrophages. In addition to a functional characterization, it will be important to perform an in-depth analysis on a single cell level on wild-type endogenous and AML mutant macrophages to determine the transcriptional overlap as well as on leukemic cells exposed to macrophages to capture in more detail the biological changes. Within this context, it is also important to note that as for other adherent stromal cells, it is possible that the current technique used, being a bone marrow aspirate, possibly only allows the study of a certain macrophage subpopulation. Furthermore, although our data shows that the exchange of mitochondria is possible between macrophages and AML cells, future studies will determine whether other proteins such as plasma membrane are exchanged or if the macrophage co-culture generates a hybrid cancer/macrophage cell. Finally, it is not demonstrated whether the metabolic changes acquired by AML cells upon macrophage co-culture persist over time and thereby contributes to the engraftment of primary APL cells.

***Conclusion***

---



## 6 CONCLUSION

Taking into account our results we can draw the following conclusions:

- In AML PB/BM samples
  - The expression of macrophage markers primarily emerges from a more mature myeloid subpopulation ;
  - The expression of macrophage markers varies across different AML patients;
  - The high expression of M2 marker detected in a more mature myeloid subpopulation can predict overall and disease-free survival in AML patients.
  
- The effect of M1 and M2 macrophages *in vitro*
  - The presence of M1 macrophages reduces AML cells proliferation and induces AML cell death;
  - The presence of M2 macrophages promotes AML survival and protects AML cells from drug induced apoptosis;
  - The co-culture of primary AML cells with macrophages repolarizes M1 into M2 macrophages.
  
- The effect of M2 macrophages *in vivo*
  - The intra-BM injection of M2 macrophages allows primary APL engraftment and progression in NSG mice;
  - The pre-culture and subsequent transplant of primary APL cells on M2 macrophages induces full-blown leukemia in NSG mice;
  - The biological effect induced on primary APL blast cells upon co-culture are maintained in a secondary transplant and present increased frequency of leukemic stem cells;
  - In line with human primary APL cells, murine primary APL cells initiate a more aggressive form of APL when pre-cultured on M2 macrophages and present a high frequency of early promyelocytes.

- The biological changes of AML cells when co-cultured on M2 macrophages
  - Primary AML cells co-cultured on M2 macrophages become resistant against phagocytosis;
  - Transcriptome analysis of primary AML cells co-cultured on M2 macrophages are enriched for the GO term cell migration and GSEA term OXPHOS compared to diagnosis or cells co-cultured on MSC cells;
  - Primary APL cells pre-cultured on M2 macrophages home better to the BM than diagnosis samples;
  - M2 macrophages transfer mitochondria to AML cell lines and primary AML samples;
  - Primary AML cells shift to a more OXPHOS-like state, which is fueled by FAO;
  - Etomoxir could be therapeutically beneficial for patients with high M2 macrophage infiltration;
  
- The clinical impact of M2 macrophages
  - The identification of good M2 prognostic markers can improve risk stratification.

***Tables***

---

## 7 TABLES

Table 1. Clinical characteristics of AML patients included

Characteristics	All patients (n=88)		
	No.	%	Median (range)
Gender			
Female	43	54.4	
Male	36	45.6	
Unknown	9	-	
Age, years			60.7 (21, 86)
18-40	10	14.5	
41-60	22	31.9	
≥60	37	53.6	
Unknown	19	-	
Leukocyte counts, ×10 <sup>9</sup> /L			61.4 (1.5, 335.6)
Platelet counts, ×10 <sup>9</sup> /L			41.5 (2, 281)
Hemoglobin, g/dL			5.8 (3.2, 11.4)
Bone marrow blasts, %			76 (3, 99)
Lactate dehydrogenase, U/dL			655.5 (197, 4632)
FAB classification			
M1	18	32.1	
M2	5	8.9	
M3	17	30.4	
M4	7	12.5	
M5	9	16.1	
Unknown	32	-	
ELN2017 risk stratification			
Favorable	15	24.2	
Intermediate	32	51.6	
Adverse	15	24.2	
Unknown	26	-	
<i>FLT3</i> mutational status			
Non-mutant	35	57.4	
ITD/TKD mutant	25	42.6	
Missing	26	-	
HSCT status			
Yes	39	66.1	
No	20	33.9	
Unknown	29	-	

Characteristics	All patients (n=88)		
	No.	%	Median (range)
Treatment scheme			
Intensive chemotherapy (3+7)	48	76.2	
Hypomethylating agents	12	19	
Best supportive care	3	4.8	
Unknown	25	-	
Treatment response			
CHR	42	72.4	
CRi	7	12.1	
No response/refractory	9	15.5	
Unknown	30	-	
Relapse status			
Relapse	15	25	
Non-relapse	45	75	
Unknown	28	-	
Survival status			
Dead	48	70.6	
Alive	20	29.4	
Unknown	20	-	
Macrophage clusters			
High M2 macrophage	39	45.2	
Low M2 macrophage	49	54.8	

FAB, French-American-British classification; ELN, European Leukemia-Net; *FLT3*, Fms Related Receptor Tyrosine Kinase 3 gene; ITD, Internal tandem duplication; TKD, Tyrosine kinase domain; HSCT, Hematopoietic stem cell transplant; CHR, Complete hematological remission; CRi, Incomplete remission

**Table 2. Univariable and multivariable analyses**

End point	Model variables	Univariable analysis				Multivariable analysis			
		HR	95% CI		P-value	HR	95% CI		P-value
OS (n=28)	Macrophage clusters: high M2 vs low M2	2.52	1.003	6.36	0.04	2.74	1.01	7.4	0.04
	ELN2017-risk stratification: Favorable vs intermediate vs Adverse	1.48	0.69	3.13	0.305	2.16	0.97	4.75	0.057
	Age at diagnosis: continuous variable	1.03	0.99	1.07	0.098	1.01	1.004	1.12	0.035
DFS (n=20)	Macrophage clusters: high M2 vs low M2	3.47	1.15	10.47	0.027	3.23	1.03	10.07	0.043
	ELN2017-risk stratification: Favorable vs intermediate vs Adverse	0.83	0.35	1.96	0.677	1.33	0.52	3.41	0.543
	Age at diagnosis: continuous variable	1.03	0.99	1.08	0.121	1.05	0.98	1.12	0.117

NOTE. Hazard ratios (HRs) > 1 or < 1 indicate an increased or decreased risk, respectively, of an event for the first category listed. Abbreviations: OS, overall survival; DFS, disease-free survival; ELN, European Leukemia-Net; HR, hazard ratio.

## *References*

---

## 8 REFERENCES

ADOLFSSON, Jörgen et al. Identification of Flt3+ lympho-myeloid stem cells lacking erythro-megakaryocytic potential: A revised road map for adult blood lineage commitment. **Cell**, [S. l.], v. 121, n. 2, p. 295–306, 2005. DOI: 10.1016/j.cell.2005.02.013.

ADOLFSSON, Jörgen; BERGE, Ole Johan; BRYDER, David; THEILGAARD-MÖNCH, Kim; ÅSTRAND-GRUNDSTRÖM, Ingbritt; SITNICKA, Ewa; SASAKI, Yutaka; JACOBSEN, Sten E. W. Upregulation of Flt3 expression within the bone marrow Lin-Sca1+c-kit+ stem cell compartment is accompanied by loss of self-renewal capacity. **Immunity**, [S. l.], v. 15, n. 4, p. 659–669, 2001. DOI: 10.1016/S1074-7613(01)00220-5.

AKASHI K; TRAVER D; MIYAMOTO T; IL, Weissman. A clonogenic common myeloid progenitor that gives rise to all myeloid lineages. **Nature**, [S. l.], v. 404, n. 6774, p. 193–197, 2000.

AL-MATARY, Yahya S. et al. Acute myeloid leukemia cells polarize macrophages towards a leukemia supporting state in a growth factor independence 1 dependent manner. **Haematologica**, [S. l.], v. 101, n. 10, p. 1216–1227, 2016. DOI: 10.3324/haematol.2016.143180.

ANA CUMANO; FRANCOISE DIETERIAN-LIEVRE; ISABELLE GODIN. Lymphoid Potential, Probed before Circulation in Mouse, Is Restricted to Caudal Intraembryonic Splanchnopleura. **Cell**, [S. l.], v. 86, p. 907–916, 1996. Disponível em: [http://ac.els-cdn.com/S009286740080166X/1-s2.0-S009286740080166X-main.pdf?\\_tid=97a5d510-7d49-11e7-92bf-00000aacb362&acdnat=1502314249\\_f55a839e9bc65ebb1efad0d5c1f60608](http://ac.els-cdn.com/S009286740080166X/1-s2.0-S009286740080166X-main.pdf?_tid=97a5d510-7d49-11e7-92bf-00000aacb362&acdnat=1502314249_f55a839e9bc65ebb1efad0d5c1f60608).

AZAD, Abul K.; RAJARAM, Murugesan V. S.; SCHLESINGER, Larry S. Exploitation of the Macrophage Mannose Receptor (CD206) in Infectious Disease Diagnostics and Therapeutics. **Journal of cytology & molecular biology**, [S. l.], v. 1, n. 1, p. 1–5, 2014. DOI: 10.13188/2325-4653.1000003. Disponível em: <http://www.ncbi.nlm.nih.gov/pubmed/24672807> <http://www.pubmedcentral.nih.gov/articlerender.fcgi?artid=PMC3963702>.

BARKAL, Amira A. et al. CD24 signalling through macrophage Siglec-10 is a target for cancer immunotherapy. **Nature**, [S. l.], v. 572, n. 7769, p. 392–396, 2019. DOI: 10.1038/s41586-019-1456-0.

BENNETT, J. M.; CATOVSKY, D.; DANIEL, Marie-Therese -T; FLANDRIN, G.; GALTON, D. A. G.; GRALNICK, H. R.; SULTAN, C. Proposals for the Classification of the Acute Leukaemias French-American-British (FAB) Co-operative Group. **British Journal of Haematology**, [S. l.], v. 33, n. 4, p. 451–458, 1976. DOI: 10.1111/j.1365-2141.1976.tb03563.x.



BENVENISTE, Patricia; FRELIN, Catherine; JANMOHAMED, Salima; BARBARA, Mary; HERRINGTON, Robert; HYAM, Deborah; ISCOVE, Norman N. Intermediate-Term Hematopoietic Stem Cells with Extended but Time-Limited Reconstitution Potential. **Cell Stem Cell**, [S. l.], v. 6, n. 1, p. 48–58, 2010. DOI: 10.1016/j.stem.2009.11.014. Disponível em: <http://dx.doi.org/10.1016/j.stem.2009.11.014>.

BEZERRA, M. F. et al. Co-occurrence of DNMT3A, NPM1, FLT3 mutations identifies a subset of acute myeloid leukemia with adverse prognosis. **Blood**, [S. l.], v. 135, n. 11, 2020. DOI: 10.1182/blood.2019003339.

BISWAS, Subhra K.; MANTOVANI, Alberto. Macrophage plasticity and interaction with lymphocyte subsets: Cancer as a paradigm. **Nature Immunology**, [S. l.], v. 11, n. 10, p. 889–896, 2010. DOI: 10.1038/ni.1937.

BLACKETT, N. M.; NECAS, E.; FRINDEL, E. Diversity of haematopoietic stem cell growth from a uniform population of cells. **Nature**, [S. l.], v. 322, n. 6076, p. 289, 1986. DOI: 10.1038/322289a0.

BOYER, Scott W.; SCHROEDER, Aaron V.; SMITH-BERDAN, Stephanie; FORSBERG, E. Camilla. All Hematopoietic Cells Develop from Hematopoietic Stem Cells through Flk2/Flt3-Positive Progenitor Cells. **Cell Stem Cell**, [S. l.], v. 9, n. 1, p. 64–73, 2011. DOI: 10.1016/j.stem.2011.04.021. Disponível em: <http://dx.doi.org/10.1016/j.stem.2011.04.021>.

BUENROSTRO, Jason D.; CORCES, M. Ryan; LAREAU, Caleb A.; WU, Beijing; SCHEP, Alicia N.; ARYEE, Martin J.; MAJETI, Ravindra; CHANG, Howard Y.; GREENLEAF, William J. Integrated Single-Cell Analysis Maps the Continuous Regulatory Landscape of Human Hematopoietic Differentiation. **Cell**, [S. l.], v. 173, n. 6, p. 1535–1548.e16, 2018. DOI: 10.1016/j.cell.2018.03.074. Disponível em: <https://doi.org/10.1016/j.cell.2018.03.074>.

CABEZAS-WALLSCHEID, Nina et al. Identification of regulatory networks in HSCs and their immediate progeny via integrated proteome, transcriptome, and DNA methylome analysis. **Cell Stem Cell**, [S. l.], v. 15, n. 4, p. 507–522, 2014. DOI: 10.1016/j.stem.2014.07.005.

CHAO, Mark P. et al. Calreticulin is the dominant pro-phagocytic signal on multiple human cancers and is counterbalanced by CD47. **Science Translational Medicine**, [S. l.], v. 2, n. 63, 2010. DOI: 10.1126/scitranslmed.3001375.

CHEN, Xiaowei et al. Bone Marrow Myeloid Cells Regulate Myeloid-Biased Hematopoietic Stem Cells via a Histamine-Dependent Feedback Loop. **Cell Stem Cell**, [S. l.], v. 21, n. 6, p. 747–760.e7, 2017. DOI: 10.1016/j.stem.2017.11.003. Disponível em: <https://doi.org/10.1016/j.stem.2017.11.003>.

CHOI, Kyunghye; KENNEDY, Marion; KAZAROV, Alexander; PAPADIMITRIOU, John C.; KELLER, Gordon. A common precursor for hematopoietic and endothelial cells. **Development**, [S. l.], v. 125, n. 4, p. 725–732, 1998. DOI: 10.1242/dev.125.4.725.

CHOW, Andrew et al. Bone marrow CD169+ macrophages promote the retention of hematopoietic stem and progenitor cells in the mesenchymal stem cell niche. **Journal of Experimental Medicine**, [S. l.], v. 208, n. 2, p. 761–771, 2011. DOI: 10.1084/jem.20101688.

CHOW, Andrew et al. CD169 + macrophages provide a niche promoting erythropoiesis under homeostasis and stress. **Nature Medicine**, [S. l.], v. 19, n. 4, p. 429–436, 2013. DOI: 10.1038/nm.3057.

CHRISTENSEN, Julie L.; WEISSMAN, Irving L. Flk-2 is a marker in hematopoietic stem cell differentiation: A simple method to isolate long-term stem cells. **Proceedings of the National Academy of Sciences of the United States of America**, [S. l.], v. 98, n. 25, p. 14541–14546, 2001. DOI: 10.1073/pnas.261562798.

CHUNG, Yun Shin; ZHANG, Wen Jie; ARENTSON, Elizabeth; KINGSLEY, Paul D.; PALIS, James; CHOI, Kyunghee. Lineage analysis of the hemangioblast as defined by FLK1 and SCL expression. **Development**, [S. l.], v. 129, n. 23, p. 5511–5520, 2002. DOI: 10.1242/dev.00149.

COPLEY, Michael R.; BEER, Philip A.; EAVES, Connie J. Hematopoietic stem cell heterogeneity takes center stage. **Cell Stem Cell**, [S. l.], v. 10, n. 6, p. 690–697, 2012. DOI: 10.1016/j.stem.2012.05.006. Disponível em: <http://dx.doi.org/10.1016/j.stem.2012.05.006>.

DE JONGE, H. J. M. et al. Gene expression profiling in the leukemic stem cell-enriched CD34 fraction identifies target genes that predict prognosis in normal karyotype AML. **Leukemia**, [S. l.], v. 25, n. 12, p. 1825–1833, 2011. DOI: 10.1038/leu.2011.172.

DE KOUCHKOVSKY, I.; ABDUL-HAY, M. ‘Acute myeloid leukemia: A comprehensive review and 2016 update’. **Blood Cancer Journal**, [S. l.], v. 6, n. 7, 2016. DOI: 10.1038/bcj.2016.50.

DEKOTER, Rodney P.; SINGH, Harinder. Regulation of B lymphocyte and macrophage development by graded expression of PU.1. **Science**, [S. l.], v. 288, n. 5470, p. 1439–1442, 2000. DOI: 10.1126/science.288.5470.1439.

DÖHNER, Hartmut et al. Diagnosis and management of AML in adults: 2017 ELN recommendations from an international expert panel. **Blood**, [S. l.], v. 129, n. 4, p. 424–447, 2017. DOI: 10.1182/blood-2016-08-733196.

DÖHNER, Konstanze; PASCHKA, Peter. Intermediate-risk acute myeloid leukemia therapy: Current and future. **Hematology (United States)**, [S. l.], v. 2014, n. 1, p. 34–43, 2014. DOI: 10.1182/asheducation-2014.1.34.

DUELLI, Dominik; LAZEBNIK, Yuri. Cell fusion: A hidden enemy? **Cancer Cell**, [S. l.], v. 3, n. 5, p. 445–448, 2003. DOI: 10.1016/S1535-6108(03)00114-4.

EMA, Hideo; NAKAUCHI, Hiromitsu. Expansion of hematopoietic stem cells in the developing liver of a mouse embryo. **Blood**, [S. l.], v. 95, n. 7, p. 2284–2288, 2000. DOI: 10.1182/blood.v95.7.2284. Disponível em: <http://dx.doi.org/10.1182/blood.V95.7.2284>.

FALOON, Patrick; ARENTSON, Elizabeth; KAZAROV, Alexander; DENG, Chu Xia; PORCHER, Catherine; ORKIN, Stuart; CHOI, Kyunghae. Faloon P, 2000.pdf. [S. l.], v. 1941, p. 1931–1941, 2000.

FARGE, Thomas et al. Chemotherapy-resistant human acute myeloid leukemia cells are not enriched for leukemic stem cells but require oxidative metabolism. **Cancer Discovery**, [S. l.], v. 7, n. 7, p. 716–735, 2017. DOI: 10.1158/2159-8290.CD-16-0441.

FINOTELLO, Francesca et al. Molecular and pharmacological modulators of the tumor immune contexture revealed by deconvolution of RNA-seq data. **bioRxiv**, [S. l.], n. July, p. 1–20, 2017. DOI: 10.1101/223180.

FORSBERG, E. Camilla; SERWOLD, Thomas; KOGAN, Scott; WEISSMAN, Irving L.; PASSEGUÉ, Emmanuelle. New Evidence Supporting Megakaryocyte-Erythrocyte Potential of Flk2/Flt3+ Multipotent Hematopoietic Progenitors. **Cell**, [S. l.], v. 126, n. 2, p. 415–426, 2006. DOI: 10.1016/j.cell.2006.06.037.

GAILLARD, Coline; SURIANARAYANAN, Sangeetha; BENTLEY, Trevor; WARR, Matthew R.; FITCH, Briana; GENG, Huimin; PASSEGUÉ, Emmanuelle; DE THÉ, Hugues; KOGAN, Scott C. Identification of IRF8 as a potent tumor suppressor in murine acute promyelocytic leukemia. **Blood Advances**, [S. l.], v. 2, n. 19, p. 2462–2466, 2018. DOI: 10.1182/bloodadvances.2018018929.

GARCIA-PORRERO, Juan A.; GODIN, Isabelle E.; DIETERLEN-LIÈVRE, Françoise. Potential intraembryonic hemogenic sites at pre-liver stages in the mouse. **Anatomy and Embryology**, [S. l.], v. 192, n. 5, p. 425–435, 1995. DOI: 10.1007/BF00240375.

GASPARETTO, Maura et al. Targeted therapy for a subset of acute myeloid leukemias that lack expression of aldehyde dehydrogenase 1A1. **Haematologica**, [S. l.], v. 102, n. 6, p. 1054–1065, 2017. DOI: 10.3324/haematol.2016.159053.

GOARDON, Nicolas et al. Coexistence of LMPP-like and GMP-like leukemia stem cells in acute myeloid leukemia. **Cancer Cell**, [S. l.], v. 19, n. 1, p. 138–152, 2011. DOI: 10.1016/j.ccr.2010.12.012. Disponível em: <http://dx.doi.org/10.1016/j.ccr.2010.12.012>.

GRAVERSEN, Jonas Heilskov; MADSEN, Mette; MOESTRUP, Søren K. CD163: A signal receptor scavenging haptoglobin-hemoglobin complexes from plasma. **International Journal of Biochemistry and Cell Biology**, [S. l.], v. 34, n. 4, p. 309–314, 2002. DOI: 10.1016/S1357-2725(01)00144-3.

GRENIER-PLEAU, Isabelle et al. Blood extracellular vesicles from healthy individuals regulate hematopoietic stem cells as humans age. **Aging Cell**, [S. l.], v. 19, n. 11, p. 1–6, 2020. DOI: 10.1111/ace1.13245.

GUBERNATOROVA, Ekaterina O.; GORSHKOVA, Ekaterina A.; NAMAKANOVA, Olga A.; ZVARTSEV, Ruslan V.; HIDALGO, Juan; DRUTSKAYA, Marina S.; TUMANOV, Alexei V.; NEDOSPASOV, Sergei A. Non-redundant functions of IL-6 produced by macrophages and dendritic cells in allergic airway inflammation. **Frontiers in Immunology**, [S. l.], v. 9, n. NOV, p. 1–14, 2018. DOI: 10.3389/fimmu.2018.02718.

GUO, Rongqun et al. Single-cell map of diverse immune phenotypes in the acute myeloid leukemia microenvironment. **Biomarker Research**, [S. l.], v. 9, n. 1, p. 1–16, 2021. DOI: 10.1186/s40364-021-00265-0.

HAFERLACH, Claudia; DICKER, F.; HERHOLZ, H.; SCHNITTGER, S.; KERN, W.; HAFERLACH, T. Mutations of the TP53 gene in acute myeloid leukemia are strongly associated with a complex aberrant karyotype. **Leukemia**, [S. l.], v. 22, n. 8, p. 1539–1541, 2008. DOI: 10.1038/leu.2008.143.

HIRAI, Hideyo; OGAWA, Minetaro; SUZUKI, Norio; YAMAMOTO, Masayuki; BREIER, Georg; MAZDA, Osam; IMANISHI, Jiro; NISHIKAWA, Shin Ichi. Hemogenic and nonhemogenic endothelium can be distinguished by the activity of fetal liver kinase (Flk)-1 promoter/enhancer during mouse embryogenesis. **Blood**, [S. l.], v. 101, n. 3, p. 886–893, 2003. DOI: 10.1182/blood-2002-02-0655.

HUR, Jin et al. CD82/KAI1 Maintains the Dormancy of Long-Term Hematopoietic Stem Cells through Interaction with DARC-Expressing Macrophages. **Cell Stem Cell**, [S. l.], v. 18, n. 4, p. 508–521, 2016. DOI: 10.1016/j.stem.2016.01.013. Disponível em: <http://dx.doi.org/10.1016/j.stem.2016.01.013>.

IKUTA, Koichi; WEISSMAN, Irving L. Evidence that hematopoietic stem cells express. **Proc.Natl.Acad.Sci., USA**, [S. l.], v. 89, n. 4, p. 1502–1506, 1992.

ITALIANI, Paola; BORASCHI, Diana. From monocytes to M1/M2 macrophages: Phenotypical vs. functional differentiation. **Frontiers in Immunology**, [S. l.], v. 5, n. OCT, p. 1–22, 2014. DOI: 10.3389/fimmu.2014.00514.

JACOBSEN, Rebecca N. et al. Mobilization with granulocyte colony-stimulating factor blocks medullar erythropoiesis by depleting F4/80+VCAM1+CD169+ER-HR3+Ly6G+ erythroid island macrophages in the mouse. **Experimental Hematology**, [S. l.], v. 42, n. 7, p. 547-561.e4, 2014. DOI: 10.1016/j.exphem.2014.03.009. Disponível em: <http://dx.doi.org/10.1016/j.exphem.2014.03.009>.

JUSTUS, Calvin R.; LEFFLER, Nancy; RUIZ-ECHEVARRIA, Maria; YANG, Li V. In vitro cell migration and invasion assays. **Journal of Visualized Experiments**, [S. l.], n. 88, p. 1–8, 2014. DOI: 10.3791/51046.

KANTARJIAN, Hagop; KADIA, Tapan; DINARDO, Courtney; DAVER, Naval; BORTHAKUR, Gautam; JABBOUR, Elias; GARCIA-MANERO, Guillermo; KONOPLEVA, Marina; RAVANDI, Farhad. Acute myeloid leukemia: current progress and future directions. **Blood Cancer Journal**, [S. l.], v. 11, n. 2, 2021. DOI: 10.1038/s41408-021-00425-3. Disponível em: <http://dx.doi.org/10.1038/s41408-021-00425-3>.

KIM, Jin A. et al. Microenvironmental remodeling as a parameter and prognostic factor of heterogeneous leukemogenesis in acute myelogenous leukemia. **Cancer Research**, [S. l.], v. 75, n. 11, p. 2222–2231, 2015. a. DOI: 10.1158/0008-5472.CAN-14-3379.

KIM, Yonggoo et al. Genetic and epigenetic alterations of bone marrow stromal cells in myelodysplastic syndrome and acute myeloid leukemia patients. **Stem Cell Research**, [S. l.], v. 14, n. 2, p. 177–184, 2015. b. DOI: 10.1016/j.scr.2015.01.004. Disponível em: <http://dx.doi.org/10.1016/j.scr.2015.01.004>.

KLCO, Jeffery M. et al. Functional heterogeneity of genetically defined subclones in acute myeloid leukemia. **Cancer Cell**, [S. l.], v. 25, n. 3, p. 379–392, 2014. DOI: 10.1016/j.ccr.2014.01.031.

KOEFFLER, H. P.; LEONG, G. Preleukemia: One name, many meanings. **Leukemia**, [S. l.], v. 31, n. 3, p. 534–542, 2017. DOI: 10.1038/leu.2016.364. Disponível em: <http://dx.doi.org/10.1038/leu.2016.364>.

KULESSA, Holger; PROGRAMME, Differentiation; MOLECULAR, European. •• Myeloblast. [S. l.], p. 1250–1262, 1995.

LANE, Steven W.; SCADDEN, David T.; GILLILAND, D. Gary. The leukemic stem cell niche: Current concepts and therapeutic opportunities. **Blood**, [S. l.], v. 114, n. 6, p. 1150–1157, 2009. DOI: 10.1182/blood-2009-01-202606.

LAURENTI, Elisa; GÖTTGENS, Berthold. From haematopoietic stem cells to complex differentiation landscapes. **Nature**, [S. l.], v. 553, n. 7689, p. 418–426, 2018. DOI: 10.1038/nature25022.

LEY, Timothy J. et al. Genomic and epigenomic landscapes of adult de novo acute myeloid leukemia. **New England Journal of Medicine**, [S. l.], v. 368, n. 22, p. 2059–2074, 2013. DOI: 10.1056/NEJMoa1301689.

LI, Bo et al. Comprehensive analyses of tumor immunity: Implications for cancer immunotherapy. **Genome Biology**, [S. l.], v. 17, n. 1, p. 1–16, 2016. DOI: 10.1186/s13059-016-1028-7.

LI, Sheng; MASON, Christopher; MELNICK, Ari. Genetic and epigenetic heterogeneity in acute myeloid leukemia. **Current Opinion in Genetics and Development**, [S. l.], v. 36, p. 100–106, 2016. DOI: 10.1016/j.gde.2016.03.011. Disponível em: <http://dx.doi.org/10.1016/j.gde.2016.03.011>.

LIN, Heng et al. Stanniocalcin 1 is a phagocytosis checkpoint driving tumor immune resistance. **Cancer Cell**, [S. l.], v. 39, n. 4, p. 480–493.e6, 2021. DOI: 10.1016/j.ccell.2020.12.023. Disponível em: <http://dx.doi.org/10.1016/j.ccell.2020.12.023>.

LINNEKIN, Diana. Early signaling pathways activated by c-Kit in hematopoietic cells. **International Journal of Biochemistry and Cell Biology**, [S. l.], v. 31, n. 10, p. 1053–1074, 1999. DOI: 10.1016/S1357-2725(99)00078-3.

LIU, C. C.; LECLAIR, P.; MONAJEMI, M.; SLY, L. M.; REID, G. S.; LIM, C. J.  $\alpha$ -Integrin expression and function modulates presentation of cell surface calreticulin. **Cell Death and Disease**, [S. l.], v. 7, n. 6, p. 1–13, 2016. DOI: 10.1038/cddis.2016.176.

LORENZ, E.; CONGDON, C.; UPHOFF, D. Modification of acute irradiation injury in mice and guinea-pigs by bone marrow injections. **Radiology**, [S. l.], v. 58, n. 6, p. 863–877, 1952. DOI: 10.1148/58.6.863.

LOVE, Michael I.; HUBER, Wolfgang; ANDERS, Simon. Moderated estimation of fold change and dispersion for RNA-seq data with DESeq2. **Genome Biology**, [S. l.], v. 15, n. 12, p. 1–21, 2014. DOI: 10.1186/s13059-014-0550-8.

MATSUOKA, Sahoko et al. Generation of definitive hematopoietic stem cells from murine early yolk sac and paraaortic splanchnopleures by aorta-gonad-mesonephros region-derived stromal cells. **Blood**, [S. l.], v. 98, n. 1, p. 6–12, 2001. DOI: 10.1182/blood.V98.1.6.

MCDEVITT, Michael A.; SHIVDASANI, Ramesh A.; FUJIWARA, Yuko; YANG, Haidi; ORKIN, Stuart H. A “knockdown” mutation created by cis-element gene targeting reveals the dependence of erythroid cell maturation on the level of transcription factor GATA-1. **Proceedings of the National Academy of Sciences of the United States of America**, [S. l.], v. 94, n. 13, p. 6781–6785, 1997. DOI: 10.1073/pnas.94.13.6781.

MEDREK, Catharina; PONTÉN, Fredrik; JIRSTRÖM, Karin; LEANDERSSON, Karin. The presence of tumor associated macrophages in tumor stroma as a prognostic marker for breast cancer patients. **BMC Cancer**, [S. l.], v. 12, p. 1–9, 2012. DOI: 10.1186/1471-2407-12-306.

MEDVINSKY, Alexander; DZIERZAK, Elaine. Definitive hematopoiesis is autonomously initiated by the AGM region. **Cell**, [S. l.], v. 86, n. 6, p. 897–906, 1996. DOI: 10.1016/S0092-8674(00)80165-8.

MÉNDEZ-FERRER, Simón; BONNET, Dominique; STEENSMA, David P.; HASSERJIAN, Robert P.; GHOBRIAL, Irene M.; GRIBBEN, John G.; ANDREEFF, Michael; KRAUSE, Daniela S. Bone marrow niches in haematological malignancies. **Nature Reviews Cancer**, [S. l.], v. 20, n. 5, p. 285–298, 2020. DOI: 10.1038/s41568-020-0245-2. Disponível em: <http://dx.doi.org/10.1038/s41568-020-0245-2>.

METZELER, Klaus H. et al. Spectrum and prognostic relevance of driver gene mutations in acute myeloid leukemia. **Blood**, [S. l.], v. 128, n. 5, p. 686–698, 2016. DOI: 10.1182/blood-2016-01-693879.

MOESTRUP, Søren K.; MOLLER, Holger J. CD163: A regulated hemoglobin scavenger receptor with a role in the anti-inflammatory response. **Annals of Medicine**, [S. l.], v. 36, n. 5, p. 347–354, 2004. DOI: 10.1080/07853890410033171.

MORITA, Kiyomi et al. Author Correction: Clonal evolution of acute myeloid leukemia revealed by high-throughput single-cell genomics (Nature Communications, (2020), 11, 1, (5327), 10.1038/s41467-020-19119-8). **Nature Communications**, [S. l.], v. 12, n. 1, p. 41467, 2021. DOI: 10.1038/s41467-021-23280-z. Disponível em: <http://dx.doi.org/10.1038/s41467-021-23280-z>.

MORRISON, Sean J.; SCADDEN, David T. The bone marrow niche for haematopoietic stem cells. **Nature**, [S. l.], v. 505, n. 7483, p. 327–334, 2014. DOI: 10.1038/nature12984.

MORRISON, Sean J.; WANDYCYZ, Antoni M.; HEMMATI, Houman D.; WRIGHT, Douglas E.; WEISSMAN, Irving L. Development-1997-Morrison-1929-39. [S. l.], v. 1939, p. 1–11, 1997. Disponível em: <papers2://publication/uuid/44A71CA9-CF17-462D-851D-B2A305E52759>.

MORRISON, Sean J.; WEISSMAN, Irving L. The long-term repopulating subset of hematopoietic stem cells is deterministic and isolatable by phenotype. **Immunity**, [S. l.], v. 1, n. 8, p. 661–673, 1994. DOI: 10.1016/1074-7613(94)90037-X.

MOSCHOI, Ruxanda et al. Protective mitochondrial transfer from bone marrow stromal cells to acute myeloid leukemic cells during chemotherapy. **Blood**, [S. l.], v. 128, n. 2, p. 253–264, 2016. DOI: 10.1182/blood-2015-07-655860.

MULLER-SIEBURG, Christa E.; SIEBURG, Hans B.; BERNITZ, Jeff M.; CATTAROSSO, Giulio. Stem cell heterogeneity: Implications for aging and regenerative medicine. **Blood**, [S. l.], v. 119, n. 17, p. 3900–3907, 2012. DOI: 10.1182/blood-2011-12-376749.

MURRAY, Peter J. et al. Macrophage Activation and Polarization: Nomenclature and Experimental Guidelines. **Immunity**, [S. l.], v. 41, n. 1, p. 14–20, 2014. DOI: 10.1016/j.immuni.2014.06.008. Disponível em: <http://dx.doi.org/10.1016/j.immuni.2014.06.008>.

MUSSAI, Francis et al. Acute myeloid leukemia creates an arginase-dependent immunosuppressive microenvironment. **Blood**, [S. l.], v. 122, n. 5, p. 749–758, 2013. DOI: 10.1182/blood-2013-01-480129.

NAKORN, Thanyaphong Na; TRAVER, David; WEISSMAN, Irving L.; AKASHI, Koichi. Myeloerythroid-restricted progenitors are sufficient to confer radioprotection and provide the majority of day 8 CFU-S. **Journal of Clinical Investigation**, [S. l.], v. 109, n. 12, p. 1579–1585, 2002. DOI: 10.1172/JCI200215272.

NERLOV, Claus; GRAF, Thomas. PU.1 induces myeloid lineage commitment in multipotent hematopoietic progenitors. **Genes and Development**, [S. l.], v. 12, n. 15, p. 2403–2412, 1998. DOI: 10.1101/gad.12.15.2403.

NEWMAN, Aaron M.; LIU, Chih Long; GREEN, Michael R.; GENTLES, Andrew J.; FENG, Weiguo; XU, Yue; HOANG, Chuong D.; DIEHN, Maximilian; ALIZADEH, Ash A. Robust enumeration of cell subsets from tissue expression profiles. **Nature Methods**, [S. l.], v. 12, n. 5, p. 453–457, 2015. DOI: 10.1038/nmeth.3337.

NISHIKAWA, Shin Ichi; NISHIKAWA, Satomi; KAWAMOTO, Hiroshi; YOSHIDA, Hisahiro; KIZUMOTO, Masami; KATAOKA, Hiroshi; KATSURA, Yoshimoto. In vitro generation of lymphohematopoietic cells from endothelial cells purified from murine embryos. **Immunity**, [S. l.], v. 8, n. 6, p. 761–769, 1998. DOI: 10.1016/S1074-7613(00)80581-6.

NOMURA, Mitsunori; LIU, Jie; ROVIRA, Ilsa I.; GONZALEZ-HURTADO, Elsie; LEE, Jieun; WOLFGANG, Michael J.; FINKEL, Toren. Fatty acid oxidation in macrophage polarization. **Nature Immunology**, [S. l.], v. 17, n. 3, p. 216–217, 2016. DOI: 10.1038/ni.3366.

OGURO, Hideyuki; DING, Lei; MORRISON, Sean J. SLAM family markers resolve functionally distinct subpopulations of hematopoietic stem cells and multipotent progenitors. **Cell Stem Cell**, [S. l.], v. 13, n. 1, p. 102–116, 2013. DOI: 10.1016/j.stem.2013.05.014. Disponível em: <http://dx.doi.org/10.1016/j.stem.2013.05.014>.

PAPAEMMANUIL, Elli et al. Genomic Classification and Prognosis in Acute Myeloid Leukemia. **New England Journal of Medicine**, [S. l.], v. 374, n. 23, p. 2209–2221, 2016. DOI: 10.1056/nejmoa1516192.



PARK, Serk In; KIM, Sun Jin; MCCAULEY, Laurie K.; GALLICK, Gary E. Preclinical mouse models of human prostate cancer and their utility in drug discovery. **Current Protocols in Pharmacology**, [S. l.], n. SUPPL.51, p. 1–27, 2010. DOI: 10.1002/0471141755.ph1415s51.

PASSLICK, B.; FLIEGER, D.; ZIEGLER-HEITBROCK, HW. Identification and characterization of a novel monocyte subpopulation in human peripheral blood. **Blood**, [S. l.], v. 74, n. 7, p. 2527–2534, 1989. DOI: 10.1182/blood.v74.7.2527.2527. Disponível em: <http://dx.doi.org/10.1182/blood.V74.7.2527.2527>.

PEI, Shanshan et al. Monocytic subclones confer resistance to venetoclax-based therapy in patients with acute myeloid leukemia. **Cancer Discovery**, [S. l.], v. 10, n. 4, p. 536–551, 2020. DOI: 10.1158/2159-8290.CD-19-0710.

PEREIRA-MARTINS, Diego A. et al. MLL5 improves ATRA driven differentiation and promotes xenotransplant engraftment in acute promyelocytic leukemia model. **Cell Death and Disease**, [S. l.], v. 12, n. 4, 2021. DOI: 10.1038/s41419-021-03604-z. Disponível em: <http://dx.doi.org/10.1038/s41419-021-03604-z>.

PIETRAS, Eric M.; REYNAUD, Damien; KANG, Yoon A.; CARLIN, Daniel; CALERO-NIETO, Fernando J.; LEAVITT, Andrew D.; STUART, Joshua A.; GÖTTGENS, Berthold; PASSEGUÉ, Emmanuelle. Functionally Distinct Subsets of Lineage-Biased Multipotent Progenitors Control Blood Production in Normal and Regenerative Conditions. **Cell Stem Cell**, [S. l.], v. 17, n. 1, p. 35–46, 2015. DOI: 10.1016/j.stem.2015.05.003.

RAAIJMAKERS, Marc H. G. P. et al. Bone progenitor dysfunction induces myelodysplasia and secondary leukaemia. **Nature**, [S. l.], v. 464, n. 7290, p. 852–857, 2010. DOI: 10.1038/nature08851.

RANZONI, Anna Maria et al. Integrative Single-Cell RNA-Seq and ATAC-Seq Analysis of Human Developmental Hematopoiesis. **Cell Stem Cell**, [S. l.], v. 28, n. 3, p. 472–487.e7, 2021. DOI: 10.1016/j.stem.2020.11.015. Disponível em: <https://doi.org/10.1016/j.stem.2020.11.015>.

REGO, Eduardo M. et al. Improving acute promyelocytic leukemia (APL) outcome in developing countries through networking, results of the International Consortium on APL. **Blood**, [S. l.], v. 121, n. 11, p. 1935–1943, 2013. DOI: 10.1182/blood-2012-08-449918.

REINISCH, Andreas; THOMAS, Daniel; CORCES, M. Ryan; ZHANG, Xiaohua; GRATZINGER, Dita; HONG, Wan Jen; SCHALLMOSER, Katharina; STRUNK, Dirk; MAJETI, Ravindra. A humanized bone marrow ossicle xenotransplantation model enables improved engraftment of healthy and leukemic human hematopoietic cells. **Nature Medicine**, [S. l.], v. 22, n. 7, p. 812–821, 2016. DOI: 10.1038/nm.4103.

RONGVAUX, Anthony et al. Development and function of human innate immune cells in a humanized mouse model. **Nature Biotechnology**, [S. l.], v. 32, n. 4, p. 364–372, 2014. DOI:

10.1038/nbt.2858.

SCHOEDEL, Kristina B. et al. The bulk of the hematopoietic stem cell population is dispensable for murine steady-state and stress hematopoiesis. **Blood**, [S. l.], v. 128, n. 19, p. 2285–2296, 2016. DOI: 10.1182/blood-2016-03-706010.

SHLUSH, Liran I. et al. Tracing the origins of relapse in acute myeloid leukaemia to stem cells. **Nature**, [S. l.], v. 547, n. 7661, p. 104–108, 2017. DOI: 10.1038/nature22993. Disponível em: <http://dx.doi.org/10.1038/nature22993>.

SMITH, L. G.; WEISSMAN, I. L.; HEIMFELD, S. Clonal analysis of hematopoietic stem-cell differentiation in vivo. **Proceedings of the National Academy of Sciences of the United States of America**, [S. l.], v. 88, n. 7, p. 2788–2792, 1991. DOI: 10.1073/pnas.88.7.2788.

SPANGRUDE, Gerald J. Hematopoietic stem-cell differentiation. **Current Opinion in Immunology**, [S. l.], v. 3, n. 2, p. 171–178, 1991. DOI: 10.1016/0952-7915(91)90046-4.

STEVENS, Brett M. et al. Fatty acid metabolism underlies venetoclax resistance in acute myeloid leukemia stem cells. **Nature Cancer**, [S. l.], v. 1, n. 12, p. 1176–1187, 2020. DOI: 10.1038/s43018-020-00126-z. Disponível em: <http://dx.doi.org/10.1038/s43018-020-00126-z>.

SUBAUSTE, C. S.; DE WAAL MALEFYT, R.; FUH, F. Role of CD80 (B7.1) and CD86 (B7.2) in the immune response to an intracellular pathogen. **Journal of immunology (Baltimore, Md. : 1950)**, [S. l.], v. 160, n. 4, p. 1831–40, 1998. Disponível em: <http://www.ncbi.nlm.nih.gov/pubmed/9469444>.

SUBRAMANIAN, Aravind et al. Gene set enrichment analysis: A knowledge-based approach for interpreting genome-wide expression profiles. **Proceedings of the National Academy of Sciences of the United States of America**, [S. l.], v. 102, n. 43, p. 15545–15550, 2005. DOI: 10.1073/pnas.0506580102.

SZABO, Susanne J.; KIM, Sean T.; COSTA, Gina L.; ZHANG, Xiankui; FATHMAN, C. Garrison; GLIMCHER, Laurie H. A novel transcription factor, T-bet, directs Th1 lineage commitment. **Cell**, [S. l.], v. 100, n. 6, p. 655–669, 2000. DOI: 10.1016/S0092-8674(00)80702-3.

TAM, Patrick P. L.; BEHRINGER, Richard R. Mouse gastrulation: The formation of a mammalian body plan. **Mechanisms of Development**, [S. l.], v. 68, n. 1–2, p. 3–25, 1997. DOI: 10.1016/S0925-4773(97)00123-8.

TANG, Qin et al. Dissecting hematopoietic and renal cell heterogeneity in adult zebrafish at single-cell resolution using RNA sequencing. **Journal of Experimental Medicine**, [S. l.], v. 214, n. 10, p. 2875–2887, 2017. DOI: 10.1084/jem.20170976.

THOMPSON, Heather L.; VAN ROOIJEN, Nico; MCLELLAND, Bryce T.; MANILAY, Jennifer O. F4/80+ Host Macrophages Are a Barrier to Murine Embryonic Stem Cell-Derived Hematopoietic Progenitor Engraftment In Vivo. **Journal of Immunology Research**, [S. l.], v. 2016, p. 15–17, 2016. DOI: 10.1155/2016/2414906.

TILL, J. E.; MCCULLOCH, E. A. A Direct Measurement of the Radiation Sensitivity of Normal Mouse Bone Marrow Cells Author ( s ): J . E . Till and E . A . McCulloch Published by : Radiation Research Society Stable URL : <http://www.jstor.org/stable/3570892> A Direct Measurement of the Rad. **Radiation Research Society**, [S. l.], v. 14, n. 2, p. 213–222, 1961.

TURLEY, Shannon J.; CREMASCO, Viviana; ASTARITA, Jillian L. Immunological hallmarks of stromal cells in the tumour microenvironment. **Nature Reviews Immunology**, [S. l.], v. 15, n. 11, p. 669–682, 2015. DOI: 10.1038/nri3902.

TYNER, Jeffrey W. et al. Functional genomic landscape of acute myeloid leukaemia. **Nature**, [S. l.], v. 562, n. 7728, p. 526–531, 2018. DOI: 10.1038/s41586-018-0623-z.

VAN GALEN, Peter et al. Single-Cell RNA-Seq Reveals AML Hierarchies Relevant to Disease Progression and Immunity. **Cell**, [S. l.], v. 176, n. 6, p. 1265–1281.e24, 2019. DOI: 10.1016/j.cell.2019.01.031. Disponível em: <https://doi.org/10.1016/j.cell.2019.01.031>.

VELTEN, Lars et al. Human haematopoietic stem cell lineage commitment is a continuous process. **Nature Cell Biology**, [S. l.], v. 19, n. 4, p. 271–281, 2017. DOI: 10.1038/ncb3493.

VON DER HEIDE, E. K. et al. Molecular alterations in bone marrow mesenchymal stromal cells derived from acute myeloid leukemia patients. **Leukemia**, [S. l.], v. 31, n. 5, p. 1069–1078, 2017. DOI: 10.1038/leu.2016.324.

WANG, Nan; LIANG, Hongwei; ZEN, Ke. Molecular mechanisms that influence the macrophage M1-M2 polarization balance. **Frontiers in Immunology**, [S. l.], v. 5, n. NOV, p. 1–9, 2014. DOI: 10.3389/fimmu.2014.00614.

WANG, Yao Chun et al. Notch signaling determines the M1 versus M2 polarization of macrophages in antitumor immune responses. **Cancer Research**, [S. l.], v. 70, n. 12, p. 4840–4849, 2010. DOI: 10.1158/0008-5472.CAN-10-0269.

WATTRUS, Samuel; SMITH, Mackenzie; HAGEDORN, Elliott; ZON, Leonard. 2008 – Adult Hematopoietic Stem Cell Clonality Is Determined By Embryonic Macrophage Sensing of Calreticulin. **Experimental Hematology**, [S. l.], v. 88, p. S30, 2020. DOI: 10.1016/j.exphem.2020.09.170. Disponível em: <https://doi.org/10.1016/j.exphem.2020.09.170>.

WEINHÄUSER, I. et al. Reduced SLIT2 is associated with increased cell proliferation and arsenic trioxide resistance in acute promyelocytic Leukemia. **Cancers**, [S. l.], v. 12, n. 11, 2020. DOI: 10.3390/cancers12113134.

WIERENGA, Albertus T. J.; SCHEPERS, Hein; MOORE, Malcolm A. S.; VELLENGA, Edo; SCHURINGA, Jan Jacob. STAT5-induced self-renewal and impaired myelopoiesis of human hematopoietic stem/progenitor cells involves down-modulation of C/EBP $\alpha$ . **Blood**, [S. l.], v. 107, n. 11, p. 4326–4333, 2006. DOI: 10.1182/blood-2005-11-4608.

WILSON, Anne et al. Hematopoietic Stem Cells Reversibly Switch from Dormancy to Self-Renewal during Homeostasis and Repair. **Cell**, [S. l.], v. 135, n. 6, p. 1118–1129, 2008. DOI: 10.1016/j.cell.2008.10.048.

WILSON, Anne; OSER, Gabriela M.; JAWORSKI, Maike; BLANCO-BOSE, William E.; LAURENTI, Elisa; ADOLPHE, Christelle; ESSERS, Marieke A.; MACDONALD, H. Robson; TRUMPP, Andreas. Dormant and self-renewing hematopoietic stem cells and their niches. **Annals of the New York Academy of Sciences**, [S. l.], v. 1106, p. 64–75, 2007. DOI: 10.1196/annals.1392.021.

XU, Zi Jun et al. The M2 macrophage marker CD206: a novel prognostic indicator for acute myeloid leukemia. **OncoImmunology**, [S. l.], v. 9, n. 1, 2020. DOI: 10.1080/2162402X.2019.1683347.

YAHATA, Takashi; ANDO, Kiyoshi; SATO, Tadayuki; MIYATAKE, Hiroko; NAKAMURA, Yoshihiko; MUGURUMA, Yukari; KATO, Shunichi; HOTTA, Tomomitsu. A highly sensitive strategy for SCID-repopulating cell assay by direct injection of primitive human hematopoietic cells into NOD/SCID mice bone marrow. **Blood**, [S. l.], v. 101, n. 8, p. 2905–2913, 2003. DOI: 10.1182/blood-2002-07-1995.

YAMAMOTO, Ryo; MORITA, Yohei; OOEHARA, Jun; HAMANAKA, Sanae; ONODERA, Masafumi; RUDOLPH, Karl Lenhard; EMA, Hideo; NAKAUCHI, Hiromitsu. XClonal analysis unveils self-renewing lineage-restricted progenitors generated directly from hematopoietic stem cells. **Cell**, [S. l.], v. 154, n. 5, p. 1112–1126, 2013. DOI: 10.1016/j.cell.2013.08.007. Disponível em: <http://dx.doi.org/10.1016/j.cell.2013.08.007>.

YAMASHITA, Masayuki; DELLORUSSO, Paul V.; OLSON, Oakley C.; PASSEGUÉ, Emmanuelle. Dysregulated haematopoietic stem cell behaviour in myeloid leukaemogenesis. **Nature Reviews Cancer**, [S. l.], v. 20, n. 7, p. 365–382, 2020. DOI: 10.1038/s41568-020-0260-3. Disponível em: <http://dx.doi.org/10.1038/s41568-020-0260-3>.

YANG, Liping; BRYDER, David; ADOLFSSON, Jörgen; NYGREN, Jens; MÅNSSON, Robert; SIGVARDSSON, Mikael; JACOBSEN, Sten Eirik W. Identification of Lin-Sca1+kit+CD34 +Flt3- short-term hematopoietic stem cells capable of rapidly reconstituting and rescuing myeloablated transplant recipients. **Blood**, [S. l.], v. 105, n. 7, p. 2717–2723, 2005. DOI: 10.1182/blood-2004-06-2159.

*Supplemental Material*

---

## 9 SUPPLEMENTAL MATERIAL



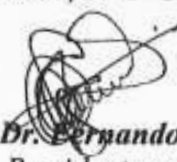
UNIVERSIDADE DE SÃO PAULO  
FACULDADE DE MEDICINA DE RIBEIRÃO PRETO  
COMISSÃO DE ÉTICA NO USO DE ANIMAIS

**CERTIFICADO**

Certificamos que o Protocolo para Uso de Animais em Experimentação nº 176/2015, sobre o projeto intitulado "*Deteção e estudo funcional de Macrófagos Associados a Tumor em um modelo transgênico de leucemia promielocítica aguda*", sob a responsabilidade do **Professor Eduardo Magalhães Rego** está de acordo com os Princípios Éticos em Experimentação Animal adotado pelo Conselho Nacional de Controle de Experimentação Animal (CONCEA) e foi **APROVADO** em reunião de 29 de fevereiro de 2016.

We certify that the protocol n° 176/2015, entitled "*Detection and functional analysis of Tumor Associated Macrophages in transgenic APL mice model*", is in accordance with the Ethical Principles in Animal Research adopted by the National Council for the Control of Animal Experimentation (CONCEA) and was approved by the Local Animal Ethical Committee from the Ribeirão Preto Medical School of the University of São Paulo in 02/29/2016.

Ribeirão Preto, 29 de fevereiro de 2016.

  
**Prof. Dr. Fernando Silva Carneiro**  
Vice-Presidente, em exercício, da  
CEUA – FMRP – USP



UNIVERSIDADE DE SÃO PAULO  
FACULDADE DE MEDICINA DE RIBEIRÃO PRETO  
COMISSÃO DE ÉTICA NO USO DE ANIMAIS

CEUA  
FMRP-USP  
Comissão de Ética no Uso de Animais  
Replacement/Reduction/Refinement

FMRP  
65 anos USP

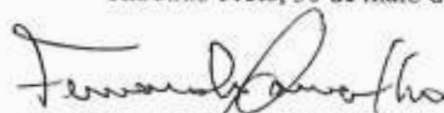
## CERTIFICADO

Certificamos que o Protocolo intitulado "*Avaliação da via TP53/TP73 na enxertia de células de leucemia promielocítica aguda em modelo de xenotransplante*", registrado com o número **067/2018**, sob a responsabilidade do **Prof. Dr. Eduardo Magalhães Rego**, envolvendo a produção, manutenção ou utilização de animais pertencentes ao *filo Chordata, subfilo Vertebrata* (exceto humanos) para fins de pesquisa científica, encontra-se de acordo com os preceitos da Lei nº 11.794 de 8 de outubro de 2008, do Decreto nº 6.899 de 15 de julho de 2009 e com as normas editadas pelo Conselho Nacional de Controle de Experimentação Animal (CONCEA), e foi **APROVADO** pela Comissão de Ética no Uso de Animais da Faculdade de Medicina de Ribeirão Preto da Universidade de São Paulo em reunião de 30 de maio de 2018.

Este Protocolo prevê a utilização de 80 camundongos NSG fêmeas pesando 22g oriundos do Serviço de Laboratório de Estudos Experimentais em Animais de Ribeirão Preto da Universidade de São Paulo. Vigência da autorização: 30/05/2018 a 06/06/2022.

We certify that the Protocol n° 067/2018, entitled "*Evaluation of the TP53/TP73 pathway in the engraftment of acute promyelocytic leukemia cells using xenotransplantation models*", is in accordance with the Ethical Principles in Animal Research adopted by the National Council for the Control of Animal Experimentation (CONCEA) and was approved by the Local Animal Ethical Committee from Ribeirão Preto Medical School of the University of São Paulo in 05/30/2018. This protocol involves the production, maintenance or use of animals from *phylum Chordata, subphylum Vertebrata* (except humans) for research purposes, and includes the use of 80 female NSG mice weighing 22g from Laboratory of Experimental Studies in Animals of Ribeirão Preto Medical School, University of São Paulo. This certificate is valid until 06/06/2022.

Ribeirão Preto, 30 de maio de 2018

  
Prof. Dr. Fernando Silva Ramalho  
Coordenador da CEUA-FMRP - USP

COMISSÃO NACIONAL DE  
ÉTICA EM PESQUISA



PARECER CONSUBSTANCIADO DA CONEP

DADOS DO PROJETO DE PESQUISA

**Título da Pesquisa:** AVALIAÇÃO DA DAUNORRUBICINA COMO AGENTE ANTRACÍCLICO NA INDUÇÃO DE REMISSÃO E CONSOLIDAÇÃO DE PACIENTES COM LEUCEMIA PROMIELOCÍTICA AGUDA

**Pesquisador:** Eduardo Magalhães Rego

**Área Temática:** A critério do CEP

**Versão:** 3

**CAAE:** 81987818.5.1001.5440

**Instituição Proponente:** Hospital das Clínicas da Faculdade de Medicina de Ribeirão Preto da USP -

**Patrocinador Principal:** FUNDAÇÃO DE AMPARO A PESQUISA DO ESTADO DE SÃO PAULO

DADOS DO PARECER

**Número do Parecer:** 3.003.975

**Apresentação do Projeto:**

As informações elencadas nos campos "Apresentação do Projeto", "Objetivo da Pesquisa" e "Avaliação dos Riscos e Benefícios" foram retiradas do arquivo Informações Básicas da Pesquisa (PB\_INFORMAÇÕES\_BÁSICAS\_DO\_PROJETO\_1049986.pdf, de 05/06/2018) e do Projeto Detalhado.

INTRODUÇÃO

A Leucemia Promielocítica Aguda (LPA) é um subtipo de Leucemia Mielóide Aguda (LMA) que se caracteriza pela parada da maturação do precursor mielóide no estágio de promielócito. Corresponde a cerca de 10% dos casos de LMA com incidência de 10.000 casos nos Estados Unidos em 2001. Entretanto, em alguns países, como Brasil e México a proporção de casos de LPA entre as LMAs é maior, situando-se entre 20 e 30%. Além das características morfológicas e citoquímicas peculiares, clinicamente apresenta-se com um quadro de coagulopatia que é o responsável pela maior morbidade dos pacientes. Do ponto de vista molecular, aproximadamente 95% dos casos de LPA apresentam uma translocação balanceada entre os cromossomos 15 e 17 (loci q22 e q21, respectivamente), gerando o gene PML-RAR. As conseqüências na regulação do ciclo celular e na terapêutica desta doença decorrentes desta alteração genética são de tal forma peculiares que, em 2001, a Organização Mundial de Saúde em sua reclassificação das hemopatias categorizou esta entidade como LMA com t(15;17). As recomendações atuais para o tratamento da

**Endereço:** SRNTV 701, Via W 5 Norte - Edifício PO 700, 3º andar

**Bairro:** Asa Norte

**CEP:** 70.719-049

**UF:** DF

**Município:** BRASÍLIA

**Telefone:** (61)3315-5877

**E-mail:** conep@saude.gov.br